1994

ANZIP Eighteenth Condensed Matter Physics Meeting

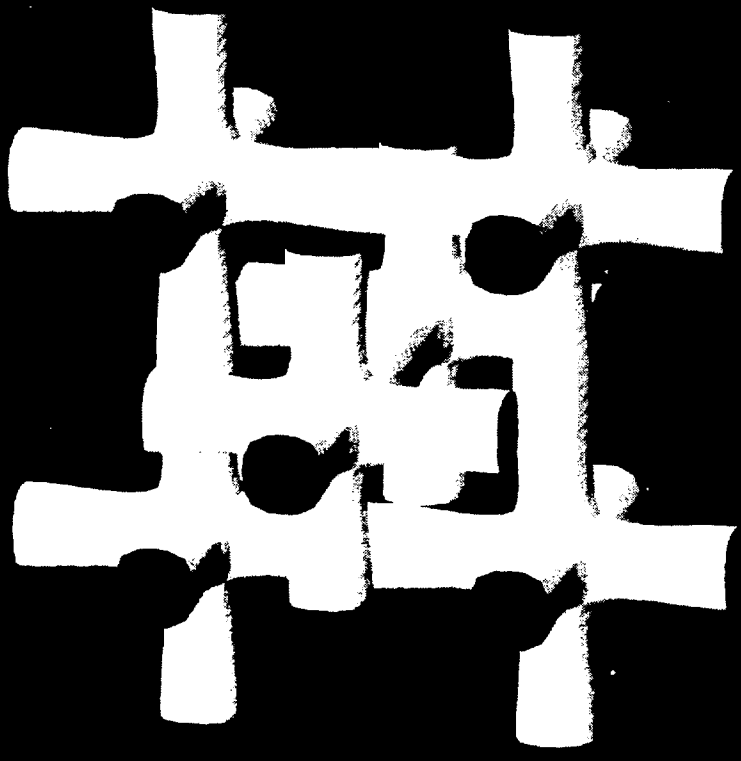

f-band Fermi surface of SmS

Wagga Wagga 9-11 February

Australian and New Zealand Institutes of Physics

18th Annual

CONDENSED MATTER PHYSICS MEETING

Charles Sturt University, Riverina

WAGGA WAGGA, NSW

9 – 11 February 1994

CONFERENCE HANDBOOK

ORGANISED BY: Don Chaplin, Wayne Hutchison, Nick Yazidjoglou and Glen Stewart

Department of Physics, University College
University of New South Wales
Australian Defence Force Academy
Canberra

with support from other members of the
Department of Physics, University College
ADFA

PAGE CONTENTS

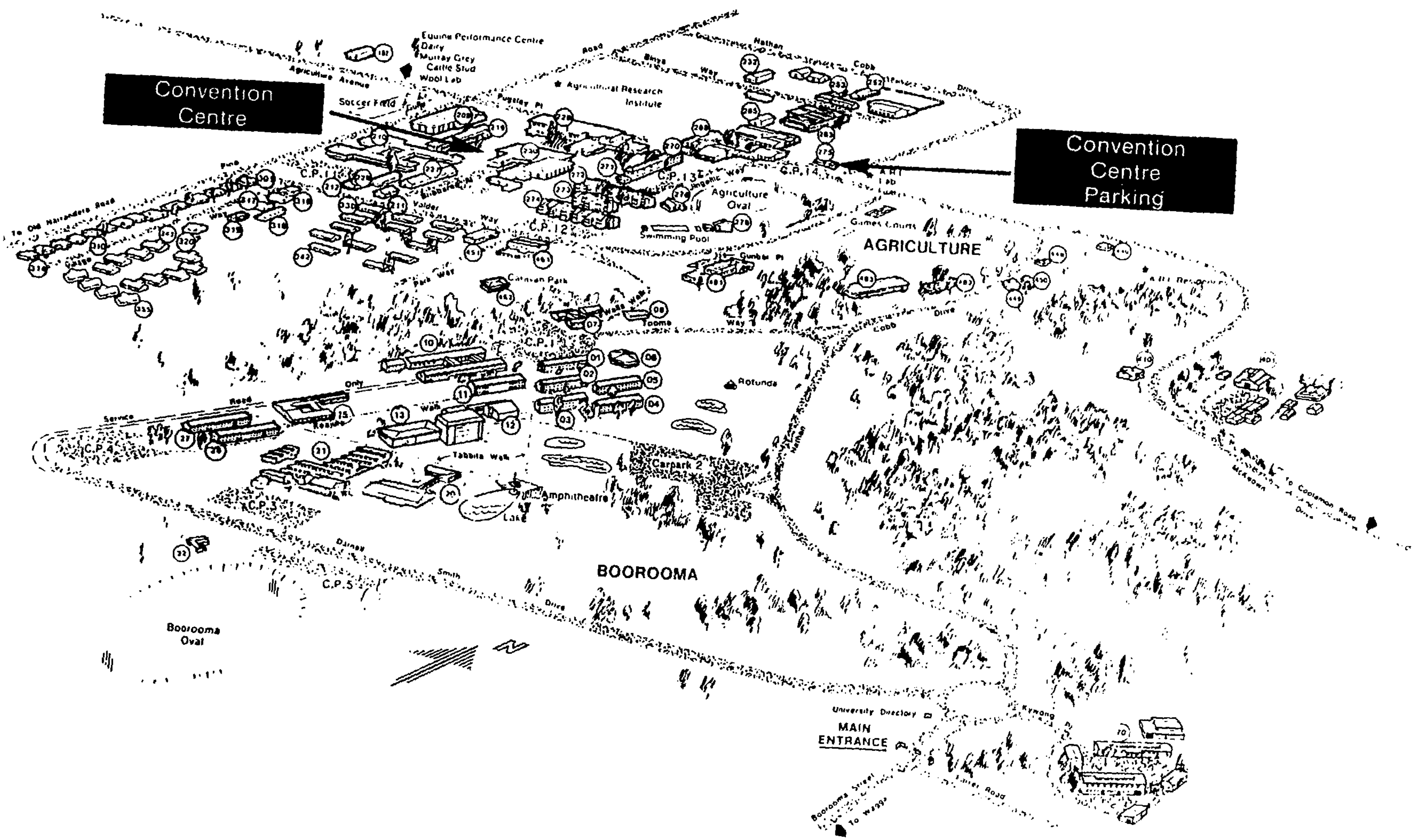

Convention Centre
Convention Centre Parking
Equine Performance Centre
Dairy
Murray Grey Cattle Stud
Wool Lab
Agricultural Research Institute
Soccer Field
Agriculture Avenue
Agriculture Oval
Swimming Pool
Games Courts
AGRICULTURE
Caravan Park
Rotunda
Carpark 2
Amphitheatre
Lake
Tabbita Walk
C.P.1
C.P.4
C.P.5
C.P.12
C.P.13
C.P.14
BOOROOMA
Boorooma Oval
University Directory
MAIN ENTRANCE
Boorooma Street
To Wagga
Coolamon Road

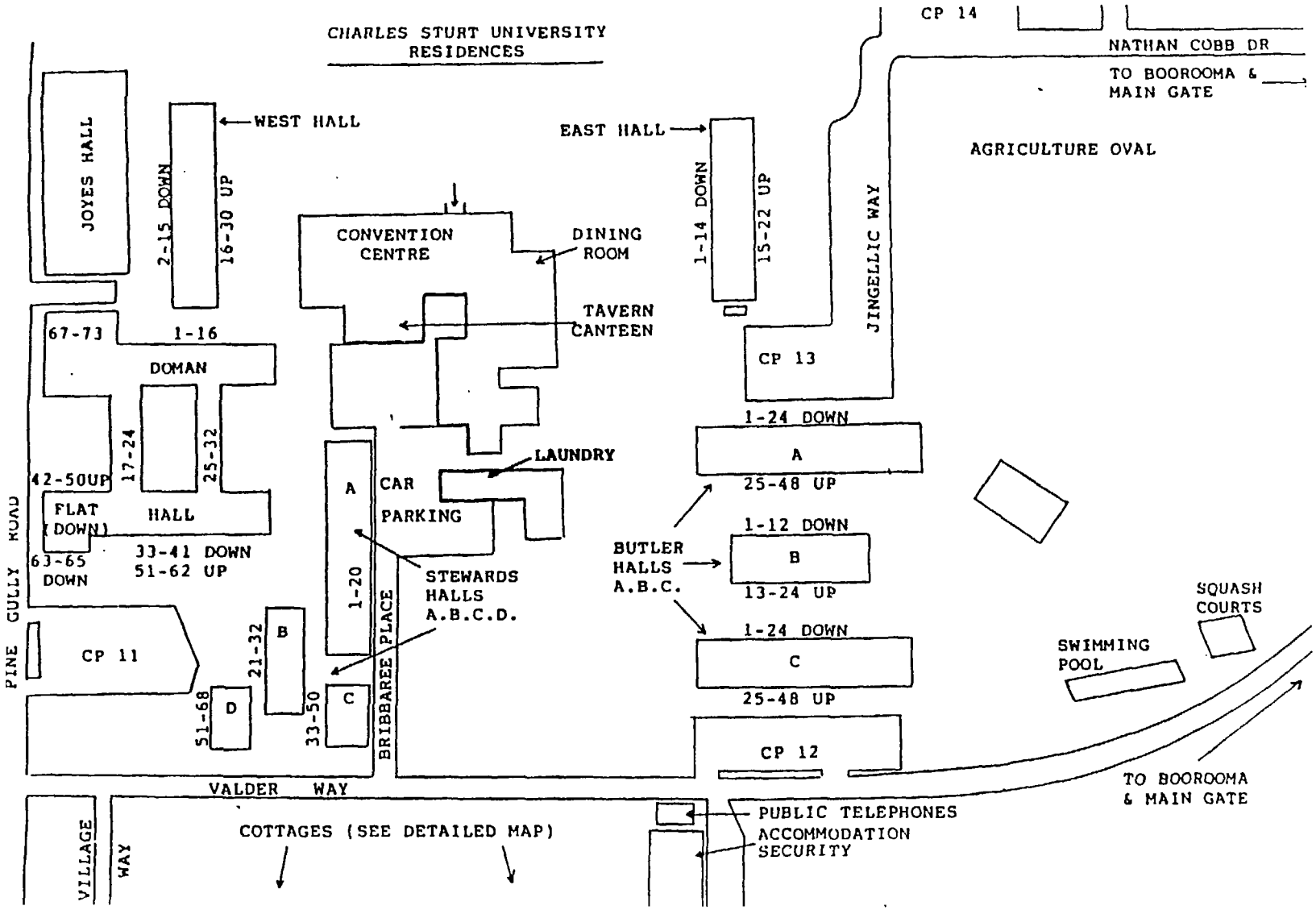
CHARLES STURT UNIVERSITY
RESIDENCES
CP 14
NATHAN COBB DR
TO BOOROOMA &
MAIN GATE
AGRICULTURE OVAL
JOYES HALL
WEST HALL
2-15 DOWN
16-30 UP
EAST HALL
1-14 DOWN
15-22 UP
JINGELLIC WAY
CONVENTION
CENTRE
DINING
ROOM
TAVERN
CANTEEN
67-73
1-16
DOMAN
CP 13
1-24 DOWN
A
25-48 UP
17-24
25-32
42-50UP
FLAT
(DOWN)
HALL
LAUNDRY
A
CAR
PARKING
1-12 DOWN
BUTLER
HALLS
A.B.C.
B
13-24 UP
63-65
DOWN
33-41 DOWN
51-62 UP
STEWARDS
HALLS
A.B.C.D.
1-20
PINE GULLY ROAD
CP 11
B
21-32
1-24 DOWN
C
25-48 UP
SQUASH
COURTS
SWIMMING
POOL
51-68
D
33-50
C
BRIBBAREE PLACE
CP 12
VALDER WAY
TO BOOROOMA
& MAIN GATE
PUBLIC TELEPHONES
ACCOMMODATION
SECURITY
COTTAGES (SEE DETAILED MAP)
VILLAGE
WAY

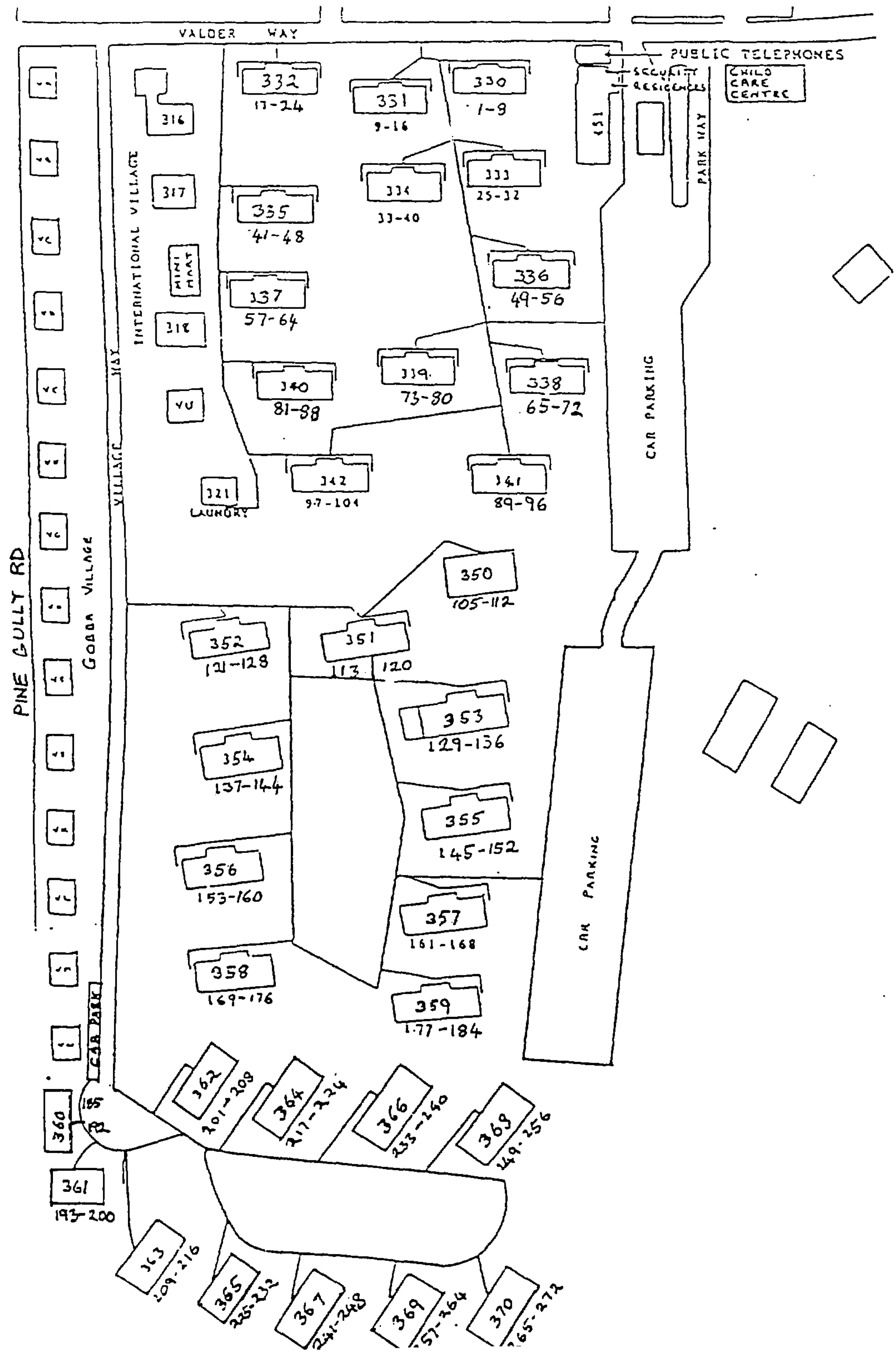
VALDER WAY
PUBLIC TELEPHONES
SECURITY
RESIDENCES
CHILD CARE CENTRE
PARK WAY
PINE GULLY RD
GOBBA VILLAGE
VILLAGE WAY
INTERNATIONAL VILLAGE
CAR PARKING
CAR PARK
LAUNDRY
332
17-24
331
9-16
330
1-8
316
317
335
41-48
334
33-40
333
25-32
336
49-56
337
57-64
318
340
81-88
339
73-80
338
65-72
342
97-104
341
89-96
321
350
105-112
352
121-128
351
113 120
353
129-136
354
137-144
355
145-152
356
153-160
357
161-168
358
169-176
359
177-184
360
361
193-200
362
201-208
363
209-216
364
217-224
365
225-232
366
233-240
367
241-248
368
249-256
369
257-264
370
265-272

WAGGA WAGGA '94

A hearty welcome to Wagga^2 '94 to all participants, especially to those who have not been here before. This year the traditional Wagga format, namely the relaxed two and a half day, no parallel session structure, has been comfortably maintained, with a few minor changes as outlined below.

All poster papers have been accommodated on either Wednesday or Thursday, which means each of the poster sessions contains in excess of 72 papers. By eliminating the Friday poster session it was therefore possible to include a larger than normal number of contributed talks. Nevertheless we regret an inability to satisfy more requests for oral delivery.

As in 1993, to give all posters a reasonable exposure, we request that on the Wednesday evening WP posters be removed, immediately after the evening WE lecture session, and Thursday's TP posters be mounted before Thursday morning's TM lecture session, as suggested in the timetable.

Posters have been grouped roughly into subject categories (e.g. magnetism, high T_C, semiconductors, etc) although in some cases there was more than one possibility. We apologise in advance to anyone whose poster may be in a slightly alien environment or not grouped as they had hoped.

The '94 committe has been pleased with the response of the condensed matter community to the suggestions made by the '93 committee on limiting the number of poster papers per presenter, or amalgamating similar material onto a single poster paper. With few exceptions restraint was shown by all which has made the committee's task a little easier.

Finally, we wish you all a stimulating and enjoyable time at Wagga Wagga 1994.

The 1994 Committee
(Don Chaplin, Wayne Hutchison, Nick Yazidjoglou and Glen Stewart)

Acknowledgements. Valuable assistance, advice and mailing lists from John Bell (Wagga '93) were greatly appreciated, as was the super-efficient work of the secretarial staff, and the assistance of Steve Harker , Vernon Edge and others at at Dept. of Physics, University College, ADFA. We also wish to thank Kathy Panarello, the convention centre programme manager, and the following people who acted as contacts at their respective institutions, both for the CMP conference and the Research Directory: T Bastow (CSIRO, DMST), D Beaglehole (Victoria), J Bell (UTS), G J Bowden (UNSW), P T Callaghan (Massey), C T Chou (Sydney), S J Collocott (CSIRO, DAP), R S Crisp (UWA), R L Davis (ANSTO), T F Finlayson (Monash), P Fisher (Wollongong), E Goldys (Macquarie), E Gray (Griffith), R Leckey (La Trobe), V McCann (Canterbury), J P D Martin (ANU), P Patterson (RMIT), S Prawer (Melbourne), C Sholl (UNE), P V Smith (Newcastle), M Staines (NZIRL) and B Usher (Telecom).

GENERAL INFORMATION

Scientific Programme

All posters and lectures will be in the Convention Centre which adjoins the dining room (see maps). Chairpersons and speakers must keep to the lecture programme schedule. If slides are to be used during a session please provide the projectionist with clearly marked slides at least 10 minutes before the relevant session. Preferably oversee their mounting and test one or two prior to the session. Overhead transparencies are, of course, catered for.

Posters must be mounted at the time specified in the timetable, i.e. on the evening prior to the day on which they are scheduled. They must also be removed early the following evening, preferably straight after dinner.

Some equipment exhibitors will be present in the Centre. They are also sponsoring the conference to help contain costs.

Administration

Please wear your name tag at all times at the Convention Centre. Registration and all other administrative matters should be addressed to the Conference desk or a committee member. For lost keys or if locked out, contact the Accommodation and Security Office near the corner of Valder Way and Park Way (the car park – see maps). After hours, phone 2288.

Convention Centre Phone Numbers : (069) 22 2184 or (069) 22 2247 (BH)

(069) 22 2288 (AH)

Meals, Coffee/Tea, Bar Facilities

All meals will be served in the dining room. You will have received a dining room pass on registration. *This must be produced at every meal.* It may also be required as ID for use of all other campus facilities (see below) which are at your disposal. Morning and afternoon tea will be served each day as indicated in the timetable. Coffee- and tea-making facilities are also available in the Common Room of each building and will be supplemented on request if necessary. In addition, at the time of the author attendance at posters on Wednesday and Thursday, the Conference Bar will open at 4.00 pm and remain open till 8.00pm. Some complimentary snacks will be available with this service to satisfy licencing rules. The other bar/canteen at the rear of the Centre is open all day and until late in the evening.

Sport and Recreational Facilities

All of the following are free (i.e. part of registration). Our old favourite, the swimming pool, is open from 6.00 am until 10.00 pm as are the adjacent squash courts. Tennis courts opposite the oval are also available. The gymnasium is on the original Agriculture campus. A wide range of facilities (exercise bikes, machines, etc) as well as table tennis tables and basketballs are available to registrants.

SPONSORS

There are a number of companies exhibiting their equipment and we encourage you to visit them during the course of the conference.

Their sponsorship, as well as that of other companies who have advertised, has helped contain costs.

The support of each of the following sponsors is gratefully acknowledged.

Balzers
Canberra Packard
Ceramic Engineering
Coherent Scientific
Coltronics Systems
Dynavac Engineering
Javac
Lastek
National Australia Bank
Nucletron
Oxford Instruments
Oxford Scientific
Rofin Australia
Stanton Scientific
Varian Australia

TIMETABLE

Tuesday ***8 February***

1400 onwards	Registration
1800 – 1900	*Dinner*
2000 – 2030	Posters WP to be mounted
2030	Poster session WP commences

Wednesday ***9 February***

0730 – 0830	*Breakfast*
0850 – 0900	Opening
0900 – 1040	Lecture session Papers WM1 – WM3
1040 – 1110	*Coffee*
1110 – 1230	Lecture session Papers WM4 – WM6
1230 – 1330	*Lunch*
1400 – 1520	Lecture session Papers WA1 – WA2
1530 – 1645	Author attencance at Posters WP1 – WP38 *(Coffee)*
1600 – 1800	*Conference Bar opens*
1645 – 1800	Author attendance at Posters WP39 – WP75
1800 – 1900	*Dinner*
1900 – 1950	*Wine tasting*
1950 – 2010	Condensed Matter studies of Wine, *prelude to*
2010 – 2140	Research Facilities and Initiatives
2140 –	Removal of WP Posters

Thursday ***10 February***

0730 – 0900	Mounting of TP Posters
0730 – 0830	*Breakfast*
0900	TP Poster session commences
0900 – 1040	Lecture session Papers TM1 – TM3
1040 – 1110	*Coffee*
1110 – 1230	Lecture session Papers TM4 – TM6
1230 – 1330	*Lunch*
1400 – 1520	Lecture session Papers TA1 – TA3
1530 – 1645	Author attendance at Posters TP1 – TP34 *(Coffee)*
1600 – 1800	*Conference Bar open*
1645 – 1800	Author attendance at Posters TP35 – TP73
1800 – 1900	*Dinner*
2030 – ?	"Teams event", main Union, Boorooma campus

Friday ***11 February***

0730 – 0830	*Breakfast*
0900 – 1040	Lecture session Papers FM1 – FM3
1040 – 1110	*Coffee*
1110 – 1220	Lecture session Papers FM4 – FM7
1220 – 1235	Prizes, wrap up
1235 – 1330	*Lunch*
1235 –	Removal of TP Posters

LECTURE SESSIONS

WEDNESDAY MORNING 9 FEBRUARY

0850 - 0900 Opening D.H. Chaplin

Session WM

Chairperson D.H. Chaplin

0900 - 0940 WM01 *Extreme cases of magnetism studied by implanted transition metal ions*
D. Riegel (Invited Lecture)

0940 - 1020 WM02 *Magnetic viscosity and magnetisation processes in thin films*
R. Street (Invited Lecture)

1020 - 1040 WM03 *Low temperature magnetic ordering of a series of structurally characterised chloroferrates*
J. Liesegang

Chairperson R.S. Crisp

1110 - 1150 WM04 *Mechanically alloyed rare earth permanent magnets*
L. Schultz (Invited Lecture)

1150 - 1210 WM05 *Preparation and properties of two-phase exchange coupled nano-composites*
D.S. Geoghegan

1210 - 1230 WM06 *Time-dependent atomic displacements in solid state diffusion*
C.A. Sholl

Chairperson G.J. Bowden

1400 - 1440 WA01 *The study of transient NMR effects by use of statistical tensor formalism*
L.N. Shakhmuratova (Invited Lecture)

1440 - 1500 WA02 *Electronic structure of graphite, diamond-like and graphitic amorphous carbon*
P. Storer

1500 - 1520 WA03 *Cross sectional imaging of single crystal materials by ion beam analysis*
D.N. Jamieson

LECTURE SESSIONS

WEDNESDAY EVENING 9 FEBRUARY

To help ease back into conference mode after the Wine tasting a small talk on condensed matter studies of wine, followed by Presentations and Discussion on Research Facilities and Initiatives

Session WE

Chairperson T.F. Smith

1950 - 2010 WE01 *Free radicals in red wine, but not in white?*
G.J. Troup

Format: 20 minutes presentation , 10 minutes for discussion & queries

2010 - 2140 WE02 *Research centres and science policy*
D. Bartels

WE03 *Semiconductor nanostructure fabrication facility*
R. G. Clark

WE04 *Applications of synchrotron radiation to materials science and the Australian National Beamline facility at the photon factory*
S. Wilkins

LECTURE SESSIONS

THURSDAY MORNING 10 FEBRUARY

Session TM

Chairperson G.A. Stewart

0900 - 0940	TM01	*Unexpected observations in metals at very low temperatures* G Eska (Invited Lecture)
0940 - 1020	TM02	*Edge phonoconductivity in a magnetically quantised two-dimensional electron gas* A.J. Kent (Invited Lecture)
1020 - 1040	TM03	*The freezing of 2D electron liquid in a random potential* J.S. Thakur

Chairperson J. Oitmaa

1110 - 1150	TM04	*How do the oxides and fullerides superconduct?* M.P. Das (Invited Lecture)
1150 - 1210	TM05	*The hole-hole superconducting pairing in the t - j model induced by the long-range spin-wave exchange* M.Y. Kuchiev
1210 - 1230	TM06	*Fabrication and properties of long Bi 2223 Ag-sheathed superconducting tapes* S.X. Dou

Chairperson G.K. White

1400 - 1440	TA01	*Long-length high-T_c superconductor processing, properties and applications* E.W. Collings (Invited Lecture)
1440 - 1500	TA02	*Growth and surface microstructure of epitaxial $YBa_2Cu_3O_{7-x}$ thin films* N. Savvides
1500 - 1520	TA03	*The decoupling between the superconducting layers in $Bi_2Sr_2CaCu_2O_8/Bi_2Sr_2Ca_2Cu_3O_{10}$ intergrowth single crystals* Y. Zhao

LECTURE SESSIONS

FRIDAY MORNING 11 FEBRUARY

Session FM

Chairperson G. Jones

0900 - 0940	FM01	*In-situ x-ray study of freezing and melting of Bi(2212) and Bi(2223)* D.K. Finnemore (Invited Lecture)
0940 - 1020	FM02	*Magnetic properties of Y 124 and Bi 2212 superconductors* N. Koshizuka (Invited Lecture)
1020 - 1040	FM03	*Charge density wave and Wigner crystal instabilities in electron-hole systems* J. Szymański

Chairperson R.J. Leckey

1110 - 1130	FM04	*Structural and electronic properties of* $C_{60}H_{36}$ L.E. Hall
1130 - 1150	FM05	*Surface plasmon observed for carbon nanotubes* L.A. Bursill
1150 - 1210	FM06	*Zeeman spectroscopy of indium acceptor impurity in silicon* R.A. Lewis
1210 - 1220	FM07	*Electron energy -loss spectroscopy study of thermal annealing of amorphous hydrogenated carbon* Y. Yin

POSTER SESSIONS

SESSION WP

POSTERS UP: Tuesday Evening 2000 -

AUTHOR ATTENDANCE:

WP01 - WP38	Wednesday 1530 - 1645
WP39 - WP75	Wednesday 1645 - 1800

POSTERS DOWN: Wednesday Evening 2140 -

WP01	**Thermal expansion of V_3Si with controlled martensite–phase morphology**	*M. Liu, T.R. Finlayson and T.F. Smith*
WP02	**Two dimensional antiferromagnetic ordering in $MnPS_3$**	*A.R. Wildes, S.J. Kennedy and T.J. Hicks*
WP03	**Electron spin resonance and intrinsic stress measurements on diamond synthesized by plasma assisted chemical vapour deposition**	*J. Khachan, P.B. Lukins, D.R. McKenzie, J.R. Pigott, I.S. Falconer and B.W. James*
WP04	**An investigation of preferential sputtering from single-phase α- and β- Cu/Zn alloys**	*D.R. Oliver and T.R. Finlayson*
WP05	**The influence of cationic and anionic surfactants on ball milled barium ferrite**	*S.J. Campbell, W.A. Kaczmarek, E. Wu and B.W. Ninham*
WP06	**Diffuse neutron scattering studies of single crystal specimens of $Fe_{3-x}Mn_xSi$**	*T. Ersez, S.J. Kennedy, T.J. Hicks and H. Kepa*
WP07	**Maximum entropy method study of the structure of Mg_2NiD_4 at 540 K using neutron diffraction data**	*E.H. Kisi*
WP08	**Magnetic properties of novel ternary phase: $Sm_3(Fe_{1-x}Ti_x)_{29}$ ($0.04 \leq x \leq 0.06$)**	*H.S Li, J.M. Cadogan, B.P. Hu, F.M. Yang, B. Nasunjilegal, J.M. Xu, H.K. Liu and S.X. Dou*
WP09	**Phase formation at the Fe-rich end of Dy-Fe-Ti system**	*J.M. Xu, H.S. Li, J.M. Cadogan, H.K. Liu and S.X. Dou*
WP10	**Mechanochemically induced reduction of zircon sand**	*T. Puclin, W.A. Kaczmarek and B.W. Ninham*

WP11	**Mechanochemical transformation of hematite to magnetite : Structural changes**	*S.J. Campbell, W.A. Kaczmarek, G. Wang and I. Onyszkiewicz*
WP12	**Magnetic properties of nano-materials of $Sm_3(Fe_{1-x}Ti_x)_{29}$ ($0.04 \leq x \leq 0.06$)**	*K.A. Reza, H.S. Li and J.M. Cadogan*
WP13	**Hyperfine magnetic fields of rare earth substituted ferrimagnets**	*R. Ramer, M. Ionescu, M. Barb, L. Diamandescu and C.C. Sorrell*
WP14	**Magnetic properties of a novel Pr-Fe-Ti phase**	*H.S. Li, Suharyana, J.M. Cadogan, G.J. Bowden, J.M. Xu, S.X. Dou and H.K. Liu*
WP15	**The magnetic properties of $Gd(Fe_{1-x}Co_x)_9Ti_2$ alloys**	*Suharyana, J.M. Cadogan, H.S. Li and G.J. Bowden*
WP16	**New feature in the magnetoresistance of silicon**	*D.J. Miller and J. Lobb*
WP17	**Transient NMRON–Recent advances**	*W.D. Hutchison, E. Jaatinen, N. Yazidjoglou and D.H. Chaplin*
WP18	**A shock-Hugoniot for $Sm_2Fe_{17}N_x$ powder**	*M.J. Lwin, P.D. Killen and N.W. Page*
WP19	**Faraday magnetometer for studying interstitially modified ferromagnets**	*T.P. Blach and E.M^{ac}A. Gray*
WP20	**The sorption of iron ions on polyurethane foams**	*D.Jinks, J.D. Cashion and W.H. Jay*
WP21	**The identification of poorly crystalline iron oxides and iron oxyhydrides**	*A.W.Y. Lee and J.D. Cashion*
WP22	**Characterisation of the sulphated ferric oxide mineral glockerite**	*D. Orloh, A.W.Y. Lee, J.D. Cashion and L.J. Brown*
WP23	**Structural and magnetic properties of $NdNi_{8.6-x}Fe_xSi_{2.4}$**	*S.J. Harker, S.J. Campbell, J.M. Cadogan and H.S. Li*
WP24	**A series study of quantum spin models on 3–dimensional lattices**	*J. Oitmaa, C.J. Hamer and Z. Weihong*
WP25	**High coercive $Sm_2Fe_{17}N_x$ powders prepared by HDDR**	*P.A.P. Wendhausen, N.M. Dempsey, B. Gebel and K.-H. Müller*

WP26	**Self-organised criticality in magnetization reversal**	*P.J. Thompson and R. Street*
WP27	**Mechanochemical activation of hematite**	*W.A. Kaczmarek and B.W. Ninham*
WP28	**Influence of air and vacuum during ball milling on morphology and structure of complex oxide powder (Effect of gas surface layer)**	*W.A. Kaczmarek*
WP29	**Magnetic properties of $ErCo_{12}B_6$:^{57}Fe**	*J.M. Cadogan, S.J. Campbell and X.L. Zhao*
WP30	**Spin glass behaviour in (Mn,Mg)S**	*G.T. Etheridge, S.J. Kennedy and T.J. Hicks*
WP31	**Molecular dynamics simulation of ion impact phenomena in 3D nickel lattice**	*P. Guan, N.A. Marks, D.R. McKenzie and B.A. Pailthorpe*
WP32	**Photoemission study of the Fermi surface of Cu**	*J.C. Foo, R. Leckey and J. Riley*
WP33	**The bond structures of closed shells in condensed nuclear matter**	*P. Norman*
WP34	**Hard disc collisions and the Lorentz gas pressure tensor**	*J. Petravic and D.J. Isbister*
WP35	**Massively parallel studies of the electronic structure of disordered micro–crystallites of transition metal oxides**	*M.T. Michalewicz*
WP36	**Classical lattice dynamics: Foreman–Lomer theory and the Blackman sum rule**	*A.M. Stewart*
WP37	**A practical appliction of the theory of hyper-complex variables: Dielectric and optical response of 3-dimensional arrays of spheres of complex permittivity**	*A.V. Vagov, R. Radchik and G.B. Smith*
WP38	**Tracer correlation factor and atomic displacements in solid state diffusion**	*P.C.L. Stephenson and C.A. Sholl*
WP39	**The polarisation of interacting and intersecting particles**	*A.V. Paley, A.V. Radchik, A.V. Vagov and G.B. Smith*

WP40	**Elimination of multiple quantum artifacts in 2D COSY NMR spectra (EMA-COSY)**	*G.J. Bowden and T. Heseltine*
WP41	**The initial thermo-instability of the Al-Cu-Mg-Ag supersaturated solid solution**	*M. Lim, P.L. Rossiter and J. Tibballs*
WP42	**Monte Carlo simulation of nanodomain textures in relaxor-type lead scandium tantalate**	*H. Qian, J.L. Peng and L.A. Bursill*
WP43	**A double monochromator system for a medium resolution neutron powder diffractometer**	*M.D. Burke and T.M. Sabine*
WP44	**Quantum well plasma effects in the tunneling current through a semiconductor double barrier structure**	*M.L.F. Lerch, C. Zhang, A.D. Martin, P.E. Simmonds and L. Eaves*
WP45	**The influence of ion, electron and photon irradiation on the level of hydrogen at the interface of metal-semiconductor systems**	*M.D. McCubbery, G.L. Nyberg and J.S. Williams*
WP46	**High energy photoelectron diffraction data from GaAs surfaces**	*A.E. Bocquet, R. Denecke, R. Eckstein, R.C.G. Leckey, J.D. Riley and L. Ley*
WP47	**Enhanced spin g-factor and split Landau-level for AlGaAs/GaAs heterostructures in strong magnetic fields**	*W. Xu and M.P. Das*
WP48	**Process optimization and characterization of Ni-Ge-Au ohmic contacts to n+ GaAs heterostructures**	*N.E. Lumpkin, G.R. Lumpkin and K.S.A. Butcher*
WP49	**Tunneling current in $Al_xGa_{1-x}As/Al_yGa_{1-y}As/GaAs$ double barrier quantum well structures**	*T. Osotchan, V.W.L. Chin, X.K. Cheng and T.L. Tansley*
WP50	**Cleavage luminescence in semiconductors**	*D.G. Li, N.S. McAlpine and D. Haneman*
WP51	**States above a quantum well in tilted magnetic fields**	*D.J. Miller and Z. Xiong*
WP52	**Porous silicon studied by soft x-ray emission spectroscopy**	*R.S. Crisp, D. Haneman and R. Sabet-Dariani*

WP53	**Lattice relaxation in strained layer semiconductors studied by in-situ x-ray topography during MBE growth**	*B.F. Usher, S.J. Barnett, G.F. Clark, B.K. Tanner, C.R. Whitehouse, A.D. Johnson, A.M. Keir, A.G. Cullis, B. Lunn, J.C.H. Hogg, W. Hagston and W. Spirkl*
WP54	**Empirical molecular dynamics calculations for the (001) and (111) reconstructed surfaces of diamond**	*A.J. Dyson and P.V. Smith*
WP55	**Ab Initio Hartree-Fock study of the B/Si(001)2X1 absorption system**	*M.W. Radny and P.V. Smith*
WP56	**Memory switching and quantum effects in amorphous hydrogenated silicon**	*M. Jafar and D. Haneman*
WP57	**Current-voltage characteristics of porous silicon**	*R. Sabet-Dariani, N.S. McAlpine and D. Haneman*
WP58	**GaAs conduction bands observed by inverse photoemission spectroscopy**	*W. Sheils, R.C.G. Leckey and J.D. Riley*
WP59	**Electrically detected magnetic resonance from a silicon p-n junction diode**	*Z. Xiong and D.J. Miller*
WP60	**Relativistic quantum mechanics in a periodic potential**	*A.J. Forsyth and A.E. Smith*
WP61	**Lifetime and bistability in electron tunneling in a double barrier structure**	*D. Fisher and C. Zhang*
WP62	**Heterojunctions of CdSe and amorphous silicon**	*S. Wu and D. Haneman*
WP63	**A high temporal resolution solid state thermal neutron detector**	*N.S. McKean, R.L. Davis, A. Bartel and E.N. Bakshi*
WP64	**Scanning deep level transient spectroscopy using an MeV ion microprobe**	*J.S. Laird, R.A. Bardos, G.R. Moloney, A.Saint and G.J.F. Legge*
WP65	**Zeeman effect of the shallow acceptors boron, gallium and thallium in germanium at magnetic fields up to 7T**	*R.J. Baker, P. Fisher, C.A. Freeth, D.S. Ryan and R.E.M. Vickers*
WP66	**Channeling contrast microscopy of defects in type II-VI MSM photodectors**	*L.C. Witham and D.N. Jamieson*

WP67	**In-situ control of solids oxidation**	*I.L. Skryabin and J.M. Bell*
WP68	**Ion beam mixing of isotopic bilayers**	*C.J. Fell*
WP69	**A study of the $Cu_3Au(110)$ surface using low energy ion scattering**	*F.M. Zhang, Y.G. Shen, B.V. King and D.J. O'Connor*
WP70	**Contact anomalies in the integral quantum Hall effect**	*B.W. Ricketts, L.D. Macks and M.M.R. Sovierzoski*
WP71	**An application of x-ray computerized tomography for examining the internal features of materials**	*G.N. Lee, M.M. Kijek and J.J. Millar*
WP72	**Analysis of compound semiconductor materials using heavy ion recoil spectrometry**	*S.R. Walker, P.N. Johnston, I.F. Bubb, W. Studd, D.D. Cohen, N. Dytlewski, M. Hult, H.J. Whitlow, C. Zahring, M. Östling, M. Andersson and J.W. Martin*
WP73	**Carbon and oxygen analysis in MOCVD grown HgCdMnTe and AlGaAs by charged particle activation**	*W.B. Studd, S.R. Walker, P.N. Johnston and I.F. Bubb*
WP74	**New automatic RBS/channeling system for thin film material analysis**	*L.S. Wielunski and M.J. Kenny*
WP75	**Determination of the deuterium order-disorder structure transition in $Pd\text{-}DO_{.65}$ at '50K'**	*S.J. Kennedy, E. Wu, E.H. Kisi, E.M. Gray and B.J. Kennedy*

POSTER SESSIONS

SESSION TP

POSTERS UP: Thursday Morning by 0900

AUTHOR ATTENDANCE:

TP01 - TP34	Thursday 1530 - 1645
TP35 - TP73	Thursday 1645 - 1800

POSTERS DOWN: Friday Afternoon 1235 -

TP01	**Investigations of ferroelectricity in $(CH_3NH_3)HgCl_3$**	*Z.T. Jiang, B.D. James, J. Liesegang*
TP02	**External control of microwave properties of dielectric materials**	*D.S. Maddison, P. Jewsbury and A. Amiet*
TP03	**Wear and friction measurements on CVD coated carbon alloy bearing surfaces**	*M.J. Kenny, L.S. Wielunski, M.D. Scott, R.A. Clissold and Q. Shaikh*
TP04	**Growth and properties of carbon nitride thin films**	*S. Kumar and T.L. Tansley*
TP05	**Tight binding calculations of the surface electronic DOS of graphite**	*B.A. McKinnon and T.C. Choy*
TP06	**Thermal characteristics of electric cables with polypyrrole coated conductors**	*R.N. Ediriweera, C. Conn, J. Unsworth and G. Tanos*
TP07	**Stability of polypyrrole tapes at high current densities**	*R.N. Ediriweera, J. Unsworth, C. Conn and E. Money*
TP08	**Investigation of carbon-nitride depositions produced by high energy density discharge in nitrogen gas atmosphere**	*V. Gurarie, A. Orlov, K. Nugent, J.L. Peng and S. Prawer*
TP09	**Determination of thin film optical constants using variable angle reflectance**	*S. Dligatch, I. Skryabin, G.B. Smith and J.M. Bell*
TP10	**Multilayer thin film colour selective filters**	*J. Barczynska and J.M. Bell*
TP11	**Preparation and characterisation of certain conducting polymer thin film devices**	*S.M. Pillai, C. Conn and J. Unsworth*

TP12	**Piezoelectric ceramic/polymer composites for damping of mechanical vibrations**	*H.H. Luo, P.L. Rossiter, L.L. Koss and G.P. Simon*
TP13	**(e,2e) measurements of thin graphite film**	*M. Vos, S. Canney, P. Storer and E. Weigold*
TP14	**Fabrication and characterisation of thin film tetrahedral amorphous carbon**	*E.G. Gerstner and D.R. McKenzie*
TP15	**Molecular dynamics study of compressive stress generation**	*N.A. Marks, D.R. McKenzie and B.A. Pailthorpe*
TP16	**Accumulated photon echoes in Nd^{3+}–doped CaF_2 and disordered CaF_2–YF_3 crystals**	*R.J. Reeves, K.W. Ver Steeg, A.Y. Karasik, R.C. Powell and T.T. Basiev*
TP17	**Zeeman shifts and splittings of hydride vibrational lines in rare-earth doped calcium fluoride**	*G. Jones and N. Strickland*
TP18	**Neutron diffraction measurements of time-dependent transformation of plastically deformed Mg-PSZ**	*W.J. Batchelor and T.R. Finlayson*
TP19	**Orientation and polarization effects in the Raman spectroscopy of (100) diamond faces in CVD deposited diamond films**	*P.S. Weiser, S. Prawer and K.W. Nugent*
TP20	**Dielectric relaxations in yttria-stabilised zirconia alloys at lower temperatures**	*Y. Chen and J.R. Sellar*
TP21	**Glassy thermal expansion of cubic stabilised zircoia alloys**	*Y. Chen and J.R. Sellar*
TP22	**Formation of iron carbide-nitrides by mechanochemical reaction between iron and organic H(CN)-ring compounds**	*I. Onyszkiewicz, W.A. Kaczmarek, A. Calka and B.W. Ninham*
TP23	**Character of electromechanical coupling in ceramic materials near F-AF phase boundary**	*Sun Da-Zhi, Dong Xian-Ling, Wang Yong-Ling and Lin Sheng-Wei*
TP24	**Fibre optic sensors for vibration monitoring of concrete beams**	*E. Tapanes, N. Pandelidis, J. Movrin, J, Williams and P. Rossiter*

TP25	**Fibre optic chemical sensors**	*E. Tapanes, J. Goode and P. Rossiter*
TP26	**Cure monitoring with fibre optic sensors**	*E. Tapanes, J. Goode, A. Hill and P. Rossiter*
TP27	**Micro-Raman studies of wear of MG-PSZ**	*G.L. Kelly, W.J. Batchelor and T.R. Finlayson*
TP28	**Inelastic neutron scattering from cubic stabilised zirconia**	*D.N. Argyriou and M.M. Elcombe*
TP29	**Low pressure growth of diamond films**	*L. Kostidis and S. Prawer*
TP30	**Transverse microanalysis of 2.5 MeV H^+ damage in diamond**	*S.P. Dooley, D.N. Jamieson, K.W. Nugent and S. Prawer*
TP31	**Zirconium x-ray emission spectra by an electron probe microanalyser**	*A. Duncan and T. Warmiński*
TP32	**Cell parameters and the orthorhombic to cubic transformation in strontium substituted perovskite ($CaTiO_3$)**	*C.J. Ball, B.D. Begg and E.R. Vance*
TP33	**The micropore structure of concrete determined by small angle neutron scattering**	*T.M. Sabine, W.K. Bertram and L.P. Aldridge*
TP34	**Modelling the microstructure of cement**	*W. Bertram, T.M. Sabine and L.P. Aldridge*
TP35	**Long-range two-hole bound states in the t - J model**	*M. Y. Kuchiev and O.P. Sushkov*
TP36	**Flux jumps in magnetization loops of melt-textured Y-Ba-Cu-O**	*K.-H. Müller and C. Andrikidis*
TP37	**Strain tolerant multifilamentary BiPb-2223 tapes for power applications**	*J. Yau, S.X. Dou and N. Savvides*
TP38	**Hall effect in Zn-doped Y-124**	*A. Mawdsley*
TP39	**A study of transition metal implanted single crystal $YBa_2Cu_3O_{7-\delta}$**	*J.W. Martin, G.J. Russell, D.D. Cohen, P.J. Evans and A. Hartmann*
TP40	**An elastic recoil time of flight spectrometer for materials analysis**	*J.W. Martin, D.D. Cohen, N. Dytlewski, G.J. Russell and D.B. Garton*

TP41	**Theory of freezing of a flux lattice in high T_c superconductors**	*D.J.C. Jackson and M.P. Das*
TP42	**Current-carrying length scale in silver sheathed Bi-Pb-Sr-Ca-Cu-O tapes**	*K.-H. Müller, C. Andrikidis, H.K. Liu and S.X. Dou*
TP43	**Magnetization studies of superconducting V_3Si**	*D.B. Lowe and T.R. Finlayson*
TP44	**Quench recovery processes associated with defect behaviour in YBCO near the critical temperature**	*Sujito, A.R. Anderson, G. Godamanne and G.J. Russell*
TP45	**Thermoelectric power of YBCO: Ag composite superconductors**	*Sujito, A.R. Anderson, G.J. Russell and G. Godammane*
TP46	**Activation energy of oxygen deficient YBCO**	*H.B. Sun and G.J. Russell*
TP47	**Electromagnetic response of high-T_c thick films**	*J.W. Cochrane and G.J. Russell*
TP48	**Anomalous time-decay in neutron depolarisation by high-T_c superconductors**	*P.A. Miles, S.J. Kennedy, K.N.R. Taylor, G.J. Russell, J. Wang, G.D. Gu, K. Takamura and N. Koshizuka*
TP49	**Variable range hopping conductivity in Y_{123}:Y_{211} composites close to the percolation limit**	*H.S. Gamchi, K.N.R. Taylor and G.J. Russell*
TP50	**Superconductivity of Fe-substituted $Bi_2Sr_2Ca_1Cu_2O_x$ single crystals**	*G.D. Gu, Y. Zhao, J.W. Cochrane, A.R. Anderson, G. Russell, K. Takamuku and N. Koshizuka*
TP51	**The relation between the ultrasonic properties and the critical temperature in Fe doped BSCCO**	*G. Godamanne, A.R. Anderson, G. Genda, G.J. Russell, N. Koshizuka and S. Tanaka*
TP52	**Oxygen stoichiometry measurements in polycrystalline $YBa_2Cu_3O_{7-x}$ by micro-Raman spectroscopy**	*J.M. Long, T.R. Finlayson, C.S. Lim and T.P. Mernagh*

TP53	**Spectral cathodoluminescence studies in $YBa_2Cu_3O_{7-x}$ and its related components**	*G. Stockton, M.R. Phillips and L. Kirkup*
TP54	**Microstructure development and phase transformation of Ag-sheathed Bi-2223 tapes**	*H.K. Liu, S.X. Dou, E.W. Collings and M.D. Sumption*
TP55	**Oxygen annealing of $Bi_2Sr_2Ca_1Cu_2O_{8+x}$ single crystals**	*H.M. Ionescu, S.X. Dou and R. Ramer*
TP56	**Microstructural and superconducting properties of Bi(2223)/Ag tapes during heat treatment process**	*Y.C. Guo, H.K. Liu and S.X. Dou*
TP57	**Electron paramagnetic resonance, magnetic susceptibility and resistance measurements on Mn doped 1:2:3 high temperature superconductors**	*G.J. Bowden, M. La Robina and E.C. Ploenjes*
TP58	**The defects of high J_c melt textured $YBa_2Cu_3O_{7-x}$ superconductors**	*J.A. Xia, P.R. Monroe, Y. Zhao, H.K. Liu and S.X. Dou*
TP59	**Vortex-glass superconductivity in low magnetic field in $YBa_2Cu_3O_{7-y}/V_2O_5$ composite**	*Y. Zhao and Y.Y. He*
TP60	**Structure and superconductivity in $YBaSrCu_{3-x}Sn_xO_y$ compound**	*Y. Zhao, G.D. Gu, J.A. Xia and G.J. Russell*
TP61	**Spin gap behaviour of $YBa_2(Cu_{(1-x)}Zn_x)_4O_8$**	*G.V.M. Williams, J.L. Tallon and R. Meinhold*
TP62	**A shock-Hugoniot for $YBa_2Cu_3O_7$ powder**	*J.R. Fitzsimmons, P.D. Killen and N.W. Page*
TP63	**Electronic structural changes in $Y_{1-x}Pr_xBa_2Cu_3O_{7-\delta}$ single crystals due to Pr4f states**	*A. Hartmann, G.J. Russell, W. Frentrup and K.N.R. Taylor*
TP64	**^{197}Au Mössbauer analysis of gold-doped YBCO**	*D. Jinks, G. Ganakas, J.D. Cashion, G. Jakovidis and M.J. Morgan*
TP65	**The behaviour of oxygen related defects in BSCCO near the critical temperature**	*A.R. Anderson, G. Godamanne, G. Genda, G.J. Russell, N. Koshizuka and S. Tanaka*

TP66	**The effect of silver on the I-V characteristics of BSCCO silver-sheathed tapes**	*D.N. Matthews, K.-H. Müller, C. Andrikidis, H.K. Liu and S.X. Dou*
TP67	**Noise in high-T_c r.f. squids**	*G.J. Sloggett, D.L. Dart, C.P. Foley, R.A. Binks, N. Savvides and A. Katsaros*
TP68	**Josephson behaviour and flux trapping effects in YBCO step edge junctions**	*C.P. Foley, G.J. Sloggett, D.N. Matthews, K.-H. Müller, S. Lam, N. Savvides and A. Katsaros*
TP69	**YBCO thin film deposition by cathodic arc and laser ablation**	*B. Jenkins, D.R. McKenzie, C.P. Foley and G.J. Sloggett*
TP70	**Anomalous flux pinning by twin boundaries in single-crystalline $YBa_2Cu_3O_7$**	*J.N. Li, A.A. Menovsky and J.J.M. Franse*
TP71	**Effect of columnar defects on the critical current anistropy of epitaxial $YBa_2Cu_3O_{7-\delta}$ thin films and $YBa_2Cu_3O_{7-\delta}/PrBa_2Cu_3O_{7-\delta}$ multilayers**	*B. Holzapfel, L. Shultz and G. Saemann-Ischenko*
TP72	**Production of superconducting thick films through cation chelated organic precursors**	*M. Yavuz and S.X. Dou*
TP73	**Charge compensation mechanisms for aliovalent impurities in perovskite and zirconolite**	*E.R. Vance, R.A. Day, B.D. Begg and M.G. Blackford*

Coherent
SCIENTIFIC

We have the laser to suit your application!

LASERS

- Argon Ion Lasers
- Carbon Dioxide Lasers
- Carbon Monoxide Lasers
- Diode Lasers
- Dye Lasers
- Excimer Lasers
- F-Centre Lasers
- Fluorine Lasers
- Helium-Cadmium Lasers
- Helium-Neon Lasers
- Krypton Ion Lasers
- Lead Salt Lasers
- Mixed-Gas Ion Lasers
- Nitrogen Lasers
- Neodymium:Glass Lasers
- Neodymium:YAG Lasers
- Neodymium:YLF Lasers
- Ruby Lasers
- Titanium:Sapphire Lasers
- Xenon-Helium Lasers

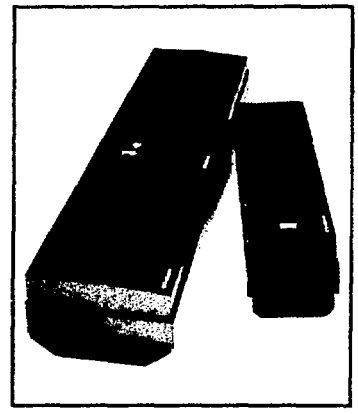

- Ion Laser & Dye Laser from Coherent (top left)
- Nd:YAG Lasers & Dye Laser from Continuum (top right)
- Ultrafast Ti:Sapphire Laser from Coherent (bottom left)
- Excimer Laser from Lambda Physik (bottom right)

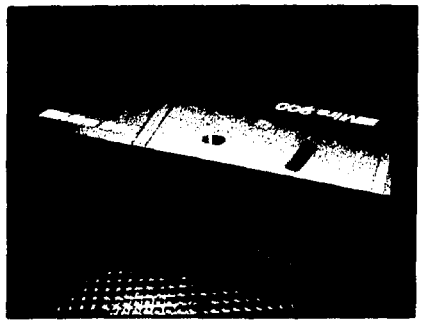

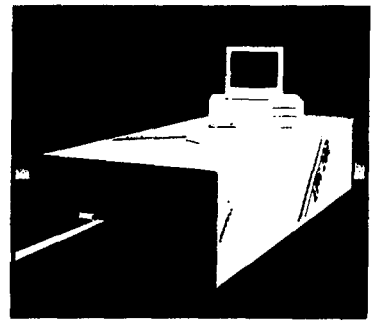

LASER ACCESSORIES

- Laser Dye
- Laser Eyewear
- Laser Flashlamps
- Laser Gases
- Laser Heat Exchangers
- Laser Power Meters
- Laser Spectrum Analysers
- Laser Mode Analysers
- Laser Beam Profilers

LASER MANUFACTURERS

- Burleigh Instruments
- Coherent Laser Group
- Continuum
- Edinburgh Instruments
- Lambda Physik
- Laser Photonics
- Lee Laser
- Melles Griot
- Omnichrome

■ 116 Burbridge Road, Hilton, South Australia 5033 ■
■ Telephone (08) 352 1111 ■ Facsimile (08) 352 2020 ■
Coherent Scientific Pty. Ltd. Inc. in S.A. ACN 008 265 969

Coherent
SCIENTIFIC

SPECTROSCOPY SOLUTIONS
from the Vacuum UV to the Far Infrared

BURLEIGH INSTRUMENTS

- Fabry-Perot Interferometers
- Laser Wavelength Meters
- Laser Spectrum Analysers

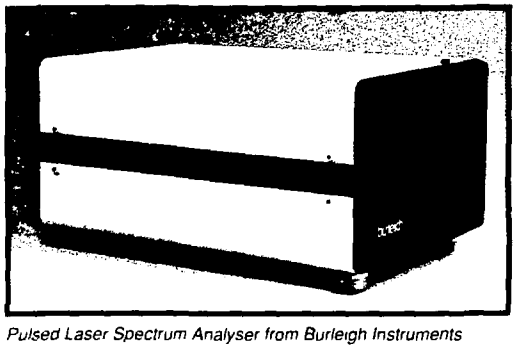

Pulsed Laser Spectrum Analyser from Burleigh Instruments

SPEX INDUSTRIES

- Grating Spectrometers
- Raman Spectroscopy Systems
- CCD and Photodiode Array Detectors
- Spectrofluorometer Systems

Single Grating Spectrometer from Spex Industries

PRINCETON INSTRUMENTS

- CCD and Intensified CCD Detectors
- Photodiode and Intensified Photodiode Array Detectors

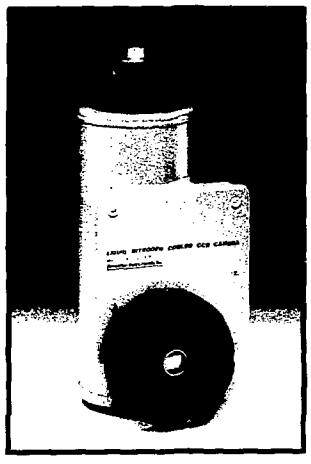

CCD Array Detector from Princeton Instruments

GALILEO ELECTRO-OPTICS

- Micro-Channel Plates (MCP's)
- Channel Electron Multipliers (Channeltrons)
- Time-Of-Flight Detectors
- Rare Earth Doped Optical Fibres

OPTRONIC LABORATORIES

- Radiometric and Photometric Calibration Standards
- Radiometers and Photometers
- UV. Visible and IR Spectroradiometers
- Detector Spectral Response Measurement Systems
- Spectral Reflectance Transmittance Measurement Systems

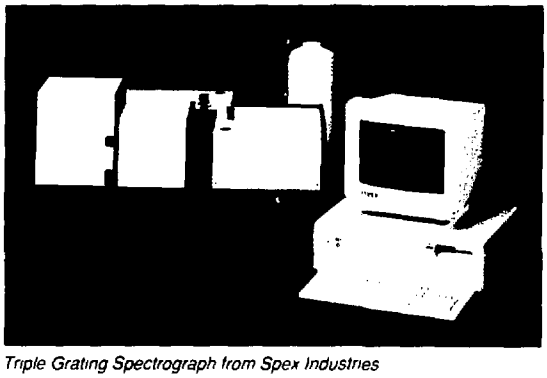

Triple Grating Spectrograph from Spex Industries

■ 116 Burbridge Road, Hilton, South Australia 5033 ■
Telephone (08) 352 1111 ■ Facsimile (08) 352 2020
Coherent Scientific Pty Ltd Inc in South Australia ACN 008 265 969

ABSTRACTS

LECTURES

WEDNESDAY POSTERS

THURSDAY POSTERS

EXTREME CASES OF MAGNETISM STUDIED BY IMPLANTED TRANSITION METAL IONS

D. Riegel
Hahn–Meitner–Institut, Berlin, Germany

Usually, the occurrence of magnetism of 3d, 4d and 5d ions in solids is restricted to certain 3d ions (Cr, Mn, Fe, Co, Ni) in alloying metallic systems and to Ti, V, Cr, Mn, Fe, Co, Ni ions in semiconductors and insulators. The application of the perturbed angular distribution method following heavy ion reaction and recoil implantation has offered an experimental way for probing the magnetic behaviour of isolated transition metal ions under extreme variations of the chemical environment. Particularly in nonalloying systems this technique allows us to produce and investigate new magnetic 3d and even magnetic 4d systems. Among these nonalloying systems are the extreme cases of local magnetism.

The recent developments in this field include :

(i) the observation of magnetic Sc ions in metallic hosts
(ii) the finding of ionic-type (including LS-coupling) magnetism for Fe ions in sp metal hosts
(iii) the observation of large local magnetic moments ($\geq 5\ \mu_B$) for 4 d ions in metals, and
(iv) the finding of strongly magnetic 4d ions in semiconductors.

In nonalloying systems, the implanted d ions often occupy substitutional and interstitial lattice sites with – depending on the host matrix – strongly different lattice site distributions. These surprisingly clear features offer the chance for aimed studies of magnetism and electronic structure for the substitutional as well as for the interstitial lattice sites.

The experimental results can be compared with theoretical predictions for both substitutional and interstitial lattice sites.

Magnetic Viscosity and Magnetisation Processes in Thin Films

R Street, Research Centre for Advanced Mineral and Materials Processing, Department of Physics, The University of Western Australia, Nedlands, WA 6009

Abstract

The parameters remanent magnetisation M_{rem} and coercivity H_c are derived from hysteresis loops. Since the discovery of magnetic hysteresis by Ewing in 1881 many attempts have been made to account for the observed values of M_{rem} and H_c in terms of elementary domain structures. Hysteresis is the consequence of the occurrence of domain structures that are in metastable equilibrium. The holomagnetic parameters M_{rem} and H_c are thus determined by the behavior and properties of microscopic metastable domain structures. Studies of these microscopic processes can provide information of value in designing magnetic materials for specific applications.

The activation energy required to initiate an irreversible transition from a metastable to a stable domain configuration can be provided by thermal activation. Experimentally this is observable as a time dependence of magnetisation M(t) at constant applied magnetic field, H_a. This phenomenon is known as magnetic viscosity or magnetic after effect. The results of observations of magnetic viscosity are conventionally presented in the form of M(t) vs lnt graphs where the origin of time is the time at which H_a is stabilised at its fixed value. The form of these graphs is determined by the activation energy function f(E), where f(E)dE = the number of metastable domain configurations which have activation energies lying between E and E + dE.

The analysis of the time dependent behaviour of a magnetic system for which, at a fixed field, changes in irreversible magnetisation are controlled by a single value of activation energy is particularly simple. I shall show that the value of a particular viscosity parameter, the fluctuation field, may be derived from sets of M(t) vs lnt data obtained under constant H_a conditions. This parameter may be directly related to the volume of material participating in the activation process, refeered to as the activation volume v_{ac}.

I have applied this analysis to data obtained by magneto optical magnetometry using TbFeCo films. For one film it was found that the value of the fluctuation field was constant at the one per cent level over more than 90% of the magnetisation of the film. For this film all the M(t) vs lnt, taken at different values of H_a fit on a single universal curve. The activation volume involved in domain magnetisation reversal is 5.3×10^{-18} cm^3. The changes in domain structures of the TbFeCo film during magnetic viscosity were followed by polarised light microscopy. It appeared that magnetisation was proceeding almost entirely by growth at the periphery of existing regions of reversed magnetisation.

I shall discuss a model in which it is assumed that magnetisation proceeds by reversal of magnetisation of single domains of average volume V. Magnetisation reversal is initiated by activation of nuclei of reversed magnetisation, of volume v_{ac} within each domain. The activation volume, v_{ac} is very much smaller than V. This model is of potential value as a pointer to the achievement of desirable improvements in magneto-optic recording media.

Finally I will consider the possible fractal nature of the growth of regions of reversed magnetisation in thin films of magnetic materials generally.

LOW TEMPERATURE MAGNETIC ORDERING OF A SERIES OF STRUCTURALLY CHARACTERISED CHLOROFERRATES

J Liesegang, B D James, M Bakalova, La Trobe Univ., Melbourne, W.M. Reiff, Northeastern Univ., Boston, USA, A.H. White, Univ. of Western Australia, Perth.

Iron-57 Mössbauer spectroscopy results are presented for a new series of related chloroferrate crystalline salts of complex ammonium cations. In particular, spectra of materials based on $FeCl_4^-$, $FeCl_5^{2-}$, $FeCl_6^{3-}$, $[FeCl_5(H_2O)]^{2-}$ and $[FeCl_5(CH_3OH)]^{2-}$ anions are discussed relative to the systematics of their isomer shifts, coordination numbers and 3D ordering at low temperatures.

The following specific systems have been studied by Mössbauer spectroscopy and have been definitively characterised by single crystal X-ray studies:

A $[CH_3NH_3^+]_4[FeCl_6][Cl^-]$ B $[Me_2N(\mu\text{-}CH_2CH_2)_2NMe_2^+][FeCl_5^{2-}]$

C $[H_3NCH_2CH_2NH_3^{2+}][FeCl_5.H_2O^{2-}]$ D $[NH_3(CH_2)_6NH_3^{2+}]_4[(FeCl_6^{3-})(FeCl_4^-)(Cl^-)_4]$

The spectral data for these complexes are discussed in the light of previous studies for systems such as E: $K_2[FeCl_5.H_2O]$ and $[Co(NH_3)_6][FeCl_6]$ N,N'-dimethyltriethylenediammonium pentachloroferrate; and the related salt F: $[FeCl_5CH_3OH]^{2-}$.

The approximate critical 3D ordering temperatures have been measured as follows:

A 1.45 K B 6.8 K C 3.45 K D <1.22 K

References

1. J.H. Zhang, W.M. Reiff, J.H. Helms, W.E. Hatfield, N. Dixon and L. Fritz, Inorg. Chem., 25 (1986) 2936.
2. M.C. Moron, F. Palacio, R. Navarro, J. Pons, J. Casibo and R.L. Carlin, Inorg. Chem., 29 (1990) 842.
3. M.C. Moron, F. Palacio, J. Pons, J. Casibo, K.E. Merabet and R.L. Carlin, J. Appl. Phys., 63 (1988) 3566.
4. A.N. Scoville, K. Lazar, W.M. Reiff and C. Landee, Inorg. Chem., 22 (1983) 3514.
5. R.L. Carlin and F. Palacio, Coord. Chem. Rev., 65 (1985) 141.
6. N.N. Greenwood and T.C. Gibb "Mössbauer Spectroscopy" (Chapman and Hall, UK 1971).
7. J Drummond and J.S. Wood, J. Chem. Soc. Chem. Commun., (1969) 1373.
8. L. Takacs, W.M. Reiff and B.D. James, Hyperfine Interactions 28 (1986) 693.

MECHANICALLY ALLOYED RARE EARTH PERMANENT MAGNETS

L Schultz
Institute for Metallic Materials, IFW Dresden and TU Dresden
D-01171 Dresden, Germany

Mechanical alloying is applied to prepare Nd-Fe-B, Sm-Fe-*TM* type (*TM*: V, Ti, Zr), and interstitial nitride and carbide permanent magnets. Starting from elemental powders, the hard magnetic phases are formed by milling in a planetary ball mill and a following solid state reaction at relatively low temperatures. For Nd-Fe-B, the magnetically isotropic particles are microcrystalline, show a high coercivity (up to 16 kA/cm for ternary alloys and above for Dy-substituted samples), and can be either used for making bonded magnets or compacted to dense isotropic magnets by hot uniaxial pressing. Magnetically anisotropic samples with a remanence up to 1.32 T and an energy product up to 333 kJ/m^3 are formed by die-upsetting. The mechanical alloying process has also been applied to prepare magnetic material of other Sm-Fe-*TM* phases providing material with high or ultrahigh coercivities (up to 51.6 kA/cm for Sm-Fe-Ti). Most promising are the interstitial nitrides or carbides of the 2:17 or the 1:12 phases. Magnetically isotropic microcrystalline $Sm_2Fe_{17}N_\chi$ samples with coercivities up to 24 kA/cm were prepared by mechanical alloying and a two-step heat treatment. Their remanence and energy product are equivalent to similarly prepared Nd-Fe-B samples, but their properties at elevated temperatures are superior because of the high Curie temperature of 470°C and the large anisotropy field of 22 T. Also for $Sm_2Fe_{17}C_\gamma$ and 1:12-type Nd-Fe-V-N, coercivities of 18.5 or 6 kA/cm, respectively, were achieved.

PREPARATION AND PROPERTIES OF TWO-PHASE EXCHANGE COUPLED NANO-COMPOSITES

D. Sean Geoghegan, R. Street

Research Centre for Advanced Mineral and Materials Processing,

Dept. of Physics, The University of Western Australia, Nedlands WA, 6009

and P. G. McCormick

Research Centre for Advanced Mineral and Materials Processing

Dept. of Mechanical and Materials Engineering, The University of Western Australia, Nedlands WA, 6009

An investigation into the exchange interaction between antiferromagnetic-ferromagnetic phases in composites prepared by mechanical alloying has been undertaken. CoO/Co, FeS/Fe and NiO/Ni composites were prepared by mechanical alloying and subsequent heat treatments, resulting in nano-scale structures. Solid phase analysis was conducted using x ray diffraction and the magnetic properties measured using a vibrating sample magnetometer. The effect of heat treatment on the properties was examined, and the magnetic behaviour attributed to exchange coupling was determined to be dependent on the heat treatment temperature. Strong evidence for exchange coupling was the observation of a discontinuity in the remanent magnetization at a temperature corresponding to the Néel point of the antiferromagnetic phase.

TIME-DEPENDENT ATOMIC DISPLACEMENTS IN SOLID STATE DIFFUSION.

J.B.H.Baker, C.J.Girard and C.A.Sholl
Physics Department, University of New England, Armidale, NSW 2351

Crystalline solids always contain point defects which diffuse through the crystal at a rate dependent on temperature. In some systems defects can also be produced by doping or by introducing a species at the surface which diffuses into the bulk of the crystal. Such solid state diffusion influences many physical properties of materials and it is the basis of some practical devices such as solid state batteries and metal-hydrogen systems for storage of hydrogen as a fuel.

There are several types of point defects and diffusion mechanisms but only the most common one, the vacancy mechanism, will be considered here. At low concentrations of vacancies, each vacancy will undergo a random walk amongst the lattice sites, in which it it exchanges places with a neighbouring atom at each step. The time-dependent displacement of a vacancy is therefore easily obtained from random walk theory. The quantity of most interest though is the time-dependent displacement of an atom and this is not a random walk.

At low concentrations of vacancies, each vacancy will, on average, exchange places with a particular atom several times before diffusing away. This sequence of interchanges is an atom-vacancy encounter and the atom is displaced by $\mathbf{l}$ with probability $W(\mathbf{l})$ as a result of the encounter.The atomic diffusion then proceeds by successive encounters with different vacancies and the diffusion is a random walk of encounters.

An integral expression for $W(\mathbf{l})$ was obtained by Sholl(1992) using recurrence relations, Fourier transforms and lattice generating functions. The present work is the corresponding analysis of the time dependence $W(\mathbf{l},t)$ of an encounter. This analysis is aimed at determining the range of validity of the encounter concept and providing the analytical basis for interpreting experimental data on solid state diffusion obtained by methods such as nuclear spin relaxation.

Reference

Sholl C.A. 1992 Phil.Mag.A 65 749-62.

The Study of Transient NMR Effects by Use of Statistical Tensor Formalism

L.N.Shakhmuratova
Kazan State Pedagogical Institute, Kazan, 420021,Russia

The fruitfullness of statistical tensor (ST) formalism in study of transient NMR and NMR on Oriented Nuclei (NMRON) is demonstrated. The approach developed in this work comes from the theory of perturbed angular correlations. On this basis the concatenation of perturbation factors for multipulsed excitation of a spin-system is established. The first application of the method has been realized in multipulsed NMR in the angular distribution of γ-radiation from oriented nuclei, where the dynamics of the second rank ST is dominant, according to the experiments from the Canberra NMRON group. The following transient NMR effects are examined by use of the developed ST formalism:

1. Formation of spin-echo in perturbed angular distribution (PAD) of γ-radiation from oriented nuclei under combined magnetic dipole and electric quadruple interactions (EQI) (equidistant and nonequidistant energy levels);the dynamics of the second rank ST is investigated.

2. Formation of the nuclear spin-echo for the first rank ST, detected in conventional NMR and PAD of β-radiation, under combined interactions; these well known results are demonstrated from the point of view of calculations without reference to a definite spin-value; the phenomenon of phase independence under magneto-acoustic excitation is investigated.

3. Oscillatory free induction decay under pure magnetic dipole interaction as well as when a small EQI is present.

4. Cumulative echo, when the accumulation of spin-echo amplitude occurs under multipulsed excitation by rf pulses of small area.

The study of other transient effects also demonstrate the ST approach to be profitable, bringing results in algebraic form, which enables express analysis of the forming signal without any preliminary calculations for a definite spin value. Irreversible relaxation can be also taken into account.

ELECTRONIC STUCTURE OF GRAPHITE, DIAMOND-LIKE AND GRAPHITIC AMORPHOUS CARBON

Peter Storer, Shane Canney, Robert Caprari, Steve Clark, Maarten Vos, Erich Weigold
Electronic Structure of Materials Centre, Flinders University of South Australia, GPO Box 2100, Adelaide 5001, South Australia

We have constructed an electron momentum spectrometer that is capable of measuring the spectral momentum density of thin free standing films using (e,2e) coincidence spectroscopy.[1] This spectrometer is the first to measure a wide range of target electron binding energies (0 to 40 eV) and momenta (0 to 3 a.u.) in parallel. The resulting count rate (of up to 6 Hz), energy resolution (1.3 eV) and momentum resolution (0.1 a.u.) is significantly better than for earlier spectrometers,[2,3,4] allowing the electronic structure of target materials to be determined with considerable detail.

Recent measurements on amorphous carbon have put a new perspective on the detailed nature of the bonding in this material, which is reflected on the electronic stucture.[5] Studies of evaporated and diamond-like amorphous carbon have shown that the bonding structure in diamond-like amorphous carbon is more random than that of evaporated amorphous carbon, but there is less evidence for diamond-like structure than implied by other methods of characterisation.[6,7] Measurements on highly oriented pyrolitic graphite are currently underway and these will explicitly determine the confidence with which these experimental results can be correlated with the theoretical spectral momentum density, which is well known for graphite.

Experiments in the near future using this new spectrometer will include studies of amorphous silicon, fullerenes and crystalline silicon.

1. P Storer, R S Caprari, S A C Clark and E Weigold, submitted to Rev Sci Instrum
2. A L Ritter, J R Dennison and R Jones, Rev Sci Instrum, **55** (1984), 1280
3. K J Nygaard, Y Chen, J Lower, P Storer and E Weigold, Microsc. Microan. Microstr., **2** (1991), 377
4. S Dey and J Williams, J Phys D: Appl Phys, **21** (1988) 18
5. A S Kheifets, J Lower, K J Nygaard, S Utteridge, M Vos, E Weigold & A L Ritter, to be published, Phys Rev B, (1994)
6. P Storer, PhD Thesis, Flinders University (1993)
7. D R McKenzie, D Muller and B A Pailthorpe, Phys Rev Lett, **67** (1991), 773

CROSS SECTIONAL IMAGING OF SINGLE CRYSTAL MATERIALS BY ION BEAM ANALYSIS.

David N. Jamieson, MARC, School of Physics, University of Melbourne, Parkville, 3052.

The technique of Nuclear Microscopy, utilizing a focused ion probe of typically MeV H^+ or He^+ ions, can produce images where the contrast depends on typical Ion Beam Analysis (IBA) processes, such as Rutherford Backscattering Spectrometry (RBS). The probe forming lens system usually utilizes strong focusing, precision magnetic quadrupole lenses and the probe is scanned over the target to produce images. If the specimen under analyis is a single crystal and the incident ion beam is aligned with a major crystal axis, then images can be produced from variations in yield from regions of differing crystal quality. This technique is known as Channeling Contrast Microscopy (CCM) [1]. The lateral spatial resolution of the images, equal to the diameter of the focused probe, can be as small as1 μm.

Owing to the relatively deep penetration of the incident ion beam into the crystal, it is possible to map image buried features. For MeV He^+ ions these may be up to 1 μm deep below the surface. For MeV H^+ ions these may be about 10 μm deep. The depth resolution with RBS is typically between 20 and 200 nm. Recently it has been demonstrated that it is possible to construct cross sectional images from the RBS signal [2-4]. This method has been called 'RBS tomography'. Applications have included the imaging of buried Ge layers, 1.6 μm thick buried under a cap layer of SiO_2 1.2 μm thick as well as the effect of annealing these layers. However, owing to the variation in the kinematic factor of the various different elements in the layers, considerable image processing was necessary to remove artifacts.

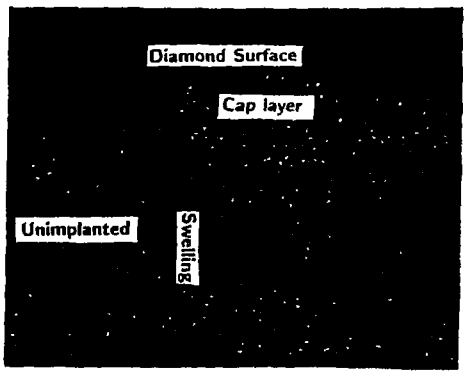

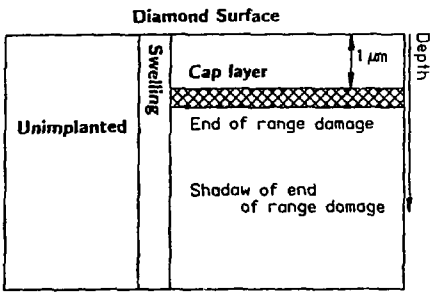

RBS tomography image of a 4 MeV As implanted diamond.

In CCM, the specimen to be imaged can consist of just one element. Therefore tomographic images can be produced that are free from artifacts caused by having more than one element in the specimen. Presented here are images produced by RBS tomography to image the damage produced by MeV As implantation into C, growth defects in HgCdTe microelectronic devices and inclusions in naturally occuring iron pyrite crystals. The new imaging method is very useful for providing an overview of the cross sectional structure of these materials.

[1] D.N. Jamieson, R.A. Brown, C.G. Ryan and J.S. Williams, Nucl. Instr. Meth., B54 (1991) 213.
[2] M. Takai, Y.Katayama and A. Kinomura, Nucl. Instr. Meth., B77 (1993) 229.
[3] A. Kinomura, M. Takai, S. Namba, M. Satou and A. Chayahara, Nucl. Instr. Meth. B45 (1990) 536.
[4] A. Kinomura, M. Takai, S. Namba, M. Satou and A. Chayahara, Nucl. Instr. Meth. B54 (1991) 275.

FREE RADICALS IN RED WINE, BUT NOT IN WHITE?

G J TROUP[1] D R HUTTON[1] D G HEWITT[2] C R HUNTER[3]

[1] Physics Department, [2] Chemistry Department, [3] Anatomy Department,
Monash University, Clayton 3168, Victoria, Australia.

Wine is clearly "condensed matter".

On reading the report of the inhibition of lipid oxidation by red wine phenolics[1], we recalled that polyphenolics can stabilise free radicals quite well, so a programme was set up to test for them, using Electron Spin Resonance (ESR) spectroscopy[2].

A Varian X-band (9.1GHz), E-12 spectrometer, capable of detecting ~ 10^{11} spins of 1 gauss linewidth, in a volume of 0.15 mL, working at liquid N_2 temperature to avoid microwave polar losses in water, was employed.

Initially, a red wine (Brown Bros., 12L. cask) and a white (Tisdall, 12L. cask), were used at their normal concentration. No free radical signal was observed. 25mL samples were then cold vacuum evaporated to ~ 1/10 of their volume, and the resulting rather syrupy liquids examined. Both samples showed Mn^{2+} signals, but only the red wine sample showed a free radical signal. The red wine had been fermented on oak, the white had not. However, a red wine not fermented on oak (Mitchelton Winery's Cab Mac) gave both Mn^{2+} and free radical signals; a semillon (Yaldara) which had been oak aged also gave both these signals.

Concentrated glycoside extracts of both red (shiraz) and white (semillon) grape juices were prepared by a standard technique[3], and examined by ESR. The red extract gave the ESR signal, the white did not. This shows that the free radical is already present in *detectable* amounts in the original red 'berry' juice, but not in white.

Treatment of red wine with cross-linked polyvinyl polypyrrolidine reduced the free radical signal by ~ 80%, showing the signal was associated with the removed polyphenolics. When a model wine containing only catechin as phenolic was allowed to oxidise slowly, the appropriate free radical signal appeared. It is suggested that the radical, with $g = 2.0038 \pm 0.0001$ and linewidth 2.0 ± 0.1 gauss, is on the B-ring of the catechin.

REFERENCES

1. E. N. Frankel, J. Kanner, J.B. German, E. Parks, J.E. Kinsella.(1993) *The Lancet* **341**; 454-57.
2. D. J. E. Ingram. (1969) *Biological and Biochemical Applications of Electron Spin Resonance*. Adam Hilger: London.
3. P.J. Williams, C.R. Strauss, B. Wilson, R.A. Massey-Westrop (1982). *Journal of Chromatography*; **235**; 471-480.

RESEARCH CENTRES AND SCIENCE POLICY

Ditta Bartels
Director of European Affairs, Vice Chancellors Unit, University of NSW
and
Immediate Past President of FASTS

This talk will examine the relationships between Australian Research Centres, with some emphasis towards Cooperative Research Centres (CRC's), and Science Policy. The CRC's are still in their formative years but what are the emerging trends? What, also, can Scientists and Technologists do to capitalize on the new found interest in a strategic vision for science and industry as recently promulgated by the Opposition Leader, Dr Hewson?

SEMICONDUCTOR NANOSTRUCTURE FABRICATION FACILITY

R G Clark
School of Physics, University of NSW, Kensington, NSW, 2033

The establishment of a fabrication facility located at the University of New South Wales to develop prototype semiconductor nanostructure devices has been supported by a major 1994 ARC Mechanism C Grant ($1M) and matching funding from the participating universities – University of New South Wales, University of Sydney, Macquarie University and University of Technology, Sydney. The facility will incorporate two leading-edge nanofabrication tools procured via an ARC Collaborative Research Grant, that will be delivered in 1994: an ultra-fine-line electron beam lithography machine (2 nanometre spot size) for nanofabrication and a combined scanning electron/scanning tunneling microscope both for imaging nanostructures and for carrying out advanced fabrication steps. The new nanofabrication facility will be combined in a clean room environment with personnel and equipment relocated from the existing UNSW Microelectronics Laboratory to provide capabilities at both micron and submicron levels for various applications.

The facility will carry out frontier research activity in the area of semiconductor nanostructures, using high resolution tools specifically designed to develop advanced prototype test structures. It represents a complementary activity to an initiative to establish a major national facility which will have a wider, commercial brief incorporating molecular engineering and new materials and semiconductor growth and processing equipment selected for device production. The entry of universities into this strategic area in advance, at a level commensurate with Mechanism C, will provide a prepared and involved scientific community active in nanotechnology and will build experience that will be instrumental in providing the step-up to a full national effort with a commercial focus at a later stage.

APPLICATIONS OF SYNCHROTRON RADIATION TO MATERIALS SCIENCE AND THE AUSTRALIAN NATIONAL BEAMLINE FACILITY AT THE PHOTON FACTORY

Stephen Wilkins
CSIRO, Division of Materials Science and Technology
PMB 33 Rosebank MDC, Clayton, Victoria 3169

The use of synchrotron radiation to probe the structure and composition of matter is one of the most exciting and rapidly developing fields of science at the present time. The present talk will explore some of these possibilities and also give a guide to the various capabilities and opportunities for SR studies using the newly operating Australian National Beamline Facility at the Photon Factory in Tsukuba, Japan. Some of the first results from the facility will be presented.

UNEXPECTED OBSERVATIONS IN METALS AT VERY LOW TEMPERATURES

G Eska
Physikalisches Institut, Universität Bayreuth, Bayreuth, Germany

In polycrystalline metallic samples sound velocity and sound attenuation was measured by P Esquinazi and coworkers. In the temperature range (100 μK < T < 100 mK) the acoustic properties are similar to what is known for amorphous materials at higher temperatures. We report on vibrating reed experiments on Ag, Ta and NbTi. We also report on NMR experiments which we performed under conditions of high nuclear spin polarization ($p \sim 0.5$; T < 1 mK; B < 1 T). As a result from high polarization, strong dipolar and/or indirect exchange fields cause considerable nonlinear corrections to the dynamics of the nuclear magnetization. Additional complications arise in metals because of the spatial variation of the nuclear magnetization due to the finite penetration depth of the rf-field. The consistent description of a pulsed NMR experiment at low temperatures is therefore based on the solution of the coupled system of Bloch's and Maxwell's equations. The NMR line shape is strongly affected by size and sign of the interaction between the nuclear spins. We show that nonlinear spin dynamics causes line splitting in the NMR of T1 and the formation of multiple spin echoes in the intermetallic compound $AuIn_2$.

EDGE PHONOCONDUCTIVITY IN A MAGNETICALLY QUANTISED TWO-DIMENSIONAL ELECTRON GAS

A. J. Kent
Department of Physics, University of Nottingham, University Park
Nottingham NG7 2RD, England

We have carried out an experimental investigation of the scattering by acoustic phonons of electrons in edge states of a magnetically quantised two-dimensional electron gas (2DEG). A phonoconductance imaging technique has been developed and was used to probe the spatial and magnetic field dependence of the phonon scattering of electrons in a GaAs device. It was discovered that a response was observed only when phonons were incident at the edge of the 2DEG. Giant oscillations in the phonoconductance with magnetic field were observed, these were periodic in $1/B$ and changed sign when the field was increased beyond 1.3T. At low field the oscillations were negative, i.e. phonon scattering caused a decrease in conductance, whereas at high field the oscillations become positive. These results are described theoretically by considering the changes in group velocity of the edge electrons upon absorbing a phonon which modifies their energy and wavevector. Assuming a sharp edge potential, an important parameter in the theory turns out to be the product of the phonon momentum component parallel to the edge and the magnetic length. If this parameter is greater than unity, then interedge state transitions leading to a decrease in electron group velocity produce the dominant effect, a decrease in conductance. However, if it is less than unity, only intraedge state transitions can take place giving rise to an increase in group velocity and hence an increase in conductance. In the more realistic case of a smooth edge potential the explanation of the results remains qualitatively the same, except that the field at which interedge state transitions are no longer possible is increased in line with the greater spatial separation of the edge channels. This makes it possible to use our data to estimate the potential gradient at the device edge. It is also demonstrated that the spatially resolved phonoconductance measurements can be used to probe the electron concentration as a function of position and the charge separation connected with the Hall effect is determined for our sample.

The freezing of 2D electron liquid in a random potential

J.S.Thakur and D. Neilson
School of Physics,
University of New South Wales,
P.O.Box 1 , Kensington
N.S.W. 2033, Australia .

Abstract

The solidification of the pure electron liquid into a wigner crystal is the subject of much experimental investigation at the moment. The electron liquid of high mobility is trapped at the interface of a gallium arsenide - gallium aluminium arsenide semiconductor heterostructure. At sufficiently low density the liquid should crystallise at low temperature $\leq$ 1K.

There is increasing experimental evidence that the presence of very small levels of defects in the underlying semiconductor substrate can increase by a factor of five or more the density at which the electron liquid solidifies. It is possible that this defect induced solid may be a wigner glass rather than a wigner crystall.

We have used a model based on the Mori memory function formalism to study the electron glass- transition of a two-dimensional electron liquid interacting with random potential. The model provides a closed non-linear equation for the self-consistent treatment of the density fluctuation in terms of the relaxation kernel . In the $t \rightarrow \infty$, the non-zero solutions of the density fluctuations are achieved either by varing the strength of coulomb interaction or the random potential. The isotropic non-zero solution is identified as an order parameter of the glassy phase of the system.

HOW DO THE OXIDES AND FULLERIDES SUPERCONDUCT ?

M. P. Das

Department of Theoretical Physics
Research School of Physical Sciences
The Australian National University
Canberra, ACT 0200

Superconductivity was discovered by Kammerlingh Onnes in Leiden in 1911. Seventy five years later Bednorz and Mueller found that doped lanthanum cuprate (an oxide) exhibit high temperature superconductivity. Their discovery created unprecedented excitements all over the world. Further to this alkali doped fullerines joined the family of high T_c superconductors. Although there is a great deal of activities in this field, yet no clear consensus seems to exist on how these novel materials superconduct.

In this talk an effort will be made to present some of our current theoretical understanding. Several basic experimental results, which are considered anomalous, will be discussed. Models dealing with strong electronic correlations will be presented as candidates for understanding high T_c phenomena.

TM 05

THE HOLE-HOLE SUPERCONDUCTING PAIRING IN THE t-J MODEL INDUCED BY THE LONG-RANGE SPIN-WAVE EXCHANGE

V.V.Flambaum, M. Yu. Kuchiev* and O. P. Sushkov†

School of Physics, The University of New South Wales

P.O.Box 1, Kensington, NSW 2033, Australia and

**A.F.Ioffe Physical-Technical Institute, 194021 St. Petersburg, Russia*

†*Budker Institute of Nuclear Physics, 630090 Novosibirsk, Russia*

The interaction of holes with magnons in 2D is shown to create the strong pairing of holes. The parameters describing the problem are taken from the 2D t-J model which is related to high-T_c superconductivity. There appears the superconducting gap $\Delta_{\mathbf{p}}$

$$\Delta_{\mathbf{p}} = C\ \mu\ \exp(-1/g)\ \sin\varphi_{\mathbf{p}}\ ,$$

where the constant C is a numerical factor, $C \approx 1$, μ is the chemical potential, g depends on the coupling constant f of magnon-hole interaction and two masses $m_1 < m_2 (m_i \equiv m_i/m_e)$ describing the hole dispersion near the minimum of the band:

$$g = (2\Lambda f^2/\pi)\ \sqrt{m_1 m_2}\ (\sqrt{m_2/m_1} + 1)^{-2}.$$

The parity of a superconducting pair is positive in spite of the dipole angular dependence $\sim \sin\varphi_{\mathbf{p}}$ of the gap.

Note two important points. First, the nonexponential factor in $\Delta_{\mathbf{p}}$ is very large, $\sim \mu$, due to the large velocity of the magnons, which is larger than the velocity of holes. Second, there has been found the strong attraction $\sim -1/r^2$ between the holes caused by magnon exchange [1]. It leads to the "collapse" effect, which results in an increase of the effective interaction between the holes. The "collapse" gives the additional factor $\Lambda > 1$ in g. As a result of both these effects the gap is very large, $\Delta_{\mathbf{p}} \sim \mu$. The numerical solution of the BCS equation with the potential arose from magnon exchange is fulfilled. It gives $max\Delta_{\mathbf{p}} = 0.7\mu$ and $T_c = 0.5 max\Delta_{\mathbf{p}} = 0.35\mu$. The approach developed requires the antiferromagnetic order to exist at least in the region of distances as large as $1/p_F$.

[1] M.Yu.Kuchiev, O.P.Sushkov. Physica C **218**, 197-207 (1993)

FABRICATION AND PROPERTIES OF LONG Bi2223 Ag-SHEATHED SUPERCONDUCTING TAPES

S.X. Dou, H.K. Liu, R. Bhasale, Q.Y. Hu, J. Yau, M. Ionescu, N. Savvides*, C. Andrikidis*, K. Muller*, E. Babic and I. Kusevic****

Centre for Superconducting and Electronic Materials,
University of Wollongong, Northfields Av. 2522,
Wollongong, Australia
* CSIRO Division of Applied Physics, Lindfield, NSW 2070, Australia
** Department of Physics, University of Zagreb, 41001, Zagreb, Croatia

Abstract

Long length Ag-sheathed Bi-based superconducting single and multifilamentary tapes up to 45 meters have been fabricated using powder-in-tube technique. A I_c up to 15 A and J_c of 8,500 A/cm^2 at 77 K over the entire length has been achieved. For short multifilament tapes, a J_c of 17,200 A/cm^2 at 77 K and 140,000 A/cm^2 at 4 K has been achieved in zero field and weak links are improved. Multiprobe measurements for a tape show that the J_c is rather uniform along the length of the tapes with a variation of 10%. The critical strains for bend tests show a dependence on the tape thickness, the number of filaments and Ag/oxide volume ratio, attributable to the improved strength and flexibility of the special interfacial layer between Ag and oxides formed during the thermomechanical processes. The results of magnetoresistance and the V-I curves of a well defined tape after correction for the parallel conduction through the Ag-sheathing and the core show a similar behaviour as single crystals and the epitaxial thin films. The effective activation energy for the flux creep is larger than those for the single crystals and thin films. The effect of mechanical deformation on the J_c will be discussed.

The authors gratefully acknowledge to Metal Manufactures Ltd. and Commonwealth Department of Industry, Technology and Commerce for financial support.

LONG-LENGTH HIGH-T_c SUPERCONDUCTOR PROCESSING, PROPERTIES AND APPLICATIONS

E.W. Collings
Battelle, Columbus, OH 43101, USA

A review is presented of the present status and future prospects of Bi:2212 and Bi:2223 powder-in-silver-tube (PIT) high-T_c superconductors (HTSCs). Both monocore tape and multicore (or multifilamentary) strands are considered. Until recently most HTSC development has focussed on the processing of short lengths of monocore tape, but only as a stepping stone towards the fabrication of long continuous lengths of twisted multifilamentary strand. For operation in the liquid-nitrogen (LN) temperature range the Bi-base material of choice is the 2223 phase. But until improvements in flux pinning materialize LN-cooled Bi:2223 will be restricted to moderate-field applications such as power transmission cables and relatively low-field magnets; of course, operation at intermediate temperatures between 4 K and 77 K is being considered. On the other hand there is a clear need for advanced high-field 4 K superconductors. All the materials presently in use or being considered – Nb_3Sn, Nb_3Al, the laves- and chevrel phases, etc – are brittle compounds that require reaction after winding. In such a context the Bi-materials with their enormous 4 K upper critical fields start to look very attractive. Both Bi:2223 and Bi:2212 are candidates for 4 K high-field operation. But the latter is preferable since it requires only one heat treatment after being mechanically processed to twisted wire. Progress in Bi:2212 long-length conductor processing worldwide is reviewed. Considered are processing details such as: starting powder, deformation processing to monocore and multifilamentary wires, and final heat treatments. Also considered are the 4 K applications of Bi:2212 PIT strand – e.g. coils and high-field magnets or magnet-inserts.

Growth and Surface Microstructure of Epitaxial $YBa_2Cu_3O_{7-x}$ Thin Films

Nick Savvides and Alex Katsaros

CSIRO Division of Applied Physics, Lindfield, Australia 2070

Superconducting $YBa_2Cu_3O_{7-x}$ thin films, grown epitaxially on crystalline substrates, are the raw materials for superconducting devices [1,2,3]. The mechanisms of nucleation and film growth, and the evolution of microstructure are important factors which determine the final surface morphology, the nature of defects and the transport properties of films.

We use a variety of high resolution microscopy techniques (SEM, STM, AFM), and transport property measurements to study the nucleation and early stages of growth, and the evolution of surface microstructure of epitaxial c-axis $YBa_2Cu_3O_{7-x}$ thin films grown *in situ* on MgO (100) substrates. The results from ultrathin films, 3 to 50 $c_\perp$ unit cells, indicate that epitaxial growth proceeds by the classical screw dislocation mediated three-dimentional island growth mode. Because of the rather large lattice mismatch at the $YBa_2Cu_3O_{7-x}$/MgO interface the films nucleate with a high density of screw dislocations, $\rho_{screw} \sim 10^9 - 10^{11}$ cm^{-2}. Consequently the growth and evolution of the surface microstructure is dominated by the accommodation of depositing species at the ledges of spirals, i.e. each three-dimentional island grows both vertically and laterally by incorporating adatoms at a spirally expanding step emanating from one or more screw dislocations.

1. N. Savvides and A. Katsaros, *Appl. Phys. Lett.* **62**, 528 (1993); *Thin Solid Films* **228**, 182 (1993).

2. N. Savvides, A. Katsaros, C.P. Foley and G.J. Sloggett, in *Advances in Cryogenic Engineering Materials*, **Vol. 40** (Plenum), (in press).

3. G.J. Sloggett, D.L. Dart, C.P. Foley, R.A. Binks, N. Savvides and A. Katsaros, *Supercon. Sci. Technol.* (in press).

The Decoupling Between the Superconducting Layers in $Bi_2Sr_2CaCu_2O_8/Bi_2Sr_2Ca_2Cu_3O_{10}$ Intergrowth Single Crystals

Y. Zhao[1], G.D. Gu[2], and G.J. Russell[2]
[1]School of Materials Science & Engineering, [2]School of Physics, University of New South Wales, P.O. Box 1, Kensington, NSW 2033, Australia

N. Nakamura, S. Tajima, K. Uehara, and N. Koshizuka
Superconductivity Research Laboratory, International Superconductivity Technology Center, 10-13 Shinonome 1-chrome, Koto-ku, Tokyo 135, Japan

A characteristic structural feature of the high-T_c superconducting cuprates is the presence of CuO_2 planes which strongly suggests two-dimensional physical properties. For Bi-Sr-Ca-Cu-O system, the normal-state resistivity ρ_c of BSCCO is several orders of magnitude larger than ρ_{ab}, and $\rho_c(T)$ has a thermally activated temperature dependence similar to that of a semiconductor, thus it provides us with a system where the superconducting layers are separated by a thermally activated resistive layer, bringing about intrinsic Josephson effect [1]. Furthermore, if in considering the thermally activated temperature dependence of $\rho_c(T)$, the Josephson interaction between the CuO_2 bilayers is weakened with decreasing temperature, and thus it is easy destroyed by applying an external field, leading to a three- to two-dimensional crossover of superconducting behaviour [2], or even the restoration of the out-of-plan resistance [3]. We report here that by the systematic measurement of the resistivity, a novel re-entrant phenomenon in the resistive transition for Bi-2212/2223 intergrowth single crystals has been observed: the sample shows a superconducting transition (zero resistance) at 105 K, but it restores to a resistive state at a lower temperature. This phenomenon is interpreted using a model where the Josephson coupling between the CuO_2 *tri*layers is weakened or destroyed by thermal activated resistance between these layers. The two steps in the resistive transition can be explained by the proximity effect along the ab-plane. The effects of the applied magnetic field or large driving current on the re-entrant phenomenon are also investigated.

References

1. R. Kleiner et al., **Phys.Rev.Lett.**, 68, 2394 (1992).
2. N. Nakamura et al., **Phys. Rev. Lett.**, 71, 915 (1993).
3. E. Rodriguez et al., **Phys.Rev.Lett.**, 71, 3375 (1993).

IN-SITU X-RAY STUDY OF FREEZING AND MELTING OF Bi(2212) AND Bi(2223)

D K Finnemore
Ames Laboratory and Department of Physics
Iowa State University, Ames, IA 50011-3160, USA

Hot stage x-ray studies of the melting and freezing of the Bi-based high temperature superconductors has been undertaken in order to provide a science base for the melt-texture processing of high performance tape conductor material that will be used in large scale magnets. The goal of the work is to determine the identity of the phases that form and the kinetics of growth or decomposition of various phases as a function of the important variables controlling the process. The work is complementary to the traditional quench techniques, but it offers the advantage that data are taken at temperature as the processes are occurring rather than looking after the fact. By making measurements at temperature in real-time as phases are growing, rather detailed "road maps" can be constructed for the processing.

Magnetic Properties of Y124 and Bi2212 Superconductors.

Naoki Koshizuka
Superconductivity Research Laboratory, ISTEC
1-10-13 Shinonome, Koto-ku, Tokyo 135, Japan

The novel physical properties of high-Tc superconductors in the normal and mixed states are closely related with their microscopic magnetic (spin) and flux behaviors. The linear temperature dependence of the electric resistivity, for example, is observed over a wide temperature region in the optimumly hole doped systems. However, the downward shift of the resistivity is observed around the "spin-gap" temperatures above Tc in the underdoped systems such as 60K class Y123 and Y124. This shows a clear correlation between the conduction of carriers and the antiferromagnetic spin fluctuation; the decrease of resistivity due to a suppression of the spin fluctuation.

The studies of spin-lattice relaxation rate and Knight shift in Ca-substituted Y124 are reviewed. This shows the enhancement of antiferromagnetic fluctuation with increase of the hole carrier concentration in the CuO_2 plane.[1] This is consistent with the occurrence of spin-singlet RVB state in the phase diagram proposed by Fukuyama et al.[2]

The correlation between the local phonon anomaly and the spin-gap formation is also discussed.

The second topic in this presentation is on the flux behaviors of Bi 2212. The behaviors of vortices and critical current densities of Bi 2212 single- and multi-crystals under different fields and temperatures are reported.

The field induced 3D-2D crossover of shielding current path in the field nearly parallel to the a-b plane are explained by the surface barrier effect on the flux penetration.[3]

The direct observation of vortex lattice by means of small angle neutron diffraction gives us much information on the correlation of the inter- and intra-plane pancake vortices in Bi 2212 single crystal. From the intensity variation of diffraction spots, it turns out that the decouping between the inter-plane pancakes takes place at about 40mT.[4] The field is independent of temperature up to ~60K and increases with reduction of the anisotropy brought by oxygen annealing. The decouping may cause the peak effect in the field dependence of magnetization for weak pinning Bi 2212 crystals.

The flux pinning behaviors in the small angle grain boundaries observed by the magneto-optical flux observation technique are discussed based on the microscopic crystalline morphology of the grain boundaries.[5]

References

[1]T. Machi et al.: Proc. 6th Int. Symposium on Superconductivity (Hiroshima, 1993).
[2]Y. Suzuyama, Y. Hasegawa, H. Fukuyama: J. Phys. Soc. Jpn. **57**, 2768(1988).
[3]N. Nakamura, G. D. Gu, N. Kosizuka: Phys. Rev. Lett. **71**, 915(1993).
[4]J. Ricketts et al.: to be published.
[5]N. Nakamura, G. D. Gu, K. Takamuku, M. Murakami, N. Koshizuka: Appl. Phys. Lett. **61**, 3044(1992).

CHARGE DENSITY WAVE AND WIGNER CRYSTAL INSTABILITIES IN ELECTRON - HOLE SYSTEMS

J. Szymański
Telecom Australia Research Laboratories, 770 Blackburn Road, Clayton, Vic. 3168

L. Świerkowski, D. Neilson
School of Physics, The University of New South Wales, Kensington 2033

Even in the current state-of-art GaAlAs/GaAs heterostructures the two-dimensional electron densities are too high to produce any significant many-body effects. In order to observe highly correlated ground states like Fractional Quantum Hall liquid or Wigner crystal in a single layer it is necessary to apply a very high magnetic field.

We have shown recently [1] that by coupling two or more layers of electrons it is possible to achieve highly correlated states in zero magnetic field at densities much higher than those that are needed in the case of a single layer. This is due to the fact that a second layer can act as a polarisable background for the first one, facilitating the transition to a nonuniform state.

In the mixed system of one layer of electrons and the other of holes the interaction between carriers in different layers is attractive. This attractive inter-layer interaction together with the repulsive interaction within each layer produces large probability of finding electron and hole close to each other. This correlation effect increases the effective interaction. It has been argued that at low temperatures and very low densities of the carriers, electrons and holes may eventually pair together to form excitons which may condense and display a superfluid ground state. Under current experimental conditions the possibility of forming the excitonic condensation is still controversial.

We show that the instability with respect to the formation of the Charge Density Wave ground state takes place at densities ($r_s \approx 5$) and layer separations experimentally attainable. (The dimensionless density parameter $r_s \equiv \sqrt{1/\pi(a_B^*)^2 n}$ where a_B^* is the effective Bohr radius and n is the electron number density.) At lower densities ($r_s \approx 15$) the preferred ground state becomes the Wigner crystal. We obtain this result by calculating the static polarisability of the system, which develops a large peak at the wave vector corresponding to the periodicity of the nonuniform state. The analysis of the pair correlation function confirms that the transition to the nonuniform state is pre-empted by the marked increase of the probability of finding a hole and an electron on top of each other.

[1] L. Świerkowski, D. Neilson, and J. Szymański, Phys. Rev. Lett. **67**, 240 (1991).

STRUCTURAL AND ELECTRONIC PROPERTIES OF $C_{60}H_{36}$

L. E. Hall*, D. R. McKenzie*, A. M. Vassallo†, R. L. Davis‡, D. J. H. Cockayne°
* Dept. of Applied Physics, University of Sydney.
† CSIRO Division of Coal and Energy Technology.
‡ Australian Institute of Nuclear Science and Engineering.
° Electron Microscope Unit, University of Sydney.

The molecule $C_{60}H_{36}$ is a readily prepared hydrogenated derivative of the fullerene molecule C_{60}. As is the case in C_{60} itself, dynamic and/or static disorder in the molecular orientation prevents the use of conventional crystallographic techniques for the determination of the internal molecular structure.

Electron and neutron diffraction patterns have been collected for $C_{60}H_{36}$ and $C_{60}D_{36}$ respectively. We obtain the radial distribution functions (RDF) by Fourier transformation of these diffraction patterns. The RDF can be used to determine the internal molecular structure, even in the presence of orientational disorder. The RDF of three isomeric structures of $C_{60}H_{36}$ were calculated using the Debye formula. When compared with the observed RDF the best fitting isomer was the one of lowest symmetry [1].

Neutrons were used to diffract off $C_{60}D_{36}$, of which deuterium can be observed much more readily than the hydrogen is from the electron diffraction data of $C_{60}H_{36}$. A large discrepancy was found between all predicted models to the experimental RDF of $C_{60}D_{36}$. A further structure proposed by Austin et al. [2] was found to give a better fit than the earlier structures. However, the positions of the deuterium from this model were altered to improve the fit to the experimental RDF.

The electrical properties of $C_{60}H_{36}$ will be presented, which will include resistivity against temperature and photoconductivity. A comparison to the corresponding results of C_{60} will be discussed.

[1]. L. E. Hall, D. R. McKenzie, M. I. Attalla, A. M. Vassallo, R. L. Davis, J. B. Dunlop, and D. J. H. Cockayne, *J. Phys. Chem.*, **97** 5741 (1993).
[2]. S. J. Austin, R. C. Batten, P. W. Fowler, D. B. Redmond, and R. Taylor, *J. Chem. Soc. Perkin Trans. 2*, 1383 (1993).

Surface plasmon observed for carbon nanotubes

L.A. Bursill, J.L. Peng and Steven Prawer
School of Physics, The University of Melbourne, Parkville, 3052, VIC , Australia

and

Pierre A. Stadelmann

Institut Interdepartementale de Microscopie Electronique
Ecole Polytechnique Federale de Lausanne, Ecublens, CH-1015, Switzer land

Electron energy loss spectroscopy and high-resolution images of carbon nanotubes, obtained using a 2nm nanoprobe and energy resolution of 0.5eV, revealed a 15eV surface plasmon for tubes containing $\leq$12 cylindrical graphitic sheets. As the number of sheets increases further the 24eV bulk plasmon quickly dominates the low-loss spectra. It is concluded that carbon nanotubes should be semimetallic, as is graphite. The first few graphitic sheets of nanotube structures act as if they are effectively decoupled electronically. As the radius of curvature increases then the interlayer structures approach the structure of graphite, as do the electronic properties. The present results do not exclude the possibility that the electronic structure of carbon nanotubes is the same as that of graphite, due to the operation of a conformal invariance principle.

This work to appear in Phys Rev B, January 15th, 1994.

ZEEMAN SPECTROSCOPY OF INDIUM ACCEPTOR IMPURITY IN SILICON*

G. Piao, R. A. Lewis and P. Fisher

Department of Physics, University of Wollongong, Wollongong NSW 2522, Australia

The mid-infrared spectrum of indium in silicon exhibits three distinct sets of transitions: the $p_{3/2}$, the $p_{1/2}$, and the Fano series, at approximately 140-160, 190-200 and 200-220 meV, respectively.[1] A recent piezospectroscopic study of these has given accurate values of deformation potential constants for the ground and first three excited states, determined unambiguously the nature of the final states of two close transitions, yielded parameters for the Fano resonances, and investigated the stress behaviour of the latter.[2]

Little has been reported on the magnetospectroscopy of acceptors in silicon. A 0.12 meV resolution study of the $p_{3/2}$ series of Si(B) has been reported by Merlet *et al.*[3] and a study of the $p_{1/2}$ series of Si(B) and Si(Al) was made by Zwerdling *et al.*[4] No Zeeman investigations of Si(In), or of the Fano lines of any system, are known. This is in contrast to several reports on the Zeeman effect in acceptors in germanium, the most recent measurements made using high resolution (0.005 meV) and fields of up to 7 T, revealing all the expected magnetic field induced components and providing reliable values of g-factors.[5]

In the present investigation, the $p_{3/2}$, $p_{1/2}$ and Fano spectra of Si(In) have been studied. A Voigt configuration, with the electric field vector polarised either parallel or perpendicular to the magnetic field, which lies along a <111> crystallographic direction, was employed, with fields of up to 1.5 T. No more detail is seen in spectra taken at 0.013 meV resolution than in those taken at 0.025 meV resolution, the intrinsic widths of the spectral lines being the limiting factor. Different groups of lines show dramatically different behaviour under the application of magnetic field. The transitions $1\Gamma_8^+ \rightarrow n\Gamma_8^-$, which make up the principal lines of the $p_{3/2}$ series, show a very slight broadening (< 0.12 meV FWHM) but no shift in energy. In contrast, transitions to Γ_6^- or Γ_7^- final states show marked splittings. The $p_{1/2}$ transitions are quenched by a moderate field, while the Fano resonances show little change.

Work supported in part by the Australian Research Council and the University of Wollongong Board of Research and Postgraduate Studies.

[1] A. Tardella and B. Pajot, *J. Physique* **43**, 1789 (1982).

[2] G. Piao, *PhD Thesis.* (University of Wollongong, 1992).

[3] F. Merlet, B. Pajot, Ph. Arcas, and A. M. Jean-Louis, *Phys. Rev. B* **12**, 3297 (1975).

[4] S. Zwerdling, K. J. Button, B. Lax, and L. M. Roth, *Phys. Rev. Lett.* **4**, 173 (1960).

[5] P. Fisher, G. J. Takacs, R. E. M. Vickers, and A. D. Warner, *Phys. Rev. B* **47**, 12999 (1993).

Electron Energy-loss Spectroscopy Study of Thermal Annealing of Amorphous Hydrogenated Carbon

Y. Yin, D.R. McKenzie and R.E. Collins

School of Physics, University of Sydney, Sydney, NSW 2006, Australia

Structure changes of annealed amorphous hydrogenated carbon (a-C:H) deposited from d.c. reactive sputtering are identified using the electron energy-loss spectroscopy (EELS) technique. The a-C:H material was heated in vacuum at temperatures up to 500°C. The density (or the mass, if the thickness changes) of the annealed film was estimated via the plasmon peak in the EELS spectrum. It was found that mass loss occurs in the material due to the heat treatment. Plasmon energy for the material is also found to be dependent of the baking temperature. With increase of baking temperature, the plasmon energy first decreases, and then increases. The temperature dependence of plasmon energy conforms that the thickness of the films does not change for heat temperatures up to about 400°C. However, heat treatment at about 500°C results in reduction of physical thickness of this material.

The baking temperature dependence of the degree of sp^2 hybridisation in the films was also studied using the EELS technique. The fraction of sp^2 carbons was determined from the normalised intensity of the π^* feature of the carbon K edge in the manner described by Berger et al.[1]. The deposited film contains about 40% sp^2 carbons, which indicates that the carbon atoms in the as-deposited films present in large fraction of aliphatic coordination. Significant increase of the sp^2 fraction occurs for films baked at temperatures above 350°C. The sp^2 fraction increases to about 100% for the films baked at 500°C. This result supports the idea that aromatisation occurs in the films at temperature above about 350°C.

[1] S.D. Berger, D.R. McKenzie and P.J. Martin, *Philos. Mag. Lett.*, **57** (1988) 288.

THERMAL EXPANSION OF V_3Si WITH CONTROLLED MARTENSITE-PHASE MORPHOLOGY

M. Liu*, T. R. Finlayson* and T. F. Smith†

* Department of Physics, Monash University, Clayton, Vic. 3168

† Vice-Chancellor's Department, La Trobe University, Melbourne, Vic. 3083

Thermal expansion measurements along the tetragonal-phase a and dominantly c axes have been made for a martensitically transforming V_3Si single crystal by using small external stress fields to control the formation of the morphologies of the low-temperature phase microstructure. A low-temperature thermal expansion anomaly was found for both the c and a axis. Based on the new data, it is suggested that the observed pre-/post-transformation anomalies are results of extension of the change in the balance between the lattice and electronic terms around the transformation to the higher/lower temperature ranges, and widely suggested electronic-driven transformation may be traced to the band overlap.

Two Dimensional Antiferromagnetic Ordering in $MnPS_3$

A R Wildes, S J Kennedy*, and T J Hicks

Department of Physics
Monash University
Clayton 3168

*Neutron Scattering Group
Australian Nuclear Science and Technology Organisation
Private Mailbag
Menai 2234

$MnPS_3$ with space group $C\frac{2}{m}$ has a layered monoclinic structure. Within the layers the manganese atoms form a hexagonal net with each manganese atom having three manganese neighbours within the layer. Below 80K the magnetic structure is three dimensional with the antiferromagnetic ordering within the layers coupled ferromagnetically between the layers and the moment direction perpendicular to the layers.

We report the discovery of a truly two dimensional antiferromagnetic ordering in the temperature range 80-130K. This order is not immediately obvious from a neutron powder diffraction pattern as the antiferromagnetic intensity appears as rods rather than spots in reciprocal space and is therefore smeared out in a powder pattern. Preliminary analysis indicates that the moment in the two dimensional structure lies in the layer plane. If this is so it would have to result from a unidirectional rather than planar anisotropy so that the system is described within the Ising model, the only model which will sustain long range magnetic order in two dimensions.

The neutron diffraction data at various temperatures will be presented along with supporting single crystal susceptibility measurements.

ELECTRON SPIN RESONANCE AND INTRINSIC STRESS MEASUREMENTS ON DIAMOND SYNTHESIZED BY PLASMA ASSISTED CHEMICAL VAPOUR DEPOSITION

J. Khachan P.B. Lukins D.R. McKenzie
J.R. Pigott I.S. Falconer B.W. James

School of Physics,
University of Sydney, Australia 2006

Abstract

An inexpensive and simple microwave-produced plasma source has recently been constructed for plasma assisted chemical vapor deposition of diamond thin-films. Electron spin resonance carried out on these films has revealed a P1 point defect structure, commonly found in natural diamond. Argon introduced into the plasma has resulted in the removal of these defects with an accompanying increase in the spin density (due to vacancies), and a dramatic change in the morphology of the film. We have also used Raman Spectroscopy and laser interferometry to measure the change in the intrinsic stress which develops in these films.

An Investigation of Preferential Sputtering from Single-Phase α- and β- Cu/Zn Alloys

D.R. Oliver and T.R. Finlayson

Department of Physics, Monash University, Clayton, VIC 3168, Australia.

Abstract

Evidence for preferential sputtering in binary alloys has been reported. Various compositions of Copper and Zinc have been alloyed to examine the sputtering behaviour of the α- and β- phase regions of the brass system. The relative sputtering efficiencies of the alloy components have been investigated using Atomic Absorption Spectroscopy. The experimental technique is detailed, and the results are examined for evidence of preferential sputtering.

THE INFLUENCE OF CATIONIC AND ANIONIC SURFACTANTS ON BALL MILLED BARIUM FERRITE

S J Campbell*, W A Kaczmarek#, E Wu* and B W Ninham#
* Department of Physics, University College, University of New South Wales, Australian Defence Force Academy, Canberra, ACT 2600
# Department of Applied Mathematics, Research School of Physical Science and Engineering, The Australian National University, Canberra, ACT 0200

Ball milling and related approaches have developed in recent years from a standard technique in powder metallurgy for particle size reduction, to a novel method in the preparation of new materials and phases. This development has been aided by the application of surface active substances in mechanical alloying. The addition of even quite small amounts of organic surfactants has been found to affect the solid state reactions which occur during milling [1].

The magnetic properties of the important magnet $BaFe_{12}O_{19}$ processed by the novel method of surfactant assisted ball milling have been reported recently [2]. Here as an extension of our earlier work [2,3] we present a comparison of the behaviour of $BaFe_{12}O_{19}$ when milled in the presence of cationic and anionic surfactants at pH values above and below point of zero charge (pH ~ 5) of the oxide surface. The structural changes taking place have been monitored by x-ray diffraction and Mössbauer effect measurements (room temperature and 4.2 K). While the behaviour of the cationic and anionic systems at the same pH value are similar, structural changes are discerned between the pH = 3 and pH = 10 systems, particularly the presence of a disordered component in the latter. The overall behaviour is linked with the interfacial properties of the surfactants and their electrostatic interactions with the charged surfaces.

[1] A P Radlinski, A Calka, B W Ninham and W A Kaczmarek, Mater.Sci.Eng. **A134** (1991) 1346

[2] W A Kaczmarek and B W Ninham, IEEE Trans. on Magnetics (in press 1994)

[3] S J Campbell, W A Kaczmarek, E Wu and K D Jayasuriya, IEEE Trans. on Magnetics (in press 1994)

DIFFUSE NEUTRON SCATTERING STUDIES OF SINGLE CRYSTAL SPECIMENS OF $Fe_{3-x}Mn_xSi$

T. Ersez*, S.J. Kennedy†, T.J. Hicks* and H. Kepa‡

* Department of Physics, Monash University, Clayton, Victoria 3168, Australia.

† Australian Institute of Nuclear Science and Engineering, PMB 1, Menai, NSW 2234, Australia.

‡ Physics Department, University of Warsaw, Poland.

Polarized neutron diffuse scattering measurements have been made of two single crystal specimens of the ordered intermetallic compounds $Fe_{2.45}Mn_{0.55}Si$ (at room temperature) and Fe_2MnSi (above and below the re-ordering temperature). The difference between spin-flip and non-spin-flip scattering cross-sections for the (111) position gave a negative diffuse peak around a positive Bragg peak, being more pronounced for the $Fe_{2.45}Mn_{0.55}Si$ crystal. This is consistent with a loss of moment on the B(Fe/Mn) site with addition of Mn. Preliminary model fitting has suggested that Mn atoms cluster on their preferred B-site.

MAXIMUM ENTROPY METHOD STUDY OF THE STRUCTURE OF Mg_2NiD_4 AT 540K USING NEUTRON DIFFRACTION DATA.

E.H. Kisi - Dept. of Mechanical Engineering, University of Newcastle, Callaghan NSW 2308.

Interstitial compounds, such as metal hydrides, characteristically contain one species (hydrogen) widely dispersed over many partially occupied sites. The hydrogen is very mobile and subject to large thermal and diffusional displacements. Conventional crystal structure models consisting of atoms confined to one or more discrete point sets within the unit cell are not always adequate.

Hydrides (deuterides) are generally studied by powder diffraction and have large amounts of line broadening, overlapping lines from pressure tight sample cans and other phases. The complexity of the model is restricted to a spherical, or at best, ellipsoidal distribution about the occupied sites by means of isotropic or anisotropic displacement parameters respectively. The data do not support the determination of higher order (anharmonic) displacement terms.

With single crystal data, the limitations of the model would be overcome by Fourier techniques to recover the actual distribution of scattering density in the unit cell. The small number of well determined reflections in most hydride experiments can lead to large truncation errors and this method is rarely used for metal hydrides. It was recently proposed [1,2] that the Maximum Entropy Method (MEM) can be applied to reconstruct the scattering density in powder diffraction experiments, with greater success for small numbers of observed reflections. In this work Mg_2NiD_4 at 540K has been studied by conventional Rietveld refinement and using MEM.

Mg_2NiD_4 at 540K is cubic (a=6.5221 A with a fluorite arrangement of metal atoms. There is broad agreement between the two techniques over the Ni atom positions, the D distribution and thermal motion in one principal D site. There are however minor differences regarding the one (conventional model) or two (MEM) secondary D sites. Quite unexpectedly, the MEM model also contains large static displacements of the Mg atoms. This observation will be discussed in relation to the D positions and the phase transition to the low temperature monoclinic phase at 507K.

[1] M. Sakata and M. Sato, Acta Cryst. (1990), A46, 263-270.
[2] M. Sakata, T. Uno, M Takata and C.J. Howard, J. Appl. Cryst. (1993), v26

MAGNETIC PROPERTIES OF NOVEL TERNARY PHASE: $Sm_3(Fe_{1-x}Ti_x)_{29}$ $(0.04 \leq x \leq 0.06)$

Hong-Shuo Li and J.M.Cadogan
School of Physics, The University of New South Wales, Kensington, NSW 2033, Australia

Bo-Ping Hu
San Huan Research Laboratory, Chinese Academy of Sciences, P.O. Box 603, Beijing 100080, China

Fu-Ming Yang and B. Nasunjilegal
Magnetism Laboratory, Institute of Physics, Chinese Academy of Sciences, P.O. Box 603, Beijing 100080, China

Jian-Min Xu, H.K.Liu and S.X. Dou
School of Materials Science and Engineering, The University of New South Wales, Kensington, NSW 2033, Australia.

Abstract

The new $Sm_3(Fe_{1-x}Ti_x)_{29}$ compound, which crystallizes in the novel ternary rare-earth intermetallic $Nd_3(Fe_{1-x}Ti_x)_{29}$ structure [1], has been successfully prepared. The powder x-ray diffraction patterns and Scanning Electron Microscope (SEM) micrographs show that the $Sm_{10}Fe_{85}Ti_5$ sample, which was annealed at 1373K for 24 hours followed by water quenching, has a dominant $Sm_3(Fe_{1-x}Ti_x)_{29}$ phase with trace of $Sm(Fe,Ti)_{12}$ impurity. The $Sm_3(Fe_{1-x}Ti_x)_{29}$ compound exhibits ferromagnetic ordering with a Curie temperature T_C= 486 K. The room temperature anisotropy field determined by Singular Points Detection (SPD) is $\mu_0 H_A$= 3.4 T. The Saturation magnetization is M_S= 125 Am^2/kg at 4.2K and M_S= 3.4 Am^2/kg at room temperature, respectively. Powder x-ray pattern of a magnetically aligned sample shows that the $(40\bar{2})$ peak is largely enhanced, which sugests that the easy-magnetzation direction is in the crystallographic b-plane.

References:

1. Hong-Shuo Li and J.M.Cadogan, R.L. Davis, A. Margarian, J.B. Dunlop and P.B. Gwan , This Meeting.

Phase formation at the Fe-rich end of Dy-Fe-Ti system

Jian-Min Xu, Hong-Shuo Li*, J.M. Cadogan*, H.K. Liu and S.X. Dou

Centre for Superconducting and Electronic Materials, the University of Wollongong, Northfields Avenue, Wollongong, NSW 2522, Australia

*School of Physics, University of New South Wales, P.O.Box 1, Kensington, NSW 2033, Australia,

Abstract

A study of the phase formation at the Fe-rich end of the Dy-Fe-Ti system has been carried out by using Scanning Electron Microscopy, Energy Dispersive X-ray Analysis (EDXA), X-ray diffraction analysis and the measurement of Curie temperature. Besides the two well known hexagonal $Dy_2(Fe,Ti)_{17}$ (2:17H) and tetragonal $Dy(Fe,Ti)_{12}$ (1:12T) phases, two new phases have been identified, (a) the orthorhombic 1:12 phase (1:12O) with an unknown crystallographic structure and (b) tetragonal $Dy(Fe,Ti)_{11}$ (1:11) phase with the $CeMn_6Ni_5$-type structure (space group P4/mbm). EDAX gives the ratio of Nd:Fe:Ti of (a) 11.3:84.1:4.6 for 2:17H, (b) 9.0:83.4:7.6) for 1:12T, (c) 8.9:81.9:9.2 for 1:12O and (c) 8.8:76.5:14.7 for 1:11. The structure transforms from Th_2Ni_{17} structure to $ThMn_{12}$ structure, 1:12O structure and the $CeMn_6Ni_5$ structure as a function of the Ti content. An explanation of Ti in stabilising the phases is proposed.

MECHANOCHEMICALLY INDUCED REDUCTION OF ZIRCON SAND

T. Puclin, W.A. Kaczmarek, and B.W. Ninham
Institute of Advanced Studies, Research School of Physical Sciences and Engineering,
The Australian National University, Canberra, ACT

The mechanochemical processing of the mineral zircon ($ZrSiO_4$) is investigated with a view to exchanging the zirconium for other metals, leading to an easily extracted zirconia (ZrO_2) phase. Current processes that are used to decompose zircon to yield zirconia can be divided into thermal and chemical routes. Zircon dissociates at temperatures in excess of 1750 °C; however, on slow cooling a partial recombination of zirconia and silica can occur. New process routes have been developed which overcome this problem; two examples are plasma dissociation followed by rapid cooling, and reduction with carbon at 2000 °C in an electric arc furnace. Zircon can also be decomposed chemically, but only by the use of aggressive reagents and elevated temperatures - two major process routes being alkali fusion and chlorination. Both thermal and chemical routes are expensive, with high specific energy inputs[1].

In this study we show the effects of room temperature ball milling of zircon with calcium and magnesium in dry conditions, and with calcium hydroxide and sodium hydroxide in wet conditions. X-ray powder diffraction, scanning electron microscopy and differential thermal analysis were employed in analysis of as-milled and annealed powders. The results indicate that mechanochemical processing significantly increases the reactivity of zircon in solid state exchange reactions with reducing metals or compounds. The effects of milling time and subsequent heat treatment on structure and morphology of zircon milled with calcium or magnesium in dry conditions, and with hydroxides of calcium or sodium in wet conditions is shown. Milling does not result in spontaneous exchange reactions; however as a result of disordered phase formation in zircon and/or the reducing metal, decomposition of the zircon can be achieved at a relatively low temperature in comparison to reduction of crystalline zircon with carbon. The most significant result of this study was the relatively low temperature range (840 °C - 920 °C) of the thermally activated decomposition of $ZrSiO_4$ dry milled with Ca or Mg metals. These reactions were found to produce crystalline $CaZrO_3$ and ZrO_2 respectively[2].

References

[1] Encyclopedia of Materials Science and Engineering, vol 7, p 5541-6
Edited by M.B.Bever (Pergamon Press, 1986).

[2] T.Puclin, W.A.Kaczmarek, and B.W.Ninham, *Mater.Sci.Eng.* (submitted).

MECHANOCHEMICAL TRANSFORMATION OF HEMATITE TO MAGNETITE : STRUCTURAL CHANGES

S J Campbell*, W A Kaczmarek#, G Wang* and I Onyszkiewicz#
* Department of Physics, University College, University of New South Wales, Australian Defence Force Academy, Canberra, ACT 2600
# Department of Applied Mathematics, Research School of Physical Science and Engineering, The Australian National University, Canberra, ACT 0200

The preparation and properties of iron oxides continue to attract considerable interest and attention because of their importance in magnetic materials technology. Part of the interest also stems from the extra scope that ball milling and related methods brings as an alternative or novel approach to the preparation of new materials and phases. This has been demonstrated recently by the preparation of Fe_3O_4 and γ-Fe_2O_3 powders by the magnetomechanical activation of α-Fe_2O_3 [1].

Here we present an x-ray diffraction and Mössbauer effect investigation of the direct transformation of α-Fe_2O_3 to Fe_3O_4 on wet milling α-Fe_2O_3 powder in low vacuum (~ 10^3 Pa) at room temperature. Excellent agreement is obtained between the two sets of data with the characteristic x-ray diffraction pattern and Mössbauer spectrum of Fe_3O_4 clearly evident after about 25 h milling, leading to complete transformation after milling periods of ~ 100 h. Comparison of the response of α-Fe_2O_3 to milling in a variety of environments suggests that the transformation has a physical rather than a chemical origin with the transformation rate inhibited greatly in the presence of a high oxygen pressure [1]. Details of the α-Fe_2O_3 to Fe_3O_4 transformation in terms of the x-ray patterns and Mössbauer spectra will be presented along with discussion of the nature and mechanism of the transformation.

[1] W A Kaczmarek and B W Ninham, IEEE Trans. on Magnetics (in press 1994)

MAGNETIC PROPERTIES OF NANO-MATERIALS OF $Sm_3(Fe_{1-x}Ti_x)_{29}$ $(0.04 \leq x \leq 0.06)$

Kazi A. Reza, Hong-Shuo Li and J.M.Cadogan
School of Physics, The University of New South Wales, Kensington, NSW 2033, Australia

Abstract

Nano form materials of new $Sm_3(Fe_{1-x}Ti_x)_{29}$ phase has been successfully prepared by splat-quencher. Powder x-ray diffraction patterns show that the samples are virtually amorphous, with trace of the 3:29 crystallites. ^{57}Fe Mössbauer spectroscopy were used to study the hyperfine field at ^{57}Fe nuclei and the Scanning Electron Microscope were employed to study the interesting micro-structure of the annealed samples of $Sm_3(Fe_{1-x}Ti_x)_{29}$.

HYPERFINE MAGNETIC FIELDS OF RARE EARTH SUBSTITUTED FERRIMAGNETICS

R. Ramer[a], M. Ionescu[a], M. Barb[b], L. Diamandescu[c], C.C. Sorrell[a]
a) University of New South Wales, Australia
b) Oklahoma State University, USA
c) Institute of Physics, Romania

Gadolinium and aluminium substituted yttrium iron garnets have easily controlled magnetic behaviour and a relatively narrow resonance linewidth. They are of great technological interest. in design of temperature stable microwave devices. Single phase polycrystalline garnets of the $Y_{3-3x}Gd_{3-3x}Fe_{5-5y}Al_{5y}O_{12}$ *(x = 0.6-1.2; y = 0.10-0.85)* were studied by transmission Mössbauer spectroscopy. The room temperature spectra could generally be resolved in double six-line Zeeman patterns, corresponding to tetrahedral *(d)* and octahedral *[a]* sublattices.

The hyperfine magnetic fields *Ha* and *Hd* were found to decrease with increasing *Al* content, and for a given value of the *Al* concentration, a decrease of the *Ha* and *Hd* values with increasing *Gd* content was observed. The distribution parameters y_a ,y_d of the substituent *Al* ions in the magnetic sublatices were determined; a practically equal *Al* distribution between *a* and *d* sites for each *Gd* content was found for samples with low *Al* concentration. For the higher *Gd* content, the shift to lower values of the *Al* concentration would correspond to equalising of the distribution. It suggests that the presence of *Gd* ions in the garnet structure leads to the *Al* preference for the *d* sites.

References

1. J. Piekoszewski, J. Suwalski, *Proc. ICAME* Tihany, (1969)
2. E. R. Czerlinsky, R. A. MacMillan, *Phys.Stat.Sol.* 41 (1970) p.333
3. T. M. Uen, D. E. Chen, C. C.Dai, P. K. Tseng, *J. Magn. Magn. Mat*, 31-34 (1983) p.789
4. D. Barb, L.Diamandescu, R. Puflea-Ramer, M. Sorescu, D. Tarina, *Materials Letters*, 12 (1991) p.109.

MAGNETIC PROPERTIES OF A NOVEL Pr-Fe-Ti PHASE

Hong-Shuo Li, Suharyana, J.M. Cadogan, G.J. Bowden, Jian-Min Xu+, S.X. Dou+ and H.K.Liu+

School of Physics & +School of Materials Science and Engineering,
The University of New South Wales, Kensington, NSW 2033, Australia.

In a systematic study of the $(Pr_{1-x}Ti_x)Fe_5$ alloy series, the $(Pr_{0.65}Ti_{0.35})Fe_5$ alloy has been found to have a dominant phase with either the rhombohedral Th_2Zn_{17} structure or the newly discovered 2:19 [1,2] phase which is now identified as $Nd_3(Fe_{1-x}Ti_x)_{29}$ structure [3], depending on the annealing procedure. Powder X-ray diffraction patterns and Scanning Electron Microscopy (SEM) show that the sample annealed at a temperature of 850°C has the 2:17 structure whereas annealing at 1000°C leads to the new 2:19 structure. EDAX analysis yields Pr:Fe:Ti ratios of 10.7 : 86.2 : 3.1 for the 2:17 phase and 9.2 : 85.9 : 4.9 for the 2:19 phase. ^{57}Fe Mössbauer Spectroscopy (at 295K) yields values for the average ^{57}Fe hyperfine field of 15.7T for the 2:17 phase and 17.5T for the 2:19 phase, respectively.

References

1. S.J. Collocott, R.K. Day, J.B. Dunlop and R.L. Davis, Proc. of the Seventh Int. Symp. on Magnetic Anisotropy and Coercivity in R-T Alloys, July, 1992, Canberra. p437.
2. Hong-Shuo Li and J.M.Cadogan, Jian-Min Xu, S.X. Dou and H.K. Liu, Int'l Conf.on Application of the Mössbauer Effect (Vancouver, August 1993) paper 15-29B.
3. Hong-Shuo Li and J.M.Cadogan, R.L. Davis, A. Margarian, J.B. Dunlop and P.B. Gwan, This Meeting.

THE MAGNETIC PROPERTIES OF $Gd(Fe_{1-x}Co_x)_9Ti_2$ ALLOYS

Suharyana, J.M. Cadogan, Hong-Shuo Li and G.J. Bowden
School of Physics, The University of New South Wales, Kensington, NSW 2033, Australia.

Four samples of $Gd(Fe_{1-x}Co_x)_9Ti_2$ with x=0.0, 0.1, 0.2 and 0.3 have been prepared by conventional arc-melting following by annealing at 1000°C for 3 days. Powder X-ray diffraction patterns of these samples show that all samples have a dominant phase with the tetragonal $CeMn_6Ni_5$ structure. Traces of $TiFe_2$ are also present. ^{57}Fe Mössbauer spectra have been collected at 80K and 295K. X-ray diffraction patterns and Mössbauer spectra on magnetically aligned samples indicate that the easy magnetization direction of these samples is the crystallographic c-axis. The Curie temperature increases monotonically with increasing cobalt concentration. The average ^{57}Fe hyperfine field at 80K reaches its maximum value of 25.8 T for x=0.2.

NEW FEATURE IN THE MAGNETORESISTANCE OF SILICON

D. J. Miller and J. Lobb
School of Physics
The University of New South Wales

We report a step-like change in the magnetoresistance of a Si Schottky diode in the range 0.1 T to 0.8 T. The change is measured using lock-in detection by modulating the magnetic field and monitoring the component of the voltage across the diode at the modulation frequency with a fixed forward-bias current. The step-like change or resonance is observed at temperatures in the range 20 K to 400 K, at forward bias currents above 10 mA and for modulation frequencies above 10 kHz. Observation of the resonance is enhanced by differentiating the lock-in signal using a digital filter.

The position of the resonance was found to depend on the angle q between the magnetic field and the Schottky barrier or current direction. The resonant field varies from 0.081 T for $q = 0^{o}$ to 0.676 T for $q = 90^{o}$.

The resonance is explained in terms of a magnetic field induced level-crossing between the singlet and triplet states of recombination centre in the space charge region of the diode. An expression is derived for the magnetic field magnitude at which the level crossing occurs, assuming that the recombination centre is an S=1 state with both isotropic exchange and dipolar spin interaction. An extremely accurate fit to the angular dependence of the resonance is obtained by choosing suitable values of the strengths of the two interactions.

The new phenomena could be a fruitful way of obtaining information about recombination centres in semiconductors.

Transient NMRON - Recent Advances

W.D. Hutchison, E. Jaatinen†, N. Yazidjoglou and D.H. Chaplin

Department of Physics, University College, The University of New South Wales,
Australian Defence Force Academy, Canberra, A.C.T. 2600, Australia

Nuclear magnetic resonance on oriented nuclei (NMRON) is a spectroscopic technique which combines the energy resolution of NMR with the sensitivity of low temperature gamma-ray detected nuclear orientation. Transient NMRON (pulsed and swept frequency extensions to basic continuous wave NMRON) allows for a larger range of measurements in a greater diversity of systems. In particular, pulsed NMRON is useful in the measurement of relaxation times and for resonanting systems with excessively fast or slow relaxation rates. The Canberra NMRON group pioneered the development of pulsed NMRON [1] and in this paper we outline some recent developments in the use of the technique. Using the seminal NMRON system ^{60}CoFe and spin echo NMRON we show the first conclusive evidence of modulation of signals by the quadrupolar interaction, as well as producing a spin-spin (T_2) relaxation measurement. The first complete NMRON Stimulated echoes, and a resulting spin-lattice (T_1) relaxation measurement are also presented.

[1] H.R. Foster, P. Cooke, D.H. Chaplin, P. Lynam and G.V.H. Wilson,
Phys. Rev. Lett. **38** (1977) 1546.

†New Address: CSIRO, Division of Applied Physics, Lindfield, NSW, 2070, Australia

A SHOCK-HUGONIOT FOR $Sm_2Fe_{17}N_x$ POWDER.

M.J.Lwin[a], P.D. Killen[a] and N.W. Page[b].
[a]Queensland University of Technology, Brisbane, Australia.
[b]The University of Queensland, St. Lucia, Australia.

The fabrication of fully dense permanent magnets from $Sm_2Fe_{17}N_x$ powder is difficult for two reasons. The material is hard (~650 VHN), so resists densification by conventional cold pressing, and is metastable, so that it decomposes if heated to temperatures high enough to soften it to facilitate densification and bonding. Thus, production of components from this material requires a process which is capable of producing very high pressures (several GPa) without the generation of heat. One such a process is dynamic (or shock) compaction in which a shock wave is used to supply the pressures required and the bulk temperature rise in the sample is very small. Previous research into the consolidation of rapidly solidified NdBFe powder at The University of Queensland[1], demonstrated that shock processing was a potential fabrication technique for such hard material. In order to determine the optimum shock conditions for densification of powdered $Sm_2Fe_{17}N_x$, a series of experiments was undertaken to enable the calculation of the shock Hugoniot[2]. Measurements of the shocked state were determined by consolidating the powder in a die using shock waves generated by the impact of high speed, 6061T6 aluminium alloy projectiles. The shock strength was determined using the impedance mis-matching technique described by Al-Tshuler[3].

REFERENCES

1. M.W.Petrie and N.W.Page, "Shock Consolidation of Rapidly Solidified Neodymium Based Rare Earth Magnet Powders" *Acta metall. mater.* **40** (11), pp3195-3203, 1992.
2. M.W.Petrie and N.W.Page, "An Equation of State for Shock Loaded Powders." *J.Appl.Phys.* **69** (6), pp3517-3524, 15 March 1991.
3. L.V.Al'Tshuler,K.K.Krupnikov,B.N.Ledenev,V.I.Zhuchiknin and M.I.Brazhnik, *Soviet Phys.* JETP 34,606 (1958)

FARADAY MAGNETOMETER FOR STUDYING INTERSTITIALLY MODIFIED FERROMAGNETS

T. P. Blach and E. M[ac]A. Gray

School of Science, Griffith University
Brisbane 4111, Australia

The introduction of interstitial impurity atoms such as H, C or N, into a metal can greatly alter its magnetic properties. Interstitial nitrides and carbides of certain rare-earth - 3d intermetallics may have Curie temperatures several hundred degrees higher than those of the host metals, with the promise of improved commercial permanent magnets if the problem of retaining the interstitial impurity at high temperatures can be solved [1].

Typically the nitrogenation and determination of magnetic properties are carried out in different apparatus, which rather limits the scope of the investigation.In our laboratory the determination of interstitial content is made gravimetrically with a microbalance, which is readily adapted to measure magnetic moments by the Faraday method. Thus the effects of interstitial content on magnetic properties can be studied directly in a single instrument of this type. Among the benefits are the possibility of cumulative treatments with several different gases, without the problems caused by exposure to the air during transfers between apparatus.

For this reason we have constructed a Faraday magnetometer based on a microbalance, with the specific aim of studying interstitially-modified ferromagnets. While under other circumstances the first choice of magnetic technique might be a SQUID or vibrating-sample magnetometer, the attractiveness of the simultaneous determination of interstitial content and magnetic moment is sufficient to justify the effort required to overcome the inherent stability problems of the Faraday magnetometer with ferromagnetic samples discussed by Stewart [2]. Presently both hydrogen and nitrogen are available, and measurements may be made at temperatures up to 550°C at gas pressures of 5.5 MPa.

In this paper we detail the design and construction of a Faraday magnetometer which is stable with strongly ferromagnetic samples, and give some examples of the data obtained for Sm_2Fe_{17} and $Nd_2Fe_{14}B$ and their nitrides.

[1] Hong Sun, J.M.D. Coey, Y. Otani and D.P.F. Hurley, *J. Phys.: Condens. Matter*, **2**, 6465-6470 (1990)

[2] A.M. Stewart, *J. Phys. E: Sci. Instr.*, **8**, 55-58 (1975).

THE SORPTION OF IRON IONS ON POLYURETHANE FOAMS

D. Jinks[1], J. D. Cashion[1] and W. H. Jay[2]

[1] Physics Department, Monash University

[2] Chemical Engineering Department, Monash University

Clayton, Vic. 3168, Australia

In order to determine some of the sorption characteristics and obtain information on the active sites in polyurethane foams we used iron in both the ferrous and ferric states and also as anions and cations. The samples were made by contacting ferric and ferrous sulphate and potassium ferri- and ferro-cyanide onto the foams. Four foams were used, principally distinguished by changing ethylene oxide to propylene oxide ratios of 1:20, 1:8, 1:5 and 3:2. Other variations included the incorporation of 40% polystyrene-acrylonitrile interpenetrating polymer as filler, differing urea contents, the use of an ethylene oxide tipped polyol and making the foam hydrophilic. The foams were immersed in a solution of the adsorbent for approximately four hours, squeezed dry and, in some cases, also washed.

The washed foams in general gave negligible absorption. The Mossbauer spectra of the sulphates on most of the dried foams at 4.2K were doublets with IS=0.52mm/s and QS=0.53mm/s for the ferric sulphate and IS=1.40mm/s and QS=3.41mm/s for the ferrous sulphate. The ferricyanide complex also gave a doublet with IS=-0.02mm/s and QS=0.54mm/s while the ferrocyanide gave a single line at 0.04mm/s. For comparison, Mossbauer spectra were also taken of frozen solutions of the salts and these agreed well with most of the observed parameters. However, potassium ferricyanide on the hydrophilic foam gave spectra which showed slow paramagnetic relaxation up to 40 K and further work on the dependence of this interaction on temperature and applied magnetic field is in progress.

THE IDENTIFICATION OF POORLY CRYSTALLINE IRON OXIDES AND IRON OXYHYDROXIDES

A.W.Y. Lee and J.D. Cashion
Physics Department, Monash University.

A series of natural and synthetic iron oxide samples were characterised by the use of x-ray diffraction, transmission electron microscopy and Mossbauer spectroscopy. The main interest was to identify the natural sediment samples, which were from a creek that drained an abandoned acidic mine in NSW, and consisted of the top hard crust layer of sediment and the spongy sublayer beneath. The synthetic samples were a series of precipitates made from a solution including Al^{3+}, SiO_3^{2-} and SO_4^{2-} ions at the same concentration as that of the water from the creek and aged for different times, namely 1 day, 4 weeks, 8 weeks and 29 weeks. These synthetic samples were made in order to assist in the identification of the natural samples.

From the x-ray diffraction patterns the major phases of the natural samples were found to be quartz, jarosite, ferrihydrite and goethite, and with the aid of the transmission electron micrographs, the aged synthetic samples were identified as representing the transformation of iron oxyhydroxysulfate in the 1 day aged precipitate to goethite in the 29 weeks aged precipitate. The transmission electron micrographs of the natural samples confirmed the presence of various phases, although the different particles seen were not conclusively distinguished, and the morphology of one type of particle was not characteristic of iron oxide precipitates. The Mossbauer spectra of the samples were taken at 4.2K in a range of applied fields parallel to the γ-ray and provide a set of spectra for qualitative comparison with those of iron oxides in the literature and so aid the identification of the samples. However, the fitting of the spectra using a computer program for antiferromagnetic polycrystalline materials based on a mean-field model is not meaningful at this stage due to the multiphase nature of most of the samples.

CHARACTERISATION OF THE SULPHATED FERRIC OXIDE MINERAL GLOCKERITE

D. Orloh[1], A.W.Y. Lee[2], J. D. Cashion[2] and L.J.Brown[2]

[1] Institute of Physics and Technology, Academy of Science, Ulan-Bator, Mongolia

[2] Physics Department, Monash University, Clayton, Vic. 3168, Australia

As part of a program on the characterisation of poorly crystalline ferric oxide/oxyhydroxide minerals, principally using Mössbauer spectroscopy at 4.2 K and in magnetic fields up to 15 T, we have studied the mineral glockerite. The ferric oxide/hydroxide minerals are ubiquitous in studies of weathering, sedimentation, soil degradation and mineral processing and because they have frequently not reached a well-crystallised state, their identification between the approximately thirteen different varieties can be quite difficult. It is also frequently complicated by the partial substitution by Al^{3+} for some of the Fe^{3+}.

The two most common oxyhydroxides are goethite, α-FeOOH, and lepidocrocite, γ-FeOOH, which can be though of crystallographically as hexagonal or fcc packing of the oxygens, with the iron ions in the octahedral interstices. However writing the formulae as α-$HFeO_2$ and γ-FeO(OH) also shows the difference in ligands. Lepidocrocite is stabilised by the presence of $SO_4^=$ ions and hence forms of it appear as a pollutant from the acid mine drainage from weathering sulphide ores. We have studied glockerite from Slovakia and synthetic $Fe_4SO_4(OH)_{10}$ which has the same nominal formula, using Mössbauer spectroscopy and TEM. Both samples show evidence of more than one phase with large differences being visible in the high field Mössbauer spectra. The majority of the synthetic sample is clearly antiferromagnetic, while the glockerite may be principally ferrimagnetic. This is possibly due to the poor crystallinity for which the very small "particles" do not necessarily have equal numbers of atoms on the two sublattices.

Structural and magnetic properties of $NdNi_{8.6-x}Fe_xSi_{2.4}$

S.J. Harker, S.J. Campbell, J.M. Cadogan† and Hong-Shuo Li†

Department of Physics, University College, The University of New South Wales, Australian Defence Force Academy, Canberra ACT 2600

†*School of Physics, University of New South Wales, Kensington NSW 2033*

$NdNi_{8.6-x}Fe_xSi_{2.4}$ alloys have been synthesised over a range of Fe concentration to elucidate further information on the magnetic structures reported for the related $RCo_{9-x}Fe_xSi_2$ (R = rare earth) alloys. These include spin reorientation at about 60 K for R = Sm and $x = 0$ and canted moments for R = Nd and $0 < x < 5$ [1–3]. The crystal structure is a variant of the $BaCd_{11}$ tetragonal structure.

The alloys were characterised by x-ray powder diffraction and ^{57}Fe Mössbauer spectroscopy; the latter was also used to investigate the magnetic structure. Preliminary results including the range of Fe content in as-cast and annealed samples, and the effects of annealing on the phases will be presented.

References

[1] Y. Berthier, B. Chevalier, J. Etourneau, H. R. Rechenberg, and J. P. Sanchez, J. Magn. Magn. Mater. **75**, 19 (1988).

[2] J. P. Sanchez, Intrinsic properties of ternary rare-earth compounds from ^{57}Fe, ^{161}Dy, ^{166}Er Mössbauer spectroscopy, in *Concerted European Action on Magnets [CEAM]*, edited by I. V. Mitchell, J. M. D. Coey, D. Givord, I. R. Harris, and R. Hanitsch, pages 300–309, Elsevier, Barking, England, 1989.

[3] F. Pourarian, S. K. Malik, E. B. Boltich, S. G. Sankar, and W. E. Wallace, IEEE Trans. Magn. **25**, 3315 (1989).

A SERIES STUDY OF QUANTUM SPIN MODELS ON 3-DIMENSIONAL LATTICES

J. Oitmaa, C.J. Hamer and Zheng Weihong
School of Physics,
The University of New South Wales,
P.O. Box 1, Kensington, NSW 2033, Australia

The linked-cluster series expansion technique has been proven to be very effective in obtaining physical results for a variety of quantum lattice models. The calculation needs a very efficient method to generate a list of clusters, connected and disconnected, on a lattice, together with their embedding constants, and an algorithm to develop the series expansion coefficients.

Recently, we have used streamlined methods of cluster generation to produce extended perturbation series for a number of quantum spin models on 2-dimensional lattices. For example, we have generated the most accurate series available for the 2-dimensional Heisenberg antiferromagnet[1], which is of interest in connection with high-T_c superconductivity. The results are found to be in good agreement with the predictions of higher order spin-wave perturbation theory[2,3] and with effective Lagrangian theory, and form a comprehensive and surprisingly accurate description of the system.

In present work, we extend the above calculations to the 3-dimensional Heisenberg antiferromagnet and Ising model with a transverse field on the simple-cubic, body-centered-cubic, and face-centered-cubic lattices. For the Heisenberg antiferromagnet, a series expansion around the Ising limit is carried out for the ground-state energy, staggered magnetization, transverse susceptibility, staggered parallel susceptibility, and energy gap. The results from analysis of the series are presented and compared with the predictions of spin-wave perturbation theory. For the Ising model in a transverse field, both weak-coupling and strong-coupling series are calculated for the ground-state energy, magnetization, susceptibility and energy gap. An analysis of the series is presented.

1. W.H. Zheng, J. Oitmaa and C.J. Hamer, Phys. Rev. B **43**, 8321 (1991).

2. C.J. Hamer, W.H. Zheng and P. Arndt, Phys. Rev. B **46**, 6276 (1992).

3. W.H. Zheng and C.J. Hamer, Phys. Rev. B **47**, 7961 (1993).

HIGH COERCIVE $Sm_2Fe_{17}N_x$ POWDERS PREPARED BY HDDR

P A P Wendhausen*, N M Dempsey, B Gebel, K.–H Müller
IFW Dresden, Postfach, 01169, Dresden, Germany
* LABMAT, Universidade Federal de Santa Catarina, 88045, Florianopolis, Brazil

The use of HDDR (Hydrogen Disproportionation Desorption Recombination) for producing $Sm_2Fe_{17}N_x$ coercive powders has been investigated. The process was applied to Sm_2Fe_{17} alloy prior to its nitrogenation. STPA (thermopiezic analyses) plots show that above 520°C a massive absorption of hydrogen takes place due to disproportionation of Sm_2Fe_{17} into a finely divided mixture of SmH_x and α–Fe. The grain-size calculated by the Scherer formula varies from 50 to 350 nm, depending on the disproportionation temperature. At certain conditions of pressure and temperature, SmH_x desorbs hydrogen and the intimate mixture of iron and Sm becomes thermodynamically unstable reverting to the more styable Sm_2Fe_{17} phase. The recombination reaction was investigated in the temperature range of 600°C to 900°C. For low temperatures (less than 700°C) the Sm_2Fe_{17} phase tends to crystallise in the disordered $TbCu_7$ structure as indicated by the absence of superstructure reflexes (211) and (204). Samples recombined at temperatures higher than 700°C and show clear superstructure reflexes after a very short time (Th_2Zn_{17} – structure). After recombination the material was pulverised and nitrogenated at 450°C for 10h. Coercivities $\mu_0 H_C$ of 0.8 to 1.5 T were achieved for samples recombined in the given temperature range. The best results are achieved for intermediate temperatures of 750°C to 800°C. For too low recombination temperatures the presence of uncombined iron or material with the $TbCu_7$ structure might be the reasons for lower values of $\mu_0 H_C$. On the other hand high temperatures lead excessive grain growth and precipitation of free Fe due to Sm evaporation, reducing the value of coercivity. The grain size of optimally recombined material as observed by SEM is smaller than 300 nm.

SELF-ORGANISED CRITICALITY IN MAGNETIZATION REVERSAL

Peter J. Thompson and R. Street
Research Centre for Advanced Mineral and Materials Processing
Dept. of Physics, University of Western Australia, Nedlands, WA 6009

Self-organised criticality is postulated to be observable in all driven, dissipative, non-equilibrium systems. It is characterised by the extinction of all scaling within the system. The irreversible magnetization processes ($\longrightarrow$ energy dissipative) which occur in a ferromagnetic ($\longrightarrow$ non-equilibrium) material in the presence of a changing applied field ($\longrightarrow$ the driving force) have been measured in the form of Barkhausen noise and indicate that the magnetization reversal mechanism may be an example of a self-organised critical process.

Once attained, the critical state is insensitive to any external parameters which may be characteristic of the system, such as the chemical composition or the microstructure of a magnet. However it is such specific characteristics of the system which determine how "viscous" the system is. The less viscous a system is, the easier it is to 'push' to the onset of the critical regime, in much the same way that a low viscosity fluid is easier to push to the onset of turbulence. Essentially it is the squareness of the hysteresis loop which influences the sweep rate of the applied field required to push the magnet to the critical regime.

Results from measurements made on various ferromagnetic materials, and the differences that the characteristics of the magnet make as regards the onset of self-organised criticality will be presented.

Mechanochemical Activation of Hematite

First Complete Room Temperature Reduction Reaction
$3Fe_2O_3 \Rightarrow 2Fe_3O_4 + 1/2O_2$

W. A. Kaczmarek and B.W. Ninham

Research School of Physical Sciences and Engineering,
Australian National University, Canberra, A.C.T. 0200

Abstract

Total phase transformation of hematite to magnetite was accomplished at room temperature by wet magnetomechanical activation of hematite [1]. Low energy mechanical activation of the oxide surface is sufficient to effect the transformation. Oxygen bonds on α-Fe_2O_3 oxide surface are apparently broken during the mechanical activation process and oxygen is released (removed) to the dispersing polar liquid. The oxygen pressure during the process as well the nature of the dispersing liquid have a critical influence on successful and fast phase transformation. Thus, all preparations performed in air, dry conditions or with nonpolar hydrocarbons (benzene, anthracene) show that the process of hematite reduction is non existent or very slow. Normal air pressure and/or application of hydrocarbons suppress the transformation.

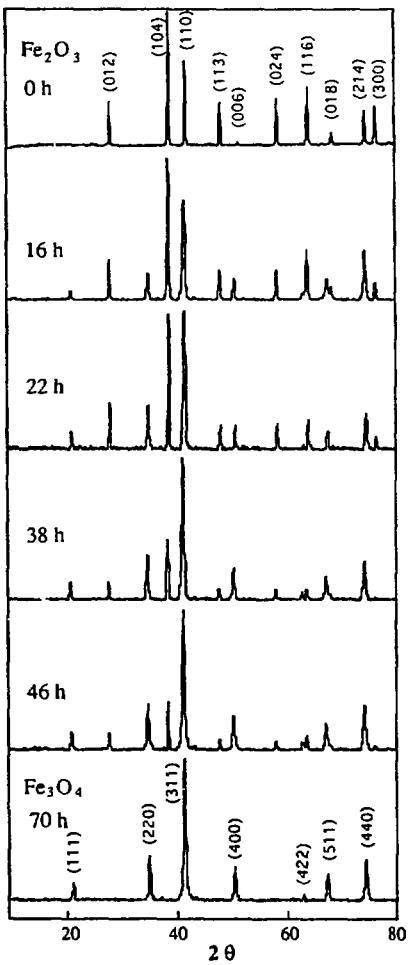

Fig. (↑) XRD patterns of hematite powder milled in wet conditions (water). Prior to milling start the air was removed from the vial (internal pressure 10^2 Pa).

[1] W. A. KACZMAREK and B. W. NINHAM, Preparation of Fe_3O_4 and γ-Fe_2O_3 powders by magnetomechanical activation of hematite, European Magnetic Materials and Applications Conference, Kosice, Slovakia, August 24-27, 1993, *IEEE Trans. Magn.* (1994) in press.

Influence of air and vacuum during ball milling on morphology and structure of complex oxide powder (Effect of gas surface layer)

W. A. KACZMAREK

Institute of Advanced Studies, Research School of Physical Sciences and Engineering

The Australian National University, Canberra, ACT, 0200, Australia.

Mechanical treatment of ferrite materials has become extremely important in many processes in technology of magnetic materials during last few decades. The overall properties of materials are governed by a complex combination of intrinsic and extrinsic properties. An intrinsic property such as saturation magnetisation is determined by material composition, whereas an extrinsic property such as magnetic coercivity is, to a large extent, determined by the microstructure which is in turn influenced strongly by the processing procedures [1]. While the nature of mechanochemical reactions involving nonmetallics has advanced somewhat, the fundamental processes governing the evolution of structure, the kinetics, and thermodynamics of resulting chemical or physical transformations remain incompletely understood. Their elucidation requires more empirical studies.

In the present study the effects of prolonged milling in air and vacuum on $BaFe_{12}O_{19}$ ionic crystal structure and particles morphology have been analysed. X-ray diffraction, scanning electron microscopy and thermal analysis experiments show that for vacuum milled material the ordered structure transforms progressively into a stable disordered nanocrystalline phase. For air milled samples apart from structural transformation, chemical decomposition was found. Application of heat treatment to the final powders restores perfect Ba-ferrite crystal structure with the particles remaining in submicron size range [2-3].

[1] W. A. KACZMAREK and B. W. NINHAM, Magnetic properties of Ba-ferrite powders prepared by surfactant assisted ball milling, European Magnetic Materials and Applications Conference, Kosice, Slovakia, August 24-27, 1993, *IEEE Trans. Magn.* (1994) in press.
[2] W. A. KACZMAREK, Ball milling of barium ferrite in air and vacuum, *J. Mater. Sci. (1993) (submitted).*
[3] W. A. KACZMAREK, Thermally activated crystalline phase restoration in disordered by ball milling barium ferrite powder, *J. Mater. Sci. (1994) (submitted).*

Magnetic Properties of $ErCo_{12}B_6$:^{57}Fe

J.M. Cadogan#, S.J. Campbell* and X.L. Zhao*+

School of Physics, University of New South Wales, P.O. Box 1, Kensington, NSW 2033, Australia
* Department of Physics, University College, University of New South Wales, Australian Defence Force Academy, Canberra 2600, Australia
+ On leave from Applied Acoustics Institute, Shaanxi Teachers University, Xian, P.R. China

This work forms part of a series of investigations into the magnetic structure of ^{57}Fe doped $RCo_{12}B_6$ compounds (R = Y, Nd, Er) using Mössbauer spectroscopy. Such compounds of rhombohedral $SrNi_{12}B_6$ structure (space group $R\bar{3}m$) are of interest in contributing to gaining an understanding of the magnetic behaviour of rare earth (R) transition metal based intermetallic compounds as a whole. As shown in our earlier work on $RCo_{12}B_6$ with nonmagnetic yttrium, the Co sublattice magnetic anisotropy direction is in the basal plane. The $NdCo_{12}B_6$ compound was found to order along or close to the crystallographic c axis at 4.2 K and undergo a spin reorientation with increasing temperature until at about 55 K the magnetisation lies in or close to the basal plane [1].

The main interest in the present work is the behaviour of $ErCo_{12}B_6$ which exhibits ferromagnetism below T_C ~130 K. Contrary to the results by Gubbens et al [2], our Mössbauer spectra reveal basal plane ordering for $ErCo_{12}B_6$ below its ordering temperature, as indicated by the splitting of the *18 h* site magnetic hyperfine field. If the second order crystal field coefficient A_{20} is negative, as predicted by the results by Gubbens et al and by our point charge model calculation, our new result requires that A_{40} and/or A_{60} be positive, in agreement with our previous work on $NdCo_{12}B_6$.

[1] J.M. Cadogan, S.J. Campbell, X.L. Zhao and E. Wu, Aust. J. Physics, **46**(1993) 679.

[2] P.C.M. Gubbens, A.M. van der Kraan and K.H.J. Buschow, J. Magn. Magn. Matter., **87**(1990) 276.

Spin Glass Behaviour in (Mn,Mg)S

G T Etheridge, S J Kennedy*, and T J Hicks

Department of Physics
Monash University
Clayton 3168

*Neutron Scattering Group
Australian Nuclear Science and Technology Organisation
Private Mailbag
Menai 2234

MnS and MgS form a solid solution with the NaCl structure. MnS is antiferromagnetic with first neighbour antiferromagnetic interactions which can never be fully satisfied because in the fcc lattice of the Mn cations first neighbours have mutual first neighbours. This competing interaction condition can lead to spin glass behaviour in a system disordered on the cation lattice.

We present magnetic susceptibility and neutron powder diffraction data which suggest that with the addition of MgS to MnS, to produce a disordered cation lattice, the antiferromagnetic phase may have a reentrant spin glass phase at low temperatures and that certainly at the composition $Mn_{0.35}Mg_{0.65}S$ the material is a classic spin glass.

MOLECULAR DYNAMICS SIMULATION OF ION IMPACT PHENOMENA IN 3D NICKEL LATTICE

P.Guan, N.A. Marks, D.R. Mckenzie and B.A. Pailthorpe
School of Physics, University of Sydney, NSW, 2006, Australia

The phenomena taking place under the surface of material after ion bombardment have been the subject of study for many years. The understanding of these phenomena are important for the modification of the properties of thin films during growth. A molecular dynamics simulation of a two-dimensional array after ion impact has already been performed and showed focussed collision sequences (or focusons) and associated bow waves [1] . To get more insight into the phenomena and obtain quantitative information about real systems, we extend our study to three dimensional systems in this paper to confirm that the focusons and bow waves are also present.

A molecular dynamics simulation of a nickel atom impacting onto a 3D nickel (fcc) lattice was performed. The interactions between atoms were described using the Lennard-Jones potentials. The lattice system has 9216 atoms and the energies of the incident atom were 200 and 500eV. Two different incident directions, (001) and (101) were used. In both cases, the focussed collosion sequences were observed along the close packed directions which are the (110) directions. The bow waves produced by the focuson, however were only found in the two <111> planes which intersect along each (110) direction. The <111> planes are the close packed planes in the fcc lattice. This is consistent with the 2D results obtained earlier. The velocities of the focuson and bow waves were found to fit the relationship $\sin\phi = c/v$, where c and v correspond to the velocities of focuson and bow waves respectively. The results confirm that the bow waves are a significant cause of energy loss from focuson and therefore important in determining their range.

[1] N.A. Marks, D.R. Mckenzie, B.A. Paithorpe, MRS Conference Proceedings, Boston, USA, 1993.

Photemission Study of the Fermi Surface of Cu

Jenice Con Foo, Robert Leckey, John Riley

Physics Department, La Trobe University, Bundoora Vic. 3083

The study of Fermi surfaces has traditionally employed the de Haas - van Alphen and Positron Annihilation techniques. The former is not suitable for alloys and the latter has significantly reduced precision. Angle Resolved Photoemission is, in principle, able to measure the Fermi surface and there have been investigations into a number of two dimensional Fermi surfaces [1]. While it is possible to measure the two dimensional Fermi surface using only a few photon energies, this is not the case for the three dimensional Fermi surface since it is necessary to extend measurements over a wide range of photon energies in order to find suitable final states of the same reduced momentum. In order to generate a Fermi surface in three dimensions information about the normal component of momentum is required, however this is not directly obtainable by photoemission measurements. By assuming free electron final states (as in this study) or using triangulation it is possible to obtain the normal component of momentum.

The capabilities of our toroidal analyser [2] allow us to collect data over all emission angles in a plane (polar angles $\pm 90°$ with resolution $\pm 1°$). By rotating the sample through a number of azimuths, transitions may be observed over the entire emission hemisphere for a given photon energy. As a consequence the large data sets required to generate the three dimensional Fermi surface may be acquired in a short time.

In this paper a comparison between the observed transitions from the Fermi surface and the idealised Fermi surface is presented.

References

[1] K.E. Smith and S.D. Kevan, Phys. Rev. B. 43, 3986-3993, (1991)

[2] R.C.G. Leckey and J.D. Riley, App. Surf. Sci. 22/23, 196-205, (1985)

The Bond Structures of Closed Shells in Condensed Nuclear Matter

Peter Norman, Physics Department,
Monash University, Frankston, 3199.

Models of the bond structures of the most abundant products of stellar nucleosynthesis based on Bernal's models of dense liquid drops show good agreement between the binding energy data and shell structures, when alpha particles are considered to be the densely packed hard spheres of Bernal's models.

In Bernal's tetrahedral models of liquid drops a hard sphere representing an atom, ion or molecule is added at whatever available position is closest to the centre of the existing cluster of spheres so that the densest possible configuration is created.

The common magic number nuclei with closed shells of nucleons are $^{4}_{2}He$, $^{16}_{8}O$, $^{40}_{20}Ca$ and $^{56}_{28}Ni$. Models of these nuclei consisting of densely packed alpha particles bound internally and externally by strong bonds between adjacent nucleons clearly exhibit the energy levels of the corresponding shell models.

References :

[1] Norman, P.D. 1993, Models of the meson bond structures of the most abundant products of stellar nucleosynthesis. *Eur. J. Phys.* 14,36.

[2] Robson, D. 1978, Alpha particle clustering and the quark structure of elementary particles, Proc. of the 3rd Int. Conference on clustering aspects of nuclear structure and nuclear reactions (Winnepeg, AIP) 348.

[3] Kukulin, V.I. 1991, A new physics in the problem of nucleon - nucleon interaction, Proc. of meeting re Pauli principle in few-body systems, (Tokyo, Inst. Nuclear Study).

[4] Pearson, J.M. 1986, Nuclear Physics : Energy and matter, (Bristol, A.Hilger)

HARD DISC COLLISIONS AND THE LORENTZ GAS PRESSURE TENSOR

Janka Petravic and Dennis J. Isbister
Department of Physics, University of NSW, University College, ADFA, Canberra, ACT 2600

The two-dimensional Lorentz model is the simplest possible model of shear flow. It consists of two particles in a periodic cell with the Lees-Edwards moving periodic boundary conditions, obeying the thermostastted Sllod equations of motion.

The potential contributions to the hard disc pressure tensor are the impulses received by the moving particle in the time intervals of vanishing duration. The collisions of hard discs were conventionally simulated using some stiff repulsive interaction potential like a stiff Hooke's law. In this work the exact solution of the hard disc collision of the particles obeying the equilibrium and sheared thermostatted Sllod equations is presented, and its implications for the potential part of the pressure tensor discussed.

In equilibrium, the trajectories of the thermostatted and unthermostatted particles are exactly the same, but the impulses received by the moving particle differ. Therefore the potential parts of the thermostatted and unthermostatted equilibrium hydrostatic pressures are different, their ratio being equal to 1.83194.

The solution of the thermostatted collision with shear shows that for the reduced shear rate $\gamma^*>4$ "forbidden" collisions may occur, when the moving particle cannot "bounce off" after the collision, but stays bound indefinitely to the scatterer. These collisions have the same origin as the artificial string phase observed in the strongly sheared soft disc systems using a linear profile thermostat.

The dependence of the potential part of the pressure tensor on shear rate can be qualitatively explained by the angular probability distributions at the collision and the collision law. To explain the change of the potential part of the elements of the pressure tensor with shear rate, it is necessary to take into account the three competing effects:

- the dependence of the impulse on the position of the point of collision
- the dependence of the impulse on the radial component of the momentum at the collision
- the value of $\cos\beta \sin\beta$, $\cos^2\beta$ and $\sin^2\beta$ at the collision, where β is the polar angle of the collision point.

The dependence of the potential part of the pressure tensor on these three different factors implies that the potential part of the pressure tensor, and the steady state, depends on shear rate and density as two separate parameters.

Massively parallel studies of the electronic structure of disordered micro-crystallites of transition metal oxides

Marek T. Michalewicz
CSIRO Supercomputing Support Group
Division of Information Technology
Commonwealth Scientific and Industrial Research Organization
723 Swanston Street, Carlton, Victoria 3053, Australia
e-mail: marek@mel.dit.csiro.au

The object of our studies is to determine the influence of defects on the electronic structure of the transition metal oxides. We investigate both point defects, such as oxygen vacancies and substitutions, as well as extended surface defects, We employ the equation of motion method to study the total, local, surface and orbital resolved density of states. We will outline methods to extend these studies to transport properties, both linear and non-linear.

The equation of motion method is very well suited to implementations on parallel processors. Parallelism is inherent in this method in a very natural way. The 3D spatial arrangement of atoms corresponds to the two dimensional computational grid of processing elements (PE) plus memory (2D + 1D). The interactions between the constituent particles correspond to the communication paths between the PEs.

Different mappings of the structure on the PE grid are possible depending on the target computer architecture. On the SIMD architecture with limited local memory fine grain parallelism (i.e. small number of atoms per PE) is perhaps most advantageous. On the other hand MIMD architectures such as Cray Research T3D with large memory would be more suitable for mapping of larger chunks of matter onto each processor, and its low latency would be well suited to long range interactions (i.e. longer communication paths).

As an example of those concepts we will report on massively parallel computations of the total and local electronic densities of states of a non-periodic micro-crystallite of rutile TiO_2. The sample size ranges from a few unit cells up to $41.5 \times 41.5 \times 1.5nm$, the largest sample consisting of 491,520 atoms or 81920 unit cells.

Mathematically, the problem *is equivalent* to solving an $n \times n$ eigenvalue problem, where $n \sim 2,500,000$. This problem was implemented on MasPar MP-1 and MasPar MP-2 autonomous SIMD computers.

The program is fully scalable in the number of atoms, i.e. the time required to run it is independent of the size of the system in x and y directions (2D PE mesh) and is linear in z direction (memory axis). The total CPU time for the largest sample, on a MasPar2 computer with 16,384 processing elements is $\sim$ 1.5 hour.

With the program described in this talk we are able to compute the electronic properties for the samples with cleaved surfaces of different Miller indices, modelling the shape of the microcrystallite in a stone-cutter fashion. The extended surface defects and fabricated features such as stepped surfaces, superlattices, modulated (non-periodic) superlattices or doped samples can now be investigated by methods described here. These features can be programmed as software masks which switch-off atoms (PE's) outside the bounds of a sample.

CLASSICAL LATTICE DYNAMICS: FOREMAN-LOMER THEORY AND THE BLACKMAN SUM RULE

A.M.Stewart
Department of Applied Mathematics
The Research School of Physical Sciences and Engineering
The Australian National University, Canberra A.C.T. 2600

It is well known that all the harmonic force components between atoms in crystals may in principle be determined if *all* the phonon eigenfrequencies and eigenvectors are known. Often the eigenvectors are not available and it is necessary to extract the maximum amount of information from the phonon frequency spectrum alone. One question of particular interest concerns the range of the atomic forces in crystals. Foreman and Lomer (1957) have provided a simple procedure for determining this in some special cases. They argued that for phonons propagating along the principal directions of *primitive cubic* crystals the Fourier series expansions of the squares of the eigenfrequencies give directly certain force constants between entire planes of atoms, each term in the Fourier series being determined by the interactions between corresponding planes.

Surprisingly, a derivation of this theorem appears never to have been given, perhaps because it seemed to be too obvious to need proving. A formal derivation of the Foreman-Lomer theorem is provided here (Stewart 1993, 1993), and it is shown how more detailed information about the range of forces may be obtained from *simple combinations* of the phonon dispersion branches rather than the individual branches themselves for certain directions both of primitive cubic crystals and of the ***non-primitive*** hexagonal close packed and diamond lattices.

As an added bonus the derivation also produces a simple, explicit and exact expression for the Blackman (1942) sum rule which states that the range of the the non-Coulombic atomic forces in a crystal of ***any*** structure may be deduced from the wavevector dependence of the *sum* of the squares of the eigenfrequencies.

BLACKMAN, M., 1942, *Proc. Roy. Soc.* **A181**, 58.

FOREMAN, A.J.E. and LOMER, W.M., 1957, *Proc. Phys. Soc. (London)* **B70**, 1143.

STEWART, A.M., 1992, *Phil. Mag.* **65**, 1137, 1993, *ibid.* **67**, 363.

A Practical Application of The Theory of Hyper-Complex Variables: Dielectric and Optical Response of 3-Dimensional Arrays of Spheres of Complex Permittivity.

A.V. Vagov

Department of Theoretical Physics, Research School of Physical Sciences, Australian National University, Canberra , ACT 0200 AUSTRALIA

A.Radchik and G.B.Smith

Department of Applied Physics, University of Technology, Sydney, PO Box 123, NSW 2007 AUSTRALIA

ABSTRACT

A powerful new formalism for solving the Laplace's equation (LE) is used to establish the dielectric response of various 3 dimensional arrays of spheres of arbitrary dielectric constant. Structure specific transformations of the 3 dimensional hyper-complex variable X into infinite dimensional hyper-complex space leads to solutions. The theory is applied to isolated spheres, pairs of spheres and touching spheres so that numerical results can be compared (for aluminium at optical frequencies) with existing theories based on the separability of the LE. The underlying technique extends to arrays for which the LE is non-separable and to arrays of composite spheres, neither of which have been previously solved.

TRACER CORRELATION FACTOR AND ATOMIC DISPLACEMENTS IN SOLID STATE DIFFUSION

P.C.L. Stephenson and C.A. Sholl
Physics Department, University of New England, Armidale, NSW 2351

Defects play an important role in determining the behaviour of many of the bulk properties of crystalline solids. Point defects are intrinsic to any crystalline solid that has non-zero temperature and can also be produced by doping with appropriate impurity atoms. The diffusion of atoms within a crystalline solid can be due to point defects and there are several types of point defects and associated diffusion mechanisms. Of these, the present work is concerned with the interstitial defect and solid state diffusion by the interstitialcy mechanism.

Diffusion by the interstitialcy mechanism occurs when an atom at an interstitial site moves on to a normal lattice site, displacing the atom at the normal lattice site on to a neighbouring interstitial site. The interstitial defect so formed is equally likely to then move to any of its nearest neighbour normal lattice sites and produce a further interstitial defect. The defect, which is not a particular atom, so moves on a lattice of interstitial sites by a random walk. The diffusion of an atom is not as straightforward since each jump consists of two parts. The first is a step from a normal to an interstitial site, which depends upon the return of the defect to the atom. The second is a step of the atom from the interstitial to a normal lattice site and this step is uncorrelated to any previous jump.

As with the vacancy mechanism (Baker *et al.* 1994), each defect will displace a particular atom several times before diffusing away. Such a sequence of interactions is termed an atom-defect encounter and the atom is displaced by $\boldsymbol{l}$ with a probability $W(\boldsymbol{l})$ as a result of the encounter. The atomic diffusion then proceeds by successive encounters with different interstitial defects and the diffusion is a random walk of encounters.

The tracer correlation factor, f, is the ratio of the atomic diffusion coefficient to the diffusion coefficient for an uncorrelated random walk and it is a measure of the correlation between atom jumps for the particular diffusion mechanism. The present work uses probability generating functions to calculate atom jump probabilities (Stephenson and Sholl 1993, Stephenson 1994) and from these, correlation factors for different types of interstitialcy mechanisms of diffusion. Simple analytic expressions for the correlation factor are obtained using a symbolic mathematics computer package. The atom jump probabilities are also used to calculate the $W(\boldsymbol{l})$ which will be used to analyse nuclear spin relaxation experiments.

References

Baker, J.B.H., Girard, C.J. and Sholl, C.A., 1994, Abstract, 18th Condensed Matter Physics Meeting.

Stephenson, P.C.L. and Sholl, C.A., 1993, Phil. Mag. A, to be published.

Stephenson, P.C.L., 1994, Submitted to Phil. Mag. A.

The Polarisation of Interacting and Intersecting Particles

A.V.Paley, A. V. Radchik, A.V.Vagov and G. B. Smith
Department of Applied Physics
University of Technology, Sydney
P.O. Box 123, Broadway, N, S. W. 2007
Australia

Abstract. The importance of electromagnetic interactions between approaching particles has been recognised for a long time but suitable models for understanding experiments have been unavailable for arbitrary dielectric constants.

The problem of polarisation of two intersecting spherical and cylindrical particles with various degrees of intersection is of great interest in the study of composites where clustering has occurred as well as in biological systems. When the applied field wavelength is significantly greater then the inclusion dimension one can invoke the quasistatic approximation. In this case the problem to be solved is an electrostatic one.

So far all solutions of such problems have been restricted to the limit of infinite conductivity or just a small degree of intersection. For the first time an exact solution of the electrostatic problem has been found for intersecting cylindrical and spherical particles with any degree of penetration and arbitrary dielectric constant.

Two slightly different shapes are particulary interesting. One case is overlapping cylinders with distance between their centre 1.2 of a radius of a particle, the other is a cardioid. In one shape, namely the cardioid, the angle of intersection between surfaces of particles is 90°, while for the cylinders it is 105.26°. A comparative example of such structures made of aluminium shows that a small difference in an angle of intersection between particle surfaces leads to a huge difference in polarisabilities, especially near the resonance wavelengths. Therefore, the polarisabity is extremely sensitive to the details of geometry near the point of intersection.

ELIMINATION OF MULTIPLE QUANTUM ARTIFACTS IN 2D COSY NMR SPECTRA (EMA-COSY)

G. J. Bowden and T. Heseltine

School of Physics, University of New South Wales
P.O. Box 1, Kensington, NSW 2033

Abstract

Correlated Spectroscopy (COSY) NMR techniques are used around the world to determine connectivities between nuclear spins, and hence the structure of very large molecules of up to 50,000 Daltons. The basic COSY sequence is just two 90^0 rf-pulses separated by a variable time t_1 (the first dimension). In practice the NMR signal is captured immediately following the removal of the second rf-pulse, in real time t_2 (the second dimension). So by successively incrementing t_1, a 2D NMR data set can be obtained in the both the t_1 and t_2 dimensions. Subsequently, a 2D Fourier transform of the NMR data set can then be used to establish connectivities between differing nuclei.

However, it has been known for some time that multiple quantum artifacts can be introduced into the COSY spectra, if the repetition time between the two rf-pulses (t_{rep}) is not long enough to allow the nuclei to relax back to thermal equilibrium. Such artifacts can lead to erroneous conclusions. However, in practice, few spectroscopists can afford the luxury of long repetition times ($t_{rep} > 5T_1 \approx 5s$) between COSY pulse sequences. So several phase cycling methods have been devised to strip unwanted MQ-artifacts from the NMR data set.

Avid readers of these columns will remember that last year we presented a new pulse sequence which could be used to strip 2D COSY spectra of MQ-artifacts arising from incomplete longitudinal relaxation between COSY pulse sequences (ELMA-COSY). This year, we have developed an even better pulse sequence which strips the NMR data of MQ-artifacts, arising from both incomplete longitudinal and transverse relaxation effects, simultaneously. We have named the new pulse sequence EMA-COSY.

THE INITIAL THERMO-INSTABILITY OF THE Al-Cu-Mg-Ag SUPERSATURATED SOLID SOLUTION

Michael Lim, P.L. Rossiter and J. Tibballs*
Department of Materials Engineering
Monash University
Clayton, Victoria 3168 Australia
Comalco Research Laboratory*
Thomastown, Victoria 3074 Australia

Unusual age hardening of Al-Cu-Mg-Ag alloys with high Cu:Mg ratios has been found to be associated with the formation of the Ω phase. Ω forms as a uniform dispersion of thin, hexagonal-shaped plates that precipitate coherently on the $\{111\}_\alpha$ planes of such alloys when they are aged in the temperature range ~120-220°C. Whilst much research has been directed at determining the morphology and composition of the Ω phase, results are still not conclusive, although the generally accepted crystal structure is orthorhombic (a=0.496 nm, b=0.895 nm, c=0.848 nm) and its composition is mainly $AlCu_2$ with traces of Ag and Mg.

Nucleation of the Ω precipitates thus appears to be preferential to formation of θ' or S' phases which are also found in alloys with high Cu:Mg ratios. Taylor has proposed that Ag and Mg may form the stable hexagonal intermetallic compounds $AgMg_3$ which could then act as nuclei for the nucleation and growth of the Ω precipitates. This suggestion was based on the fact that the intermetallic compounds $AgMg_3$ has a hexagonal structure with a=0.493 nm, which is close to a value for Ω of 0.496 nm, and that the favoured ratio of Ag:Mg is around 1:3. In this regard, Cousland and Tate have investigated the Al-Ag-Mg ternary alloy by X-ray diffraction but failed to isolate $AgMg_3$ particles even at high Mg:Ag ratio, and found instead MgAg compounds. More recent atom probe field ion microscopy studies by Hono have found evidence of MgAg clustering in Al-Cu-Mg-Ag during the early stages of ageing (aged for 15 sec at 180°C) after quenching.

The present project is aimed at identifying these nuclei at the early stage of the nucleation process by means of thermodynamic modelling. A computer routine called THERMOCALC developed by a Swedish group is being used for calculation.

MONTE CARLO SIMULATION OF NANODOMAIN TEXTURES IN RELAXOR-TYPE LEAD SCANDIUM TANTALATE

H. QIAN, J. L. PENG and L. A. BURSILL
School of Physics, The University of Melbourne, Parkville, 3052

Chemical domain textures for lead scandium tantalate (PST) are modelled using Monte Carlo (MCS) and next-nearest-neighbour Ising (NNNI) models. A wide range of degrees of short- and long-range ordering of the (Ta,Sc) atoms occur in ceramic specimens, depending on processing routes. The simulations help us understand and quantify the chemical domain textures, chemical domain wall configurations and other chemical defects which may occur in certain relaxor-type perovskite-type oxides. The results are compared to dark-field transmission electron microscopic observations.
Some new types of small defects were discovered. These are described and classified. The results provide a first step towards the development of a microscopic statistical physics framework for analytical theories of the dielectric response of relaxor-type ceramics, where the frequency and temperature variation of the permittivity are due essentially to dipolar-type fluctuations on nanometer scales.

A DOUBLE MONOCHROMATOR SYSTEM FOR A MEDIUM RESOLUTION NEUTRON POWDER DIFFRACTOMETER

M. D. Burke, Prof. T. M Sabine;
University of Technology, Sydney

The efficiency of conventional neutron powder diffractometers is still less than is desired for a number of experimental applications.

With detector technology having gone almost as far as it can, attention has been turned to improvements in efficiency of the monochromator system.

The double monochromator System we have designed will match a conventional single monochromator system such as used in HIFAR (Howard et al 1983) for resolution at a high take-off angle, yet is expected to provide a greater flux output. The flux output will improve by a calculated factor of 1.6, Thus improving the efficiency by the same amount.

In addition, an infinitely variable wavelength may be selected using the double monochromator system we have proposed which is not possible with a single monochromator.

The monochromating crystals themselves have also been under investigation. We are in the process of developing crystals with characteristics to produce maximum reflectivity within resolution constraints since the two are directly, positively correlated.

The crystals initially chosen for this investigation are Germanium for their favourable characteristics (Freund 1983).

References

1. Howard C.J., Ball C.J., Davis R.L., Elcombe M.M.; 1983 Aust. J. Phys 36 507-518.
2. Freund K.; 1983 Nucl. Inst. Methods 213 495-501.

Quantum Well Plasma Effects in the Tunneling Current through a Semiconductor Double Barrier Structure

M.L.F. Lerch, C. Zhang, A.D. Martin, P.E. Simmonds and L. Eave.

Department of Physics, University Of Wollongong, Wollongong, 2522.

†*Department of Physics, University Of Nottingham, Nottingham, NG7 2RD, England.*

Abstract

This paper reports on calculations and experimental measurements on resonant tunneling in a double barrier semiconductor structure. A new technique developed recently enables regions of apparent bistability in the electrical characteristics of some of these structures to be probed. One such structure shows complex behaviour inside the bistability at low temperatures. Theoretical calculations based on a transfer Hamiltonian model and path integral method together with magnetic field measurements will be presente[1]. These results indicate that this behaviour may be associated with plasma oscillations in the two dimensional electron gas which forms due to charge build up in the central quantum well of the device when it is biased near resonance.

THE INFLUENCE OF ION, ELECTRON AND PHOTON IRRADIATION ON THE LEVEL OF HYDROGEN AT THE INTERFACE OF METAL - SEMICONDUCTOR SYSTEMS.

M.D.McCubbery*, G.L.Nyberg* and J.S.Williams#
*Dept of Physical Chemistry, LaTrobe University, Bundoora 3083.
#Dept of Electronic Materials Engineering, A.N.U.

We have studied the level of hydrogen at the interface of metal (Al) - semiconductor (Si) systems using the forward scattering mode of RBS, commonly known as elastic recoil detection analysis (ERDA)[1]. Here we detect forwardly recoiled protons and the spectra obtained comprise two peaks corresponding to surface and interface hydrogen. In addition to confirming[2] a substantial decrease in interfacial hydrogen under ion beam (He 2-3 MeV) irradiation, we have also observed changes in the interfacial hydrogen concentration for electron and photon irradiated samples. Previously it has been found that ion[3] , electron[4] and photon[5] irradiation leads to a marked adhesion enhancement of the metal film to the substrate, and it is generally believed that changes in chemical bonding across the interface generated by secondary electrons are responsible for the improved adhesion. These results will be discussed in terms of possible irradiation-induced chemistry involving H-bond breaking and subsequent bonding rearrangement at the interface[2,6] .

---

[1] see for instance Turos, A and Meyer, O. *Nucl. Inst. and Methods B* (1984) 92-97 and Arnold Bik, W.M. and Habraken, F.H.P.M. *Reports on Progress in Physics* v56 n7 (1993) 859-902

[2] Seiberling, L.E. *Nucl. Inst. and Methods B* 24/25 (1987) 526-530

[3] Griffith, J.E., Qui, Y. and Tombrello, T.A. *Nucl. Inst. and Methods* 198 (1982) 607

[4] Mitchell, I.V., Williams, J.S., Smith, P. and Elliman, R.G. *Appl. Phys. Lett* 44 (1984) 193

[5] Mitchell, I.V. Nyberg, G. and Elliman, R.G. *Appl. Phys. Lett* 45 (1984) 137.

[6] Tombrello, T.A. *Nucl. Inst. and Methods B* 24/25 (1987) 517-521.

High energy photoelectron diffraction data from GaAs surfaces.

A.E Bocquet†, R. Denecke*, R. Eckstein*, R.C.G Leckey†, J.D Riley† and L. Ley*

† Department of Physics, LaTrobe University, Melbourne, Australia
* Institut für Technische Physik II, Universität Erlangen–Nürnberg, Germany

Currently there is interest in applying the holographic principle to obtain real-space atomic images of crystal surfaces using measured photoelectron diffraction spectra. The acquisition of such data has traditionally relied on conventional single angle spectrometers resulting in excessively long collection times. This has been particularly inconvenient for users of synchrotron radiation due to the limited availability of beam-time. This poster displays data obtained by an unique toroidal analyser which simultaneously acquires a complete set of angle resolved data covering the full range of polar angles. Photoelectron diffraction spectra are obtained by rotating the sample through a range of azimuthal angles. Typical acquisition times ranged between 1–6 hours.

Enhanced spin g-factor and split Landau-level for AlGaAs/GaAs heterostructures in strong magnetic fields

W. Xu and M.P. Das
Department of Theoretical Physics,
Research School of Physics Sciences and Engineering,
The Australian National University, Canberra, ACT 0200 Australia

Abstract

Recent experimental data showed[1,2] that in the presence of the strong magnetic fields the spin g-factor for AlGaAs/GaAs heterojunctions will be enhanced by exchange interaction. The enhanced value of Landé factor g^* has been observed up to 10 in contrast with the bare value $g^* = 0.44$ for the bulk GaAs at low temperatures. The enhanced g-factor results in the split Landau-levels (LL) and asymmetric density of states (DOS) and in the saw-tooth-shaped Shubnikov-de Haas oscillations observed by our recent measurements[3].

In this work we study theoretically the enhanced g-factor and split LLs in heterojunctions in strong magnetic fields. The Green's function for the LLs, the electron self-energy, and the spin g-factor are calculated self-consistently including the electron interaction with impurities and with phonons. Our theoretical results show: 1) a split LL structure, i.e., the saw-tooth-shaped DOS; and 2) the oscillation of g^* with magnetic fields. We also look into the influence of sample mobility, electron density, temperature and spacer distance on the enhanced g-factor. The results obtained from our theoretical calculations agree with those obtained from the experimental measurements.

References

[1] R.J. Nicholas, R.J. Haug, K.v. Klitzing, and G. Weimann, Phys. Rev. **B 37**, 1294 (1988).

[2] B.B. Goldberg, D. Heiman, and A. Pinczuk, Surf. Sci. **299**, 137 (1990).

[3] A.A. Allerman, N. Hauser, C. Jagadish, and W. Xu, Appl. Phys. Lett., to be published.

PROCESS OPTIMIZATION AND CHARACTERIZATION OF Ni-Ge-Au OHMIC CONTACTS TO n^+ GaAs HETEROSTRUCTURES

Nancy E. Lumpkin[1], Gregory R. Lumpkin[2] and K. S. A. Butcher[3]

[1] Division of Radiophysics, CSIRO, P.O. Box 77, Epping, NSW 2121
[2] Advanced Materials Program, ANSTO, P.M.B. 1, Menai, NSW 2234
[3]Department of Physics, Macquarie University, NSW, 2109

A process for the formation of low resistance Ni-Ge-Au ohmic contacts to n^+ GaAs heterostructures was optimized using multivariable screening and response surface experiments [1,2]. Of seven variables screened by a fractional factorial experiment, the strongest effects were: total Ge+Au evaporative thickness, Ge:Au ratio and post-alloy cooling time. A response surface experiment run on these three variables enabled the development of an empirical model of ohmic contact resistance (R_c), with a predicted optimum value of 0.07 ± 0.03 Ωmm. Twenty confirmation runs yielded an average R_c of 0.07 ± 0.04 Ωmm, a reduction of 50% on the standard average process value of 0.14 ± 0.1 Ωmm.

A non-optimized ($R_c = 0.17$ Ωmm) and an optimized ($R_c = 0.04$ Ωmm) sample were characterized using SEM-EDS, cross-sectional AEM, and XPS techniques. The non-optimized sample has prominent surface dendrites and a heterogeneous microstructure consisting of blocks of $Ni_{0.5}Ge_{0.4}As_{0.1}$ in a matrix of $Au_{0.7}Ga_{0.2}As_{0.1}$ and Ge-rich phases. Some of the Ge-rich crystals extend downward 50 nm into the substrate and are epitaxial to the n^+ GaAs. The optimized sample has faint surface dendrites and a homogeneous fine-grained microstructure consisting of islands of $Ni_{0.5}Ge_{0.25}As_{0.25}$ in a matrix of $Au_{0.8}Ga_{0.15}As_{0.05}$. XPS depth profiles are in qualitative agreement with these results--the non-optimized sample shows a higher Ge content in the metal layer and less Ge in the GaAs substrate relative to the optimized sample.

This work shows that 1) multivariable experimental methods can be used to optimize Ni-Ge-Au ohmic contacts to n^+ GaAs, 2) the critical parameters for this process are Ge+Au layer thickness, Ge:Au ratio, and post alloy cooling time, and 3) lower R_c values are realized by effective diffusion of Ge from the metal layer into the GaAs substrate [3].

1. G.E.P. Box and N.R. Draper, Empirical Model Building and Response Surfaces, John Wiley, New York, 1987.
2. D.C. Montgomery, Design and Analysis of Experiments, John Wiley, New York, 1984.
3. T.S. Kuan, P.E. Batson, T.N. Jackson, H. Rupprecht, and E.L. Wilkie, J. Appl. Phys. **54**, 6952 (1983).

TUNNELLING CURRENT IN $Al_xGa_{1-x}As/Al_yGa_{1-y}As/GaAs$ DOUBLE BARRIER QUANTUM WELL STRUCTURES

T. Osotchan, V.W.L. Chin, X.K. Cheng and T.L. Tansley
School of Mathematics, Physics, Computing and Electronics
Macquarie University, NSW 2109.

In this paper, we present the simulation of the current-voltage characteristics of $Al_xGa_{1-x}As/Al_yGa_{1-y}As/GaAs$ double-barrier quantum well structure as functions of Al mole fraction and the width of each material layer. Using the Airy function as a basic wave function, the transmission coefficient with bias voltage was calculated by the transfer-matrix method[1]. Three typical device structures were studied by varying the Al mole fraction in each layer; 1) a single barrier when $x=y$ for bound-to-bound quantum well infrared photodetector (QWIP)[2], 2) a double barrier resonant tunnelling diode for $x=0$ and 3) a double barrier quantum well when $x<y$ for bound-to-quasibound QWIP. We describe the relationship between the resonance energies and the voltages where the peak currents occur for a number of design parameters.

---

1) R. Tsu and L. Esaki, Appl. Phys. Lett. **22**, 562 (1973).

2) S.R. Andrews and B.A. Miller, J. Appl. Phys. **70**, 993 (1991).

CLEAVAGE LUMINESCENCE IN SEMICONDUCTORS

D.G. Li, N.S. McAlpine and D. Haneman
Surface Physics Laboratory, School of Physics, University of New South Wales,
P.O.Box 1, Kensington 2033, Australia

Cleavage luminescence, as a novel experimental approach for the determination of surface and bulk structures of semiconductors, has been studied from *Si, Ge, GaAs, InP*, and there are different Ge_xSi_{1-x} alloys. All materials show a common characteristic in that there are at least two emissions in different wavelength regions. One group appears from cleavages in vacuum only, and is of relatively long duration for the elemental semiconductors, being of band gap origin, whereas the other emission appears also in air and is of short (20 μs or less) duration for all the materials. The latter signals are ascribed to surface defects, being apparently a property of many cleaved semiconductor surfaces.

[1] D.G. Li, N.S. McAlpine and D. Haneman, "Surface barriers and potentials from luminescence on cleaved Si, GaAs, and InP", Surface Science Letters, 281, L315, 1993.

[2] D.G. Li, N.S. McAlpine and D. Haneman, "Precision determination of long-wavelength cleavage luminescence energy and derivation of minimum surface state gap on clean cleaved Si Surfaces", Surface Science Letters, 289, L609, 1993.

STATES ABOVE A QUANTUM WELL IN TILTED MAGNETIC FIELDS

D. J. Miller and Z. Xiong
School of Physics
The University of New South Wales

There has been interest recently in the quasibound electron states in the continuum of levels above a quantum well (QW) or above the wells in superlattices. The states have potential applications in the context of photodetection and optical modulators.[1] It is interesting to consider the effect of magnetic fields on these states.

Consider first the bound states in the QW. The effects of the component of a magnetic field perpendicular to the growth direction of a QW are well-known. The component of the field perpendicular to the two-dimensional electron gas (2DEG) exerts a Lorentz force with a component in the growth direction and therefore competes with the strong confining electric field in the QW. Thus this component of the magnetic field has only a second order effect and is significant only for fields in excess of 10 T for a typical QW.

The effect of the parallel component of the magnetic field on states above the well will be quite different. The electrons are not confined and have large momentum in the growth direction above the well. Therefore the Lorentz force due to the parallel component of the magnetic field will be large and, unlike the case for bound electrons, that the parallel component of the field will have a significant effect on the energy states.

Using a semi-classical approach we have derived the energy levels and density of states of the magnetic-filed induced states above the QW and show that they have features which would be interesting to investigate experimentally.

1. See for example, C. Parks et al, Phys. Rev. B 45, 14215 (1992).

POROUS SILICON STUDIED BY SOFT X-RAY EMISSION SPECTROSCOPY

by R S Crisp
Department of Physics, The University of Western Australia, Nedlands, 6009,

and

D Haneman & R Sabet-Dariani.
School of Physics, The University of New South Wales, Kensington, 2033,

Porous silicon (PS) is usually prepared by anodising single crystal silicon surfaces in hydrofluoric acid and the resulting material, grown on the surface, exhibits a number of interesting and useful optical and electrical properties [1, 2]. We have sought information on the electronic band structure, and thus indirectly on the physical structure, through soft X-ray emission studies of the conveniently intense Si-L_{23} emission band which falls at about 135Å or 95eV.

Many workers [3], including ourselves, have previously studied c-Si, a-Si, a-Si:H and the oxides and carbides of silicon through the Si-L_{23} and Si-Kβ bands and the relationship of the band shapes to the structure and chemical bonding state of the Si atoms is in large measure understood. While the materials mentioned above are themselves more or less stable and well defined the same is not true for PS which incorporates significant amounts of carbon and oxygen presumably from uptake of atmospheric CO_2 and in the present study showed a tendency to convert to the oxide so that over periods of about one month exposure to atmosphere spectra show a significant trend towards that of silicon oxide.

Our studies show that PS does not resemble c-Si, rather it is related to a-Si and while large amounts of oxygen and carbon are incorporated into the material and seen by us through the O-Kα and C-Kα emission these are not held as the oxide or carbide of silicon. When PS samples are annealed at only a moderate temperature (250C) the Si-L23 band takes on a form more characteristic of a crystalline structure.

1. H. Takai and T. Itoh, J Appl Phys **60** 222 (1986)
2. N. Koshida and H. Koyama, Appl Phys Lett **60** 347 (1992)
3. R.S. Crisp, D. Haneman and V. Chacorn, J Phys C 21 975 (1988)
   G. Wiech and E. Z. Kurmaev, J Phys C 18 4393 (1985)
   A. Meisel et al eds, (1989) "X-ray Spectra and Chemical Bonding", Springer Verlag

Lattice Relaxation in Strained Layer Semiconductors Studied by in situ X-Ray Topography during MBE Growth

B.F.Usher, S.J. Barnett‡, G.F. Clark§, B.K. Tanner¶,
C.R. Whitehouse‡, A.D. Johnson‡, A.M. Keir‡, A.G. Cullis‡,
B.Lunn†, J.C.H. Hogg†, W. Hagston†and W. Spirkl¶.

Telecom Australia Research Laboratories
770 Blackburn Rd
Clayton VICTORIA 3168

Abstract

X-ray topography is able to image individual dislocations over large areas of sample and so is a useful tool with which to investigate the initial stages of lattice relaxation in strained-layer semiconductors. Topographs provide an insight into the origin of the first misfit dislocations, which define the critical thickness and make possible quantitive analysis of the initial strain relaxation process. A unique MBE facility which allows X-ray topography during the growth of strained layers is described, together with results from the first experiments.

‡DRA (Malvern),St Andrews Rd, Malvern, Worcs WR14 3PS, U.K.
§SERC Daresbury Laboratory, Warrington WA4 4AD, U.K.
¶Physics Department, University of Durham, South Road, Durham DH1 3LE, U.K.
†Department of Applied Physics, University of Hull, Hull HU6 7RX, U.K.

Empirical molecular dynamics calculations for the (001) and (111) reconstructed surfaces of diamond.

A. J. Dyson and P. V. Smith,
Department of Physics, University of Newcastle, Callaghan,
Australia, 2308.

Reconstructions of the C(001) and C(111) surfaces have been examined with molecular dynamics simulations, employing the Tersoff [1], Brenner [2] and modified Stillinger-Weber [3,4] empirical potential functions. Stable symmetric dimerization of the (001) surface is predicted by all three potentials. Spontaneous dimerization at room temperature was observed for the Brenner and SW potentials. For the (111) surface, the pi-bonded chain configuration is a local energy minimum for all three potentials, but is higher in energy than the unreconstructed surface. Activation barriers were estimated for the reconstructions by stepping the system in geometry space from the relaxed unreconstructed surface through to the reconstructed surface. Migration paths for adatoms on these reconstructed surfaces were also investigated, by calculating the energy of adsorbed carbon atoms at a grid of points over the surface unit cell. In this study we have observed notable differences in geometrical predictions between the three model potentials, such that choice of a particular potential function will strongly affect the results of any calculation where geometrical structure is important.

[1] Tersoff, J., *Phys.Rev.B* 61 (1988) 2879

[2] Brenner, D.W., *Phys.Rev.B* 42 (1990) 9458

[3] Stillinger, F.H., Weber, T.A., *Phys.Rev.B* 31 (1985) 5262

[4] Mahon, P., Pailthorpe, B.A., Backsay, G.B., *Phil.Mag.B* 63 (1991) 1419

AB INITIO HARTREE-FOCK STUDY OF THE B/SI(001)2X1 ADSORPTION SYSTEM

M.W.Radny and P.V.Smith
Physics Department, The University of Newcastle,
Callaghan, N.S.W., Australia, 2308

Many applications require semiconductor surfaces which are less reactive and more stable against contamination, oxidation, and so on. The adsorption of boron seems to provide one of the most promising processes for producing such stable surfaces because of its ability to form unique structures compared with those of other metals [1]. To address the issue of the optimum B/Si(001) surface geometry theoretically we have performed ab initio all-electron linear combination of atomic orbitals (LCAO) Hartree-Fock calculations for periodic slabs [2]. We have found four stable adsorption geometries which exhibit a (2x1) reconstruction of the boron-covered Si(001) surface. While two of these have non-dimer geometries which are identical to previously discussed structures [1], the most stable configuration is predicted to be an ad-dimer on top structure in which the B dimers are oriented parallel to the Si dimers in the same row. The fourth geometry is one in which boron is chemisorbed just below the relaxed silicon surface layer. This subsurface configuration is 0.08 eV higher in energy than the ad-dimer topology and 0.07 eV lower in energy than the two non-dimer adsorption geometries.

REFERENCES

[1] R.Cao, X.Yang, and P.Pianetta, J.Vac.Sci.Technol. B 11 (1993) 1455

[2] C.Pisani, R.Dovesi, and C.Roetti, Hartree-Fock ab initio Treatment of Crystaline Systems, Lectures Notes in Chemistry Vol. 48 (Springer, Heidelberg, 1988)

MEMORY SWITCHING AND QUANTUM EFFECTS IN AMORPHOUS HYDROGENATED SILICON

M. Jafar and D. Haneman
School of Physics, University of New South Wales

Amorphous hydrogenated silicon (ASIL) double Schottky switching diodes in which one contact is vanadium, formed to produce switching, can show discrete steps in the room temperature I-V characteristics in the ON state. These steps frequently occur at resistances of $h/2ne^2$, where n is an integer. We have explained [1] the quantum phenomena on the assumption that the metal from the vanadium electrode penetrates the amorphous silicon during the initial and essential forming treatment, and are now in the process of formulating a model to explain the switching phenomena based on the same assumption. Our recent experimental data show that the forming temperature of the device is in excess of 1100 K, which can allow diffusion. Depth profiling Anger Electron Spectroscopy (AES) shows that the vanadium electrode penetrates significantly into the amorphous silicon film in the formed devices. An elemental composition of the diffused metal region, over the less than 100 μm electrode cross section, has been obtained. Resistance plots at various temperatures have been made as an alternative method of checking the presence of vanadium particles in the amorphous silicon matrix. The results have been found to be consistent with conduction in granular structures [2].

[1] M. Jafar and D. Haneman, Phys. Rev. B 47, 10911 (1993).
[2] A. Moser and H. Rohrer, Solid State Comm. 17, 939 (1975).

CURRENT-VOLTAGE CHARACTERISTICS OF POROUS SILICON

R. Sabet-Dariani, N.S. McAlpine and D. Haneman
School of Physics, University of New South Wales

The recent discovery of visible-light emission from porous silicon (PS) has stimulated both experimental and theoretical investigation on application of Si to optoelectronics. Previously, we have measured photoluminescence, atomic composition [1], electroluminescence [2], and recently current-voltage characteristics. The I-V data were taken under single shot voltage pulse conditions, using a gold semitransparent top contact to the PS. The forward current increased at first slowly, and then approx. linearly with voltage pulse magnitude. The reverse current was much smaller. Exposure to the atmosphere clearly affected the I-V curves, indicating that the resistance of PS increased. Annealing treatments on the PS also caused change, with a slight increase in current at a given voltage. The data are discussed in terms of proposed structures of PS.

[1] R. Sabet-Dariani, D. Haneman, A. Hoffman, D.D. Cohen, J. Appl. Phys. 73, 2321 (1993).

[2] R. Sabet-Dariani, N.S. McAlpine, D. Haneman, J. Appl. Phys., submitted (1993).

GaAs conduction bands observed by Inverse Photoemission Spectroscopy.

W. Sheils, R.C.G. Leckey, and J.D. Riley
Physics Department, La Trobe University, Bundoora, Victoria. 3083

Because of the technological importance of GaAs, much experimental and theoretical effort has been devoted to elucidating its electronic band structure. The valence band structure of GaAs is considered to be well known due the correspondance between band calculations and the results of many Photoemission Spectroscopy (PES) experiments. PES has also been used to examine the conduction bands of GaAs that lie above the vaccuum level, where the agreement between theory and experiment is not so close. PES is unable to probe conduction band states that lie below the vacuum level. In this energy region Inverse Photoemission Spectroscopy is the preferred method of investigation.

This work compares the data from an inverse photemission study with theoretical bands generated by an LMTO calculation. The bands lying close to the conduction band minimum are the main focus of the study. The IPS experiments were performed in the isochromat mode at 11.4eV using a solid-state band-pass detector.

ELECTRICALLY DETECTED MAGNETIC RESONANCE FROM A SILICON p-n JUNCTION DIODE

Z. Xiong and D. J. Miller
School of Physics
The University of New South Wales

Electrically detected magnetic resonance (EDMR) is a relatively new technique which involves the detection of the change in the conductivity of a semiconductor due to a resonant change in the nonradiative recombination time of minority carriers. The technique is similar to optically detected magnetic resonance (ODMR) which involves the electron spin dependence of radiative recombination centres. EDMR is particularly useful because nonradiative recombination is dominant in indirect band gap semiconductors at room temperature. The resonant change occurs due to microwave induced transitions between energy levels split by a magnetic field. The transitions alter the proportion of singlet and triplet states and hence the recombination time because of the large difference in recombination rates from initial singlet and triplet states to the final singlet state

We report a modified theory of EDMR which is shown to agree extremely well with measurements of the EDMR signal from a commercial Si diode. The theory is tested against experimental results taken under different conditions including over the range 200 K to 350 K. It is shown that the signal can be enhanced by modulating both the microwaves and the applied magnetic field. By fitting the results at different temperatures, we have been able to determine the energy level relative to the conduction band edge of the recombination centre responsible for the EDMR signal. Thus both the EPR signature, which can lead to structural information about the recombination centre on the atomic level, and the energy level has been determined for the centre in the same experiment. Usually these two types of information have to be determined in independent experiments and related by inference. Unfortunately in this instance the EPR spectrum consists only of a single line but other EDMR signals with a more complex EPR spectrum could be investigated by the new technique reported here leading to identification at the microscopic level of centres with known energies.

RELATIVISTIC QUANTUM MECHANICS IN A PERIODIC POTENTIAL

A. J. Forsyth and A. E. Smith
Department of Physics
Monash University
Clayton, 3168, AUSTRALIA.

A theoretical analysis is outlined for the rigorous application of the Dirac equation to the problem of high energy electron scattering in condensed matter physics (e.g. electron microscopy) /1/. The so-called Fujiwara equation is obtained, this being a modified form of the Schroedinger equation /2/. In particular, a simple two level band structure problem is studied using the Dirac equation and first order perturbation theory analogous to the nearly free model (or 2 beam electron microscopy) for the non-relativistic Schroedinger equation /3,4/. It is shown that the degeneracy caused by the overlap of two relativistic free electron quasi-parabolae is split by a weak potential by a factor of $2|V_K|$, (and not $2|\gamma V_K|$ as one may intuitively expect) where V_K is the coefficient of the Fourier expansion of the periodic potential. The Dirac equation has been reduced to the relativistic Schroedinger equation by neglecting small spin terms /1/, but it can be shown that for a one-dimensional two level system that the spin does not contribute to the band gap at the Bragg plane, and that its contribution far from the Bragg plane is minimal.

The solution of the nearly free electrons converges to the free electron solution far from the Bragg plane on the scale of V. While the rate of convergence for the non-relativistic nearly free electron parabolae is very rapid, the non-relativistic nearly free electron parabolae do not seem to converge to the relativistic free electron solution within the space of a Brillouin zone /5/. This indicates that the free electron picture may not be an accurate picture in the relativistic case.

/1/ D.M. Bird and B.F. Buxton, Proc. Roy. Soc. London, A379, 459-479 (1982).
/2/ K. Fujiwara, J.Phys. Soc. 16, 2226-2238 (1961).
/3/ N. W. Ashcroft and N. D. Mermin, Solid State Physics, Holt, Reinhart and Winston (1976).
/4/ C. Kittel, Introduction to Solid State Physics, e.g. 4th edition, John Wiley and Sons Inc., New York (1971).
/5/ A.J. Forsyth, Honours Thesis, Monash University (1993).

Lifetime and Bistability in Electron Tunneling in a Double Barrier Structure

D. Fisher and C. Zhang

Department of Physics, University of Wollongong, NSW 2500, Australia

Abstract

The level width of a quasibound state due to electron tunneling in a double barrier resonant tunneling structure in an external electric field is investigated. The result for the width rests on the S-matrix resonant tunneling formalism. The inverse lifetime obtained in this manner is free of small parameter expansion and is exactly the width at the half maximum of the resonant tunneling rate. It is found that for a system exhibiting current bistability, the level broadening of a quasibound state is not a monotonic function of the applied bias and has a minimum at some intermediate field strength. With the use of the exact tunneling rate, we were able to incorporate the effect of electron-electron interaction in the resonant tunneling current and obtained multiple stable tunneling states.

HETEROJUNCTIONS OF CdSe AND AMORPHOUS SILICON

S. Wu and D. Haneman
School of Physics, University of New South Wales

We have fabricated and analysed hetero-junctions of n:CdSe and p-type amorphous hydrogenated silicon (p:APIL) using previous techniques.[1] The mechanisms of current flow at positive and reverse biases were studied. Capacitance-voltage behaviour indicated the presence of interface states. Optical internal photo-emission measurements under various bias conditions showed that the band offsets for the cell structures are 0.025 eV and 0.056 eV for conduction and valence bands respectively.

[1] S. Wu and D. Haneman, J. Appl. Phys. 73, 265 (1993).

A High Temporal Resolution Solid State Thermal Neutron Detector

N.S.McKean*, R.L. Davis *, A.Bartel* , E.N. Bakshi* .

*Physics Department , .Swinburne University of Technology

* Neutron Scattering Group, A.N.S.T.O

Neutron diffraction is a major method for investigation of material structure at a molecular level and has applications in investigation of metals , ceramics , polymers and organic molecules. There are two major methods , **1.** diffraction using a monochromatic beam and **2.** diffraction based on the Laue time-of-flight method.[1,2,3,4,5] The Laue time-of-flight technique has considerable advantage , due to the total utilisation of the neutrons.The integrated intensity of the Laue-spot from a single crystal in simple form is

$$\mathscr{I}^{\lambda} = i(\lambda)\lambda^4 \frac{N_c^2 F^2}{2\sin^2\theta}$$ where $\mathscr{I}^{\lambda}$ is the integrated intensity

λ is the wavelength of neutrons

and F is the structure factor.

To extract structural information care has to be taken in evaluating λ since $R^{\lambda} \propto \lambda^4$.The design goal was to build a thermal-neutron detector capable of a time resolution at least two orders of magnitude better than that currently available .The thermal-neutron detector consists of a thin foil of Gadolinium on which a beam of thermal-neutrons is incident , and whose isotropically scattered internal conversion electrons[6] are detected by a Passivated Implanted Planar Silicon (PIPS) detector .This detector will be incorporated in a time-of-flight diffractometer with much greater wavelength resolution , which will enable greater precision in determination of molecular structure of materials.The detector will also be applied to a new instrument currently being designed at HIFAR[8,9] based on the "Time Correlated Diffraction Method" [7].

References

1. WILSON , S.A. and COOPER , M.J. (1973) *Acta crystallogr.* **A29** , 90-1.
2. BACON , G.E. *Neutron Diffraction* (Clarendon Press).
3. HUBBARD , C..R., et al. (1972). *Acta crystallogr.* **A28** , 236-45.
4. BRUGGER , R.M. et al (1967). *Phys. Lett.* **24A** , 714.
5. BURAS , B. (1967) . *AEC - ENEA Seminar* , Santa Fe , New Mexico.
6. AMALDI , E and RASETTI , F ., (1939) Ric. Sci. **10** , 115.
7. BAKSHI , E.N.(1990). "Time -Correlated Diffraction", Meas.Sci.Tecnol.,1,1990,1123-1125.
8. BARTEL , A , McKEAN , N.S , DAVIS , R.L , BAKSHI , E.N, (1992) "An Instrument for Evaluating a new Time-Correlated Diffraction Method" , Proc. of ACA , **20** , 149.
9. BARTEL , A , McKEAN , N.S , DAVIS , R.L , BAKSHI , E.N , " High Frequency Piezoelectrically excited quartz crystals as neutron beam monochromators/modulators", In preparation.

Scanning Deep Level Transient Spectroscopy Using An MeV Ion Microprobe.

J.S.Laird, R.A.Bardos, G.R.Moloney, A.Saint and G.J.F.Legge
MIcro-Analytical Research Centre (MARC)
School of Physics, University of Melbourne

Abstract:

The existence of impurities and intrinsic defects in a semiconductor greatly alter the electrical characteristics of a device through their activation in the form of deep levels in the bandgap. Using techniques such as Deep Level Transient Spectroscopy one is able to characterize such levels and their affect on device performance . For a more complete understanding of the role of traps it is advantageous to be able to spatially map the traps and their concentrations across a device.

Although in the past the SEM has been used to such ends, its limited range of less than a few microns and the large degree of starggle severly limit the range of its applications. We present here work carried out to date on the development of a new technique termed Scanning Ion Deep Level Transient Spectroscopy. The charge collection physics underlying the technique as well as the data collection system and current results shall be discussed. Further , we also present the various modes in which the data may be collected to obtain a more comprehensive view of the sample being studied.

Zeeman Effect of the Shallow Acceptors Boron, Gallium and Thallium in Germanium at Magnetic Fields up to 7T*

R.J. Baker, P. Fisher, C.A. Freeth, D.S. Ryan and R.E.M. Vickers
Department of Physics, The University of Wollongong, Northfields Ave, Wollongong 2522.

Recent[1,2] observations of the effect of high magnetic fields on the spectra of boron and gallium impurities in germanium have revealed measurable and significant differences in the ground states of these two impurities. These studies were made with **B**, the magnetic field, along <100> directions. Measurements have now been extended to thallium in germanium for **B**||<100> and to boron, gallium and thallium for **B**||<111>. These three group III impurities have been chosen because their ionisation energies span the range covered by all five of the shallow acceptors, *vis.*, boron, aluminium, gallium, indium and thallium. The magnitude of the ionisation energy should indicate the relative effects of the central cell corrections for these impurities and thus a systematic variation in the Zeeman splitting of the ground state might be expected. This is indeed found to be the case, the linear splitting for **B**||<100> of the $\pm\frac{1}{2}$ Zeeman states of the ground state decreases with increasing binding energy of the acceptor whilst the splitting of the $\pm\frac{3}{2}$ state increases. These data will be presented along with those for the excited states of the two lowest energy transitions, the G and D lines. For the latter states some very dramatic interaction effects are observed which are predicted by recent theory[3,4]; comparisons between theory and experiment will be given.

* Work supported by the Australian Research Council and the University of Wollongong Board of Research and Postgraduate Studies.

1. G.J. Takacs, R.E.M. Vickers, P.Fisher and C.A. Freeth, Mater.Sci. Forum **117-118**, 123 (1993); P. Fisher, G.J. Takacs, R.E.M. Vickers, and A.D. Warner, Phys Rev B **47**, 12999 (1993)
2. Seventeenth Australian Institute of Physics Condensed Matter Physics Meeting, Wagga Wagga 1993
3. J. Broeckx and P. Clauws, Solid State Commun. **28**, 355 (1978); J. Broeckx et al., J. Phys. C **12** 4061 (1979)
4. W.O.G. Schmitt, E Bangert and G Landwher, J. Phys. Condens. Matter **3**, 6789 (1991)

Channeling Contrast Microscopy of defects in Type II-VI MSM Photodetectors

Lachlan C. Witham and David N. Jamieson,
Micro Analytical Research Centre,
School of Physics,
University of Melbourne,
Parkville, 3052.

ABSTRACT

Characterization of defects in MSM photodetectors fabricated from Mercury Cadmium Telluride (MCT) was performed using Channeling Contrast Microscopy (CCM) with a 2MeV He ion beam. Devices found by this technique to contain defects correlated with anomalies in the dark current - voltage characteristics of these devices. A quantitative correlation between the degree of defectiveness of the MCT active layer and the size of anomalies in the current - voltage characteristic was also found.

IN-SITU CONTROL OF SOLIDS OXIDATION.

WP 67

I.L.Skryabin and J.M.Bell
Department of Applied Physics, University of Technology, Sydney
P.O. Box 123 Broadway NSW 2007.

At present methods of oxygen determination in solids based on interaction with electromagnetic wave (ESCA), collisions with electrons (AES) or ions (SIMS) are broadly used. Positive features of these methods are high space resolution (up to 1μm) and absolute sensitivity (up to 10^{-12}g). However, the possibilities of application of these methods are restricted by high cost of equipment, calibration problems and special sample preparation requirements.

The method of differential thermal analysis (DTA) where the increase or decrease of the amount of oxygen in the sample is estimated by sample's mass variation during oxidation is also well known (*in situ* technique). However, this method does not take in account the interaction with side gases, which can cause significant errors.

In present work we discussed the inverse DTA technique - method of gas differential electrochemical analysis (GDA). Here the oxygen input or output to the sample is measured by variation of it's amount in gas phase. It's advantage is simplicity and low equipment cost. The mass sensitivity in GDA is the same as in DTA (10^{-10}g). The scheme of GDA method for oxidation process control (in constant oxygen partial pressure) is presented on figure.

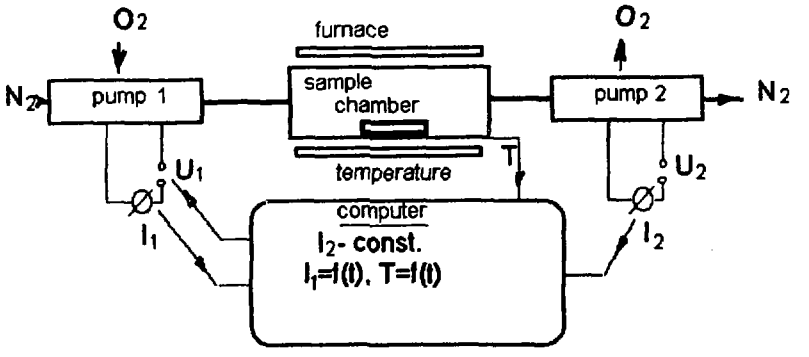

The electrochemical oxygen pump 1 is used for pumping oxygen from atmosphere to a system. The partial pressure of oxygen in system is a function of 1st pump current I_1 and nitrogen flow rate. The 2nd pump is pumping oxygen out of the system. If there is no oxygen consumption in sample chamber then $I_1=I_2$. In the case of oxidation I_1-I_2 is a measure of oxidation rate (g/s). The constant pressure of oxygen in a sample chamber means I_1-constant.. For this purpose computer varies value of U_2. The difference between new value I_2' and I_2 is the measure of oxidation rate in a constant oxygen partial pressure.

As an example, oxidation curves of coated and uncoated graphite presented. Analytical characteristics of system as a function of system geometry discussed. The system can operate in a noble gas environment or in vacuum

ION BEAM MIXING OF ISOTOPIC BILAYERS

C J Fell,
Dept. of Physics, University of Newcastle, Callaghan, 2308

The field of ion beam irradiation as a means of materials modification stands to benefit from an increased understanding of the processes which occur at an atomic level. Ion beam mixing studies can contribute to this understanding by revealing the dependence of the magnitude of mixing on physical, mechanical, thermal and electronic properties of the solid, as well as on different ion beam parameters.

Recent studies of metallic bilayers suggest that the broadening, due to irradiation, of a sharp layer interface may be strongly dependent on the rate of cooling of the collision cascade, which in turn depends on the efficiency with which heat is transferred between the lattice and the electronic system.

A Secondary Ion Mass Spectrometry study is to be carried out using specially grown monocrystalline bilayers of ^{58}Ni / ^{60}Ni so as to eliminate the effects of preferential sputtering, chemically driven mixing, grain boundary diffusion and microtopography. The results will be directly comparable with other low-energy mixing results for Cu, which has a similar mass to Ni, but a weaker electron-phonon coupling and hence a lower cascade cooling rate.

An important aspect of the work is the preparation of high quality single-crystal thin films. Ni layers have been grown on the (110) surface of pure Ni and verified for crystallinity using Reflection High-Energy Electron Diffraction and Rutherford Backscattering channelling analysis. RHEED is used to confirm the two-dimensional crystallinity of the surface before and after deposition of each layer, and channelling used to confirm bulk film crystallinity.

Analysis of a Ni (110) surface using RHEED at 9 kV shows a streak spacing which corresponds to a lattice spacing of 2.47 $\pm$ 0.09 Å. This value is consistent with an unreconstructed Ni surface along the $<110>$ direction, which has a row spacing of 2.49 Å. Results of channelling analysis on a Ni (110) substrate using 2 MeV $^{4}He^{++}$ shows a χ_{min} value of 0.027, which agrees with the theoretically attainable value of 0.020.

A Study of the $Cu_3Au(110)$ Surface Using Low Energy Ion Scattering

F.M.Zhang, Y.G.Shen, B.V.King and D.J.O'Connor

Department of Physics, The University of Newcastle,
Newcastle, NSW 2308, Australia

ABSTRACT

The surface composition and structure of $Cu_3Au(110)$ have been investigated by using combination techniques of low energy ion scattering spectroscopy and low energy electron diffraction. Using 1 keV Li^+ and He^+ ions, the compositions of the first and second layers have been determined using selected scattering geometries from the measurements of the ion intensity and from comparison of the scattered ion intensity with calibration measurements on pure Cu(110) and Au(110). The results indicate a surface composition of 55% Cu-45% Au in the first layer, while 77% Cu-23% Au in the second layer at room temperature respectively. The Au enrichment of the first layer is compensated by the Au depletion of the second layer. The temperature dependence of the surface composition at temperature range from 300 K to 650 K has also been measured. The surface structure has been obtained by analyzing the Li^+ incident angle dependence along the [001], [$1\bar{1}2$], [$1\bar{1}1$], [$3\bar{3}2$] and [$1\bar{1}0$] azimuthal orientations on the basis of the shadowing and blocking features. The results demonstrate that the Au atoms of the first layer are not clustered in domains, and that the atoms of the first layer are all in the same plane within the experimental accuracy of 0.05 Å. This is consistent with our LEED observation, showing 2x1 structure. The evidence has been further tested by using 2 keV K^+ ion scattering along the [001] azimuth, showing the Au-Au double scattering peaks.

Contact Anomalies in the Integral Quantum Hall Effect

B W Ricketts[1], L D Macks[2] and M M R Sovierzoski[1]

[1] CSIRO Division of Applied Physics, PO Box 218, Lindfield 2070
[2] School of Physics, University of New South Wales, PO Box 1, Kensington 2033

The use of the integral Hall effect as a precise resistance standard is now routine [1]. The standard is normally realized by using a Hall bridge of GaAs/AlGaAs heterostructure. Each Hall bridge has to be carefully characterized to ensure that the quantized Hall resistance steps are in fact flat and that any effect on the resistances of the non–zero temperature of the Hall bridge is known to the required accuracy.

During the characterization of the Hall bridges the greatest difficulties are usually caused by the ohmic contacts that connect the two dimensional electron gas to the measuring circuit. Some contacts are grossly non–ohmic and can be quickly identified but others have deficiencies that are only revealed during precision measurements. This paper discusses a contact anomaly of the latter type found in a GaAs/AlGaAs Hall bridge with diffused indium contacts. The results obtained are discussed in relation to recent publications on the effects of contacts on the integral quantum Hall effect [2].

[1] GW Small, BW Ricketts and PC Coogan, IEEE Trans Instr. and Meas., 38, 245, 1989

[2] S Komiyama et al, Phys. Rev., 40, 12566, 1989

An Application of X-Ray Computerized Tomography for Examining the Internal Features of Materials

Lee G. N., Kijek M. M. and Millar J.J.

Department of Applied Physics, Royal Melbourne Institute of Technology,
GPO Box 2476V, Melbourne, Vic 3001, Australia.

Abstract - Most of the advanced materials are either composites or metal alloys and are designed to have specific properties required for a particular application. Despite the advantage of the customised properties provided, most of these materials are difficult and complicated to produce. Inappropriate manufacturing or handling processes may result in internal defects which are not visible from the outside. Some of the typical defects are voids, cracks, porosity, delamination, non-uniformities and fibre misalignment. A non-destructive method is desirable to inspect the internal features of materials. Computerized tomography has been successfully used in examining the internal features of various materials. A brief introduction of the technique and some application examples are presented. Experimental results for example the propagation of fracture formed during solidification in the AZ91 Mg Alloy (sample courtesy Material Science Divison, CSIRO) and porosity distribution within a bone (sample courtesy Medical Radiation Science Department, RMIT) are included.

ANALYSIS OF COMPOUND SEMICONDUCTOR MATERIALS USING HEAVY ION RECOIL SPECTROMETRY

Scott R. WALKER[1], Peter N. JOHNSTON[1], Ian F. BUBB[1], Warren STUDD[1], David D. COHEN[2], Nick DYTLEWSKI[2], Mikael HULT[3], Harry J. WHITLOW[3], Carina ZAHRING[4], Mikael ÖSTLING[4], Margaretha ANDERSSON[5] and Jarrod W. MARTIN[6].

[1]Department of Applied Physics, Royal Melbourne Institute of Technology, GPO Box 2476V, Melbourne 3001, Australia
[2]Australian Nuclear Science and Technology Organisation, PMB 1, Menai 2234, Australia
[3]Department of Nuclear Physics, Lund Institute of Technology, Sölvegatan 14, S-223 62, Lund, Sweden
[4]Department of Solid State Electronics, The Royal Institute of Technology, Box 1298, S-164 28, Kista, Sweden
[5]Institute of Chemistry, Uppsala University, Box531, S-751 21 Uppsala, Sweden
[6]School of Physics, University of New South Wales, Kensington, Sydney

Heavy Ion Recoil Spectrometry has been used to examine various semiconductor material systems which cannot easily be studied using convensional ion beam techniques such as RBS. The technique enables the determination of seperate energy spectra for individual elements. This enables it to be used in many situations where RBS is inappropriate due to the superimposition of signals in the backscattering spectrum.

We have employed Recoil Spectrometry to study; light element impurity concentrations, stoiciometry and metalisation contact systems for various compound semiconductor materials.

The experiments were performed at the ANTARES (FN Tandem) accelerator facillity at Lucas Heights using 61-91 MeV ^{127}I ions. The incident ^{127}I ions cause nuclei of the sample to recoil following Rutherford scattering. The recoiling target nuclei are then analysed by a Time Of Flight and Energy (TOF-E) detector telescope composed of two timing pickoff detectors and a surface barrier (energy) detector. From the time of flight and energy, the ion mass can be determined and individual depth distributions for each element can be obtained.

ACKNOWLEDGEMENTS

The authors wish to acknowledge the support of the Australian Institute of Nuclear Science and Engineering (AINSE), the Australian Department of Industry, Technology and Commerce (DITAC), the Swedish Institute and the Craaford Foundation. SRW also acknowledges the support of an Australian Postgraduate Research Award and an AINSE Postgraduate Research Award. The Si_xGe_{1-x} and $Al_xGa_{1-x}As$ structures were produced at the Australian National University Department of Electronic Materials Engineering.

Carbon and Oxygen Analysis in MOCVD Grown HgCdMnTe and AlGaAs by Charged Particle Activation.

Warren B. Studd, Scott R. Walker, Peter N. Johnston and Ian F. Bubb

Department of Applied Physics, Royal Melbourne Institute of Technology. G.P.O. Box 2476V, Melbourne 3001 Australia

Metal Organic Chemical Vapour Deposition (MOCVD) offers the capability of epitaxial growth on various substrates with high wafer throughput but is often subject to carbon and oxygen contamination. The impurity level is a critical factor in the performance and reliability of devices manufactured from these materials. There are few suitable chemical methods with sufficiently high sensitivity to make them suitable for the determination of trace carbon and oxygen in semiconductor materials.

The suitability of Charged Particle Activation Analysis (CPAA) as an absolute method to determine low concentrations of light impurities or dopants at the ppm level has been investigated at RMIT. In particular the levels of carbon and oxygen in MOCVD grown $Hg_{1-x-y}Cd_xMn_yTe$ and $Al_xGa_{1-x}As$ thin films have been examined by CPAA using the $^{12}C(^3He, \alpha)^{11}C$ and $^{16}O(^3He, p)^{18}F$ reactions.

Acknowledgments

The work has been supported by the Australian Research Council. HgCdMnTe samples supplied by Telecom Research Laboratories. AlGaAs samples supplied by Department of Electronics Materials Engineering, Australian National University.

New Automatic RBS/Channeling System for Thin Film Material Analysis.

L.S. Wielunski and M.J. Kenny
CSIRO, Division of Applied Physics
P.O.Box 218 Lindfield, NSW 2070

Abstract

Rutherford Backscattering Spectrometry (RBS) is an ion beam analysis technique used in many fields. The high depth (20nm) and mass (1amu) resolution of RBS make this technique very useful in thin film material science including semiconductors, high tc superconductors, wear and chemical resistant coatings as well as new biomaterials and biosensors. The use of ion channeling in combination with RBS creates a powerful technique which can provide information about crystal structure and quality in addition to mass and depth resolution. The presence of crystal defects such as interstitial atoms, dislocations, dislocation loops or twins can be detected and profiled. In many cases in order to fully identify defect type or position the multidirectional channeling analysis is required. In complex cases the total analysis time can be many hours and is very strong function of the goniometer operator and its skill in localising different channeling directions used in the analysis.

In this paper we describe the new automatic RBS/channeling system which is designed to automatically collect RBS data in fixed position and/or rotational random and/or channeling position for up to forty individual samples without operator assistance. Different channeling directions can be chosen by selecting initial position (direction) within 5 deg from selected channeling orientation. The automatic channeling procedure is based on computer controlled two dimensional angular scanning within 5 deg from initial direction. This procedure is fast, very effective, reliable and independent of the operator. The system is equip with RBS data analysis program "HYPRA" which allows analysis of complex thin film structures in very short time.

The examples of RBS and channeling analysis of different materials and thin film structures will be shown.

DETERMINATION OF THE DEUTERIUM ORDER-DISORDER STRUCTURE TRANSITION IN Pd-$DO_{.65}$ at '50K'

S J Kennedy[1], E Wu[2], E H Kisi[3], E M Gray[2] and B J Kennedy[4]

[1] Neutron Scattering Group, ANSTO, PMB 1, Menai, NSW 2234
[2] School of Science, Griffith University, Nathan, Queensland 4111
[3] Department of Mechanical Engineering, University of Newcastle, NSW 2308
[4] Department of Inorganic Chemistry, University of Sydney, NSW 2006

Anomalies in the heat capacity and the electrical resistance of Palladium Hydride at ~50K were first reported in the 1950's(1). Since then a number of experimental techniques have been applied in attempts to determine the origin of these anomalies. These techniques have included XRD and neutron diffraction. All crystallographic studies have been hampered by the sluggishness of this transition (ie it takes several days to complete). Early powder diffraction results suggested a phase transition involving migration of H (or D) atoms from sites of octahedral symmetry to sites of tetrahedral symmetry(2). Later evidence from single crystal neutron diffraction studies indicated an order-disorder transition within the octahedral sites(3). Neither description has found global support because conclusive evidence has not been produced.

We have just completed a time resolved powder neutron diffraction study of the structural transition in b-Pd-$D0_{.65}$ at 54K using the new Medium Resolution neutron Powder Diffractometer (MRPD) at the HIFAR research reactor. Our results show that the latter description of an order-disorder transition of the octahedral sites is correct. The 'ordered' crystal structure can be accurately described with space group Pm3n and by doubling the lattice constant from the high temperature structure (Fm3m). The transition to the ordered phase involves diffusion from specific 'D' sites from nearest 'D' neighbour positions to second nearest 'D' neighbour positions. This eventually produces 97% and 33% occupancy of the favoured and unfavoured sites respectively.

(1) D M Nace and J G Aston, J. Amer. Chem. Soc., 79, 3623 (1957)
(2) G A Ferguson, A J Schindler, T Tanaka and T Morita, Phys. Rev., 137, A2 (1965)
(3) I S Anderson, C J Carlile and D K Ross, J. Phys. C: Sol. State Phys., 11, L381

OXFORD SCIENTIFIC

Regardless of your application, no matter how small or large consult our experts at Oxford Scientific. If your research requires any of the following we can help.

- **Cooled and ambient PMT Housings**
- **Cryogenic Instruments and Cryostats**
- **High voltage power supplies**
- **MCA Cards**
- **Mossbauer systems**
- **Open and closed cycle refrigeration systems**
- **Powder X-Ray diffraction instruments**
- **Scanning surface resistance analyser**
- **SQUID systems and sensors**
- **SEM's and TEM's**
- **Scanning magnetic microscope**
- **Superconducting magnet systems**
- **And More**

CS-Series Closed-Cycle Systems

Features:

Refrigerator

- No consumption of liquid or gaseous nitrogen or helium
- Twenty years of proven reliability
- Compact, inline profile - operates in any orientation
- Only two moving parts - easily maintained in the field
- Custom interfaces available
- Vacuum shroud rotatable - 360° under vacuum

OXFORD SCIENTIFIC
P.O. Box 232, RYDALMERE NSW 2116
PH: (02) 638-1244 FAX: (02) 638-0878

*** APTEC * AMERICAN MAGNETICS * APD * BERTAN**
*** CRYO-INDUSTRIES * CONDUCTUS * ISI**
*** PRODUCTS FOR RESEARCH * RMC * RANGER**
*** SCINTAG**

Investigation of Ferroelectricity in $(CH_3NH_3)HgCl_3$

Z. T. Jiang, Bruce D. James and John Liesegang
La Trobe University, Bundoora, VIC 3083, Australia

Alkyl Ammonium Halides form different double salts with mercury (II) halides. A number of the complexes have the formula $(R_XNH_{4-X})HgX_3$ where R=alkyl, X=Cl, Br, and I. Some of these complexes exhibit structural phase transitions with change in physical properties, e.g. ferroelectricity. One of these complexes, $(CH_3NH_3)HgCl_3$, undergoes a ferroelectric phase transition at $T_C \approx 60°C$ and has been extensively studied by X-ray diffraction[1], NQR[2], and Dielectric[3] measurements. A hydrogen bond, N-H---Cl, is contained in $(CH_3NH_3)HgCl_3$ to link the cation and anion; however, the phase transition is associated with a disordering of the $CH_3NH_3^+$ cation dipole moment. In this paper, we investigate the piezoelectric phase transition of this crystal using IR, XPS, DSC, and a Piezoelectricity Test. Temperature-dependent XPS spectra, core level binding energy shifts of N(1s), Cl(2p), and Hg(4f) indicate that the charge distributions on these atoms are totally different in the ferro- and paraelectric phases. The IR spectra are reported for the cation group $(H_3C\text{-}NH_3)$ in the temperature range of 25-91°C. Analysis of the thermosensitive bands also confirms the phase transition. The observed temperature dependence of the splitting of the ν_9 (NH_3 asym. deformation) mode[4] and the disappearance of the ν_6 (C-N torsional) mode around 60°C have been attributed to a dynamical tumbling motion of the $H_3C\text{-}NH_3$ cation through the order-disorder transition. Surprisingly, N-H stretching modes fail to show any temperature dependence through T_C. These results support the notion that H-bonding is not central to the existence of ferroelectric behaviour in this crystal.

References:

[1]. M. Korfer and H. Fuess, ***Zeitschrift fur Kristallographie***, **183**, pp. 27-41, 1988.
[2]. F. Milia and M. Voudouris, ***Solid State Communication***, **60, 3**, pp.261-2, 1986.
[3]. M. Taya, T. Asaji and D. Nakamura, ***Phys. stat. sol. (a)***, **114**, pp.157-60, 1989.
[4]. P. S. R. Prasad and H. D. Bist, ***J. Phys. Chem. Solids***, **50,** pp.1033-1040, 1989.

EXTERNAL CONTROL OF MICROWAVE PROPERTIES OF DIELECTRIC MATERIALS

D.S. Maddison, P. Jewsbury, A. Amiet
maddison@ssmd.mrl.dsto.gov.au, jewsbury@ssmd.mrl.dsto.gov.au, amiet@ssmd.mrl.dsto.gov.au
DSTO-Materials Research Laboratory, PO Box 50, Ascot Vale, VIC, 3032, Australia

Certain microwave applications call for the need to be able to control the dielectric properties of a material such as permittivity. Uses might include applications such as phase shifters used in electronically scanning "phased-array" antennas, time delay lines in microwave radar sets or other applications where the ability to alter the dielectric properties of a material is needed. Materials whose dielectric properties can be externally altered fall into the realm of the emerging class of "smart" materials and offer potential cost savings (due to simplicity) and new applications. Materials with this property include piezoelectrics, ferromagnetics, liquid crystals and electrorheological fluids.

Currently we are investigating the use of piezoelectric materials such as lead zirconate titanate (PZT) and electrorheological fluids. Piezoelectric materials have the ability to alter the dimensions of their unit cells and/or realign grain orientations under the influence of electric fields and thus their dielectric properties can potentially be altered. Electrorheological fluids comprise of polarisable particles suspended in an insulating fluid, in our case the particles are metallic and are coated by a hydrophilic polymer suspended in a hydrophobic oil. A dipole is induced on each of the particles when an electric field is applied and the particles then form filamentary structures, the size of which is determined by the applied field. The reorganisation of the central metallic cores influences material dielectric properties.

Measurements of the complex permittivity of samples were performed with an HP 8510B network analyser. The samples under investigation were placed between two horns about 30 cm apart and the transmission component of the scattering matrix (S-matrix) was determined. The complex permittivity was determined from this S-matrix component. The following preliminary results have been obtained and further results will be presented at the conference. A sample of unpoled PZT was obtained and an electric field was applied to it whilst the sample was simultaneously probed with an HP microwave network analyser. The applied field was found to cause an increase in the permittivity of the sample. This was determined to be due to poling of the sample because once the sample was poled there was only a modest change in permittivity with applied field. Another sample was poled before measurement and it was found that for one sample orientation the imaginary permittivity increased as the electric field was increased but this did not happen when the electric field was reversed. Changes were also detectable upon the application of an electric field to an electrorheological fluid.

The assistance of Louis Chew is gratefully acknowledged.

WEAR AND FRICTION MEASUREMENTS ON CVD COATED CARBON ALLOY BEARING SURFACES

M.J.Kenny, L.S.Wielunski, M.D.Scott, R.A.Clissold and Q.Shaikh(+)
CSIRO, Division of Applied Physics, PO Box 218 Lindfield, NSW, 2070

A series of ball-on-disc wear and friction measurements has been made for surfaces which have a CVD layer deposited on a carbon substrate (fine grain POCO graphite or carbon fibre reinforced carbon). The CVD process produces a coating which is typically fifty microns thick and is itself moderately hard. The deposited surfaces were then polished using progressively finer materials beginning with 800 mesh SiC and finishing with Polipla compound containing submicron alumina. Ion Irradiation with nitrogen ions at a dose of 2 x 10^{16} ions cm^{-2} was then used to produce a radiation damaged wear resistant layer 0.15 microns thick(1).

Ball-on-disc wear measurements were made using a Swiss / CSEM tribometer machine maintaining the same parameters for both irradiated and unirradiated sections of the same ball so as to eliminate any influence of alloy composition on the surface. Both upper curved surfaces were run against the same irradiated flat which showed no evidence of wear due to its larger exposed area. The consistent environment was distilled water, 200 RPM (9 mm track radius) lower contact velocity and 40 g load. The flattened contact zone was 180μ diameter and wear occurred in this area only. After 60000 revolutions approximately the same diameter scar was observed in both instances, but the volume of material removed as measured by interferometry showed the irradiated specimen shed only half as much material as the unirradiated specimen.

The friction coefficient was measured simultaneously and found to be 0.11 for the unirradiated sample and 0.07 for the irradiated sample as top contact.

It is therefore possible to produce a carbon bearing surface with low friction coefficient and high resistance to wear suitable for use in environments which are hostile to other bearing materials.

(1) M.J.Kenny, J.T.A.Pollock and L.S.Wielunski, Nucl. Instr. and Meth. in Research B39 (1989) 704

(+) Visiting Scientist at CSIRO

GROWTH AND PROPERTIES OF CARBON NITRIDE THIN FILMS

Sunil Kumar and T. L. Tansley
Solid State Science and Technology Laboratories
Physics Department, Macquarie University
Sydney, NSW 2109.

Abstract

The current interest in carbon nitride (C-N) thin films stems from the recent theoretical work by Liu and Cohen predicting the extreme hardness of this material, comparable to or greater than that of diamond. The relatively shorter bond length (1.47 Å) and low bond ionicity (~ 7%) of the C-N bond as compared to ß-Si_3N_4 with a Si-N bond length of 1.74 Å and bond ionicity of 30% suggest the superiority of the former material over the latter in terms of hardness and high temperature applications. Apart from its predicted extreme hardness, carbon nitride can prove to be a remarkable novel material for device applications such as an insulator in MIS structures, much like its homolog, Si_3N_4. The formation of C-N thin films has recently been reported, employing deposition techniques such as plasma CVD, magnetron sputtering and ion assisted dynamic mixing.

In the present paper, we report on the growth of carbon nitride thin films on various substrates using a purpose-built low power radio frequency reactive sputtering system. The results on the morphology, structure and optical properties of the films thus deposited, obtained using scanning electron microscopy (SEM), X-ray photoelectron spectroscopy (XPS) and optical spectrophotometry, are presented. A quantitative analysis using X-ray photoelectron spectroscopy shows that the films contain about 80 at.% C and 20 at.% N. Scanning electron microscopy suggests a mixture of amorphous and crystalline phases present in the films. Nitrogen atoms incorporated in the film chemically bond to carbon atoms as revealed by X-ray photoelectron and infrared absorption spectroscopies. Typically, a 500 nm thick C-N film exhibits a band gap of about 2.5 eV with high optical transmission.

Tight Binding Calculations of the Surface Electronic DOS of Graphite

B. A. McKinnon and T. C. Choy

Department of Physics, Monash University

With the rapid expansion of surface physics over the last decade, in particular the study of chemi- and physisorption, the understanding of surface electronic structure has become increasingly important. Surface probes such as Scanning Tunneling Microscopy and Angle Resolved Photoemission Spectroscopy have proved valuable experimental tools in this pursuit. However, theoretical understanding lags behind, as is illustrated by the interpretation of the STM image of the familiar graphite. Anomalous features are observed, arising purely from the electronic interaction of the STM tip with the surface.

We have previously calculated the electronic density of states of Bernal graphite within the framework of a parametrized Tight Binding Hamiltonian, using a Green's function technique. This work has been extended, following an approach developed by Thorpe and Weaire. We first investigate a terminated, semi-infinite system, and then extend our method by means of Dyson's equation to include perturbations to the surface electronic environment. We can use this method to investigate the conditions for the existence of surface states.

In addition, we discuss the implications of our work for the experimentally observed STM images of Bernal graphite.

References

[1] E-Ni Foo, M.F. Thorpe, and D. Weaire. Effective surface potential method for calculating surface states. *Surf. Sci.*, 57:323, 1976.

[2] B. A. McKinnon and T. C. Choy. A tight binding model for the density of states of graphite-like structures, calculated using green's functions. *Aust. J. Phys.*, 46:1, 1993.

THERMAL CHARACTERISTICS OF ELECTRIC CABLES WITH POLYPYRROLE COATED CONDUCTORS

R.N. EDIRIWEERA, C. CONN, and J. UNSWORTH
Centre for Materials Technology, University of Technology, Sydney
and
G. TANOS, MM Cables, Liverpool, Australia.

The current rating of a polymer insulated electric cable is determined by the maximum temperature that the polymer can withstand. A coating of polypyrrole on the conductor of the cable would act as a thermal barrier between the heat generating conductor and the polymer insulator, enabling the cable to pass a higher current while still keeping the polymer insulation below its maximum operating temperature.

Polypyrrole doped with p-toluene sulphonic acid have been deposited on tinned copper wires at different concentrations, temperatures and for different time periods giving polypyrrole coatings of different thicknesses and morphologies.

The thermal stability and thermal conductivity values of these coatings are reported. The temperature distribution within cables made up of polymer insulated, polypyrrole coated, tinned-copper wires are presented and advantages compared to conventional cables are discussed.

STABILITY OF POLYPYRROLE TAPES AT HIGH CURRENT DENSITIES

R.N. EDIRIWEERA, J. UNSWORTH, C. CONN and E. MONEY
Centre for Materials Technology
University of Technology, Sydney.

Conducting polymers have been proposed for use in a wide variety of applications and hence its stability is of prime importance. Considerable work has been done investigating their stability with respect to temperature and environment. However, the effect of high current densities has not been reported so far.

Our investigations have found the maximum current density that polypyrrole tapes doped with p-toluene sulphonic acid and synthesised in aqueous media can carry is of the order of 1 A/mm^2. The dependence of this maximum current density on the film properties is reported. The effect of lower current densities on the conductivity stability of these tapes is presented and possible breakdown mechanisms discussed.

Investigation of Carbon-Nitride Depositions Produced by High Energy Density Discharge in Nitrogen Gas Atmosphere

V. Gurarie, A. Orlov, K. Nugent, J.L. Peng and S. Prawer
School of Physics, University of Melbourne, Parkville, VIC. 3052

A number of theoretical investigations have predicted the possibility of synthesising new hard materials. Among them covalent solids formed between carbon and nitrogen were demonstrated to be good candidates for extreme hardness [1]. Recent experiments show that the nitrogen content changes the structure and improves wear resistance [2], hardness [3], tribological [4] and other properties of diamond-like and amorphous C-N films. Experimental realisation of the covalent solid carbon nitride β-C_3N_4, which has been predicted to be harder than diamond, has also been reported [5]. A key to further progress in this area is the development of new plasma and laser deposition techniques of varying physical parameters.

The present work explores carbon-nitride depositions produced by an intense gas discharge of a powerful capacitor battery between carbon electrodes in nitrogen atmosphere. The energy of the discharge, the threshold electric field, initial nitrogen pressure, number of discharges and geometrical parameters of the method are varied to establish their effect on nitrogen content, mechanical, structural and geometrical characteristics of the carbon-nitride films deposited. The structural diagnostics includes optical and scanning electron microscopy, as well as Auger and Raman spectroscopy, Rutherford Backscattering and TEM.

The experiments indicate the formation of two major types of C-N depositions differing by structure and mechanical properties. One of them is C-N films, containing up to 35 at% nitrogen, and which have an amorphous structure similar in many respects to that obtained by the rf plasma method [4]. These films are formed on the periphery of the plasma affected area at a relatively low plasma shock pressure and exhibit relatively low microhardness, ~ 1.5 GPa. In the region of higher plasma pressure and temperature the C-N deposition consists of high density, closely packed crystal-like grains growing perpendicular to the substrate surface and displaying a cauliflower-like morphology. The thickness of the latter deposition is ~ 10 μm (following about 1000 discharges) and its microhardness is extremely high, reaching 15 GPa, as measured by the Vickers method. The grains vary in size between 5 and 10 μm in length and between 1 and 3 μm in diameter. Further investigations are in progress to ascertain the structure of these crystals.

1. A.Y. Liu and M.L. Cohen, Physical Review B, 41, 15, pp. 10727-10733 (1990).
2. M. Iwaki, K. Takahashi and A. Sekiguchi, J. Mater. Res., **5**, 11, pp. 2562-2566 (1990)
3. D.Li, Y. Chung, M. Wong and W.D. Sproul, J. Appl. Physics, **74**, 1, pp. 219-223 (1993)
4. C.J. Torng, J.M. Siversten, J.H. Judy and C. Chang, J. Mater. Res., **5**, 11, pp. 2490-2496 (1990)
5. Ch. Niu, Yu. Z. Lu and C.M. Lieber, Science, **261**, pp. 334-337 (1993).

DETERMINATION OF THIN FILM OPTICAL CONSTANTS USING VARIABLE ANGLE REFLECTANCE.

S.Dligatch, I.Skryabin, G.B.Smith, J.M.Bell

Department of Applied Physics, University of Technology, Sydney, Australia

The angular dependence of the light transmittance $T(\phi)$, and reflectance $R(\phi)$, is important in the study of thin films for energy efficient windows [1]. Accurate optical constants are needed for modelling these important quantities, especially when multilayers or composites are involved. Optical constants (n,k) and thickness d of the coating can be calculated using $R(\phi)$ measurements . This is the main aim of this work.

The ideal device for the experimental measurements of the $R(\phi)$ is an automatic optical goniometer, which has been used for this task [2]. The advantage of such a system is its direct measurement of the absolute reflectance for all possible angles of incidence ($0<\phi<90$). But such systems are relatively expensive. Less expensive Variable Angle Attachments for commercial spectrophotometers (eg Cary-05E) perform only relative reflectance measurements. For solving this problem we developed a method and program for calculation of optical constants of the coating using relative reflectance measurements of $R(\phi)$ with the bare substrate as reference sample.

The steps required are :

-measurement of the bare substrate reflectance $R_{sub}(\phi_i)$ (i=1,...n, for n different angles ϕ_i);

-measurements of the coated surface reflectance $R_C(\phi_i)$ for the same angles ϕ_i ;

-calculations of the experimental relative reflection function $f^*(\phi_i)=R_{sub}/R_C$;

-determination of the parameters- n,k,d for the coating by minimisation of the function

$$\sum_{p,s,\phi} [f(n,k,\phi,d,n_O)-f^*(n,k,\phi,d,n_O)]^2$$

where $f(n,k,\phi,d,n_O)$ is the calculated relative reflectance, p and s the polarisation of the incident light, and n_O the refractive index of the substrate.

This method was applied to the determination of the optical parameters of commercial ITO/glass samples. Our results are in good agreement with other published data in the visible range [3]. In this range, where $k \cong 0$, n was also estimated by Brewster angle measurements where $f^*(\arctan(n))\sim 1$ [4].

1. G.B.Smith, M.W.Ng, A.J.Reuben, A.V.Radchik and S.Dligatch *Fine tuning the spectral response of metal insulator composites for specific solar applications.* Proc. SPIE 2717, 1993 (in press).

2. G.Bader, P.V.Ashrit, S.Elouabik, F.E.Girouard and Vo-Van Truong *Determination of thin film optical constants with an automatic reflectance and transmittance goniometer.* Rev.Sci.Instrum. 62(10), October 1991, p.2398-2404.

3. John.A.Woollam, W.A.McGalan and B.Johs. *Spectroscopic ellipsometry studies of indium tin oxide and other flat panel display multilayered materials.* E-MRS 1993, Symposium C, Paper C-IX/PII.

4.O.S.Heavens *Optical properties of Thin Solid Films.* Butterworths, London, 1955.

MULTILAYER THIN FILM COLOUR SELECTIVE FILTERS

J. Barczynska, J. M. Bell
Department of Applied Physics, University of Technology, Sydney
P.O. Box 123 Broadway NSW 2007

Abstract

The production of relatively cheap coloured coating on glass is in commercial interest of one of a leading Australian producers of art glass. We are aming to produce the desired strong colours in reflection or transmission using multilayer dielectric thin films deposited by a sol-gel process.

The use of sol-gel dipping technique can be adapted for coating three dimensional objects. The shape of an object and changes in the angle of incidence can provide variation of colour enhancing the aesthetic appeal of the finished artworks.

The influence of the sol-gel deposition technique on multilayer filter reflectance has been investigated. The changes in processing parameters , such as temperature of firing and dipping speed result in variation of thin film thickness and refractive index. These changes have been taken into account in the optical design of the colour selective filters. The variation of colours with the angle of incidence has also been investigated.

The variation of film thickness from the nominal value changes the position of the transmittion or reflection band of the filter, the intensity of reflected light and the sequence of colours reflected at different angles.

Modeling of optical properties of multilayer stacks, and optical characterisation (calculation of n and k) of the individual sol-gel deposited films to be used in the filters will be presented.

Preparation and characterisation of certain conducting polymer thin film devices

S. M. Pillai, C. Conn and J. Unsworth

Departments of Materials Science and Chemistry, University of Technology, Sydney
P O Box 123 Broadway N.S.W 2007, Australia

Solution processable polyaniline (PAn) and poly phenylene - vinylene (PPV) are two recent and important polymer electronics materials. Transparent conducting thin films of PAn of transparency >70% over the wavelength range 475 to 675 nm and surface resistance less than 100 ohms per square have been prepared [1]. They are stable and can be prepared at room temperature. Because of these desirable qualities PAn is becoming increasingly an attractive material for optoelectronic applications. PPV can be prepared in the *n* and *p* type form and has conductivities of the order of 10^4 S/cm. It is emerging as a promising organic light emitting material[2] in its undoped form.

At UTS we have prepared the solution processable polyaniline, and PPV and have undertaken a systematic study of the optical and electrical characteristics to facilitate their application in various electronic and opto-electronic devices.

Thin films of solution processable polyaniline were prepared by the doping and complexation of polyaniline with camphor sulphonic acid and then dissolving it in meta-cresol and spin casting on glass substrate. Thin films of PPV were prepared by first spin coating a PPV precursor polymer on the desired substrate and then converting to PPV by a thermal conversion process. It is found that the optical absorption and fluorescence characteristics of the undoped PPV is a strong function of this thermal conversion process.

Optical absorption studies of these films have been carried out and the effective optical band gap was estimated. An electronic device was fabricated using PPV as the active material and polyaniline as the transparent electrode and we studied its I-V, impedance and opto-electronics characteristics at various temperatures. A possible model to explain the observed results is presented.

---

[1] Y. Cao, P. Smith, A. J. Heeger, Synth. Met., 48, 91(1992)
[2] A. N. Burroughs, D. D. C. Bradley, A. R. Brown, A. N. Marks, K. Mackay, R. H. Friend, P. L. Burns and A. B. Holmes, Nature, 347, 539 (1990)

PIEZOELECTRIC CERAMIC/POLYMER COMPOSITES FOR DAMPING OF MECHANICAL VIBRATIONS

H.H. Luo, P.L. Rossiter, L.L. Koss* and G.P. Simon
Department of Materials Engineering
Department of Mechanical Engineering*
Monash University
Clayton, Victoria 3168 Australia

The piezoelectric ceramic (piezo-ceramic) component of a piezoelectric ceramic/polymer composite converts mechanical energy into electrical energy and this electrical energy is dissipated as Joule heat in a load resistance, R_x, simulated by a shunted resistance but provided in practice by a conductive polymer matrix. The composite therefore dissipates the input mechanical energy via the damping mechanism provided by piezoelectric ceramic/conductive matrix material as well as the conventional viscoelastic damping provided by the polymer. Mathematical models have been developed to characterize the damping behaviour of the composites. Equations for the composite damping, polymer damping and the damping provided by the piezo-ceramic have been derived. The maximum damping ratio of composites can be as high as 23%. A two-degree-of-freedom (2DOF) experimental setup was developed to test the validity of the models. The experimental results are in good agreement with the theoretical predictions and hence support the models. Promising applications for such composites may be found in the damping of mechanical vibrations.

(e,2e) MEASUREMENTS OF THIN GRAPHITE FILM

M. Vos, S. Canney, P. Storer and E. Weigold
Electronic Structure of Materials Centre, School of Physical Sciences, The Flinders University of South Australia, GPO Box 2100, Adelaide, S.A. 5001, Australia.

(e,2e) spectroscopy is a technique being developed for solids to study quantitatively the energy dispersion and momentum density of electrons with momentum. In this contribution we present our first results for crystalline carbon films.

Thin films of highly oriented pyrolitic graphite (HOPG) were prepared by a cleaving procedure, followed by plasma etching in an Argon/Oxygen atmosphere. The surface condition was checked by Auger spectroscopy. It was found that directly after plasma etching oxygen was incorporated in the near surface layer, but a clean C surface could be prepared by annealing.

In the (e,2e) measurements of the films directly after plasma etching two structures are found, whereas only one is predicted by theory for crystalline C. After annealing one of these structures disappears almost completely and is thus attributed to adsorbed Oxygen. This demonstrates the surface sensitivity of the (e,2e) technique in the present configuration. The remaining structure after annealing shows clear dispersion of energy with momentum and resembles the theoretical calculations of (e,2e) spectra of HOPG fairly well.

FABRICATION AND CHARACTERISATION OF THIN FILM TETRAHEDRAL AMORPHOUS CARBON

E. G. Gerstner, D. R. McKenzie
School of Physics, University of Sydney, NSW, 2006

Tetrahedral amorphous carbon (ta-C) is a hydrogen free form of diamond-like carbon with an sp^3 bonding fraction approaching 90%. Thin film ta-C is made at the University of Sydney using a filtered vacuum arc deposition system, whereby an arc discharge is generated on a pure carbon cathode and ions are guided to the substrate by a curved solenoid, removing macro-particles and neutral species. The properties of ta-C are similar to those of crystalline diamond, with a short range tetrahedral order and a density approaching that of diamond. It also has a similar hardness, chemical inertness and thermal stability to that of diamond.

Associated with the growth of high sp^3 fraction films are large compressive stresses (up to 5 GPa) which provides an explanation for the formation of tetrahedral sp^3 bonded structures over graphitic sp^2 bonded structures[1]. These high stresses, however, cause adhesion failure when the film thickness exceeds some critical value. One approach to improve adhesion is to deposit an intermediate reactive metal or metal oxide layer, to effectively "stick" the film and the substrate together. This should allow the deposition of ta-C onto virtually any smooth surface material.

As well as its fabrication and physical properties, an important thrust of research into ta-C is of its electrical properties. The mobility gap of ta-C is around 2eV (versus 5eV for crystalline diamond) making it a suitable candidate for use as a semiconducting material for large area and high temperature device applications. Experiment suggests that undoped ta-C is slightly p-type, and with the introduction of nitrogen or phosphorous can be doped n-type[2]. Resistance versus temperature measurements will be presented that indicate conduction in undoped ta-C occurs by a combination of both thermal activation and electron hopping, with the latter mechanism increasing with increased nitrogen doping. Detailed results of current-voltage measurements on metal - ta-C junctions are consistent with a thin, highly sp^2, graphitic layer on the surface of ta-C films. Measurements of photoconductivity in ta-C films will also be presented.

[1] D.R. McKenzie, D.A. Muller, B.A. Pailthorpe, *Phys. Rev. Lett.* **67**, (1991), 773-776.
[2] V.S. Veerasamy, G.A.J. Amaratunga, C.A. Davis, A.E. Timbs, W.I. Milne, D.R. McKenzie, *J. Phys.: Condens. Matter* **5** (1993), 169-174.

MOLECULAR DYNAMICS STUDY OF COMPRESSIVE STRESS GENERATION

N. A. Marks, D.R. McKenzie, B.A. Pailthorpe
Applied Physics, University of Sydney, NSW, 2006

There is a great deal of current interest in the properties of thin films grown with energetic ion beams and the mechanisms behind their growth. Properties such as density, electrical resistivity and compressive stress often exhibit a characteristic dependence on the ion beam energy, namely, an energy window in which the quantity is a maximum. In the case of ta-C, the fraction of sp^3 exhibits the same characteristic dependence [1].

Kaukonen and Nieminen [2] performed simulations of film growth using the Tersoff potential which permits both sp^2 and sp^3 bonding. They found the density and the sp^3 density fraction to be largest when the ion beam energy was in the range 40 to 70 eV. We too have performed simulations of film growth using mono-energetic ions which were individually deposited onto a substrate at 300 K. Our simulations were two-dimensional and the atomic interactions were modelled using the Stillinger-Weber potential parametrised for graphite.

Films were grown at ion energies of 1, 10, 30 and 50 eV. The film grown with 1 eV ions had a voided, columnar structure and exhibited tensile stress. Those grown at higher energies had a high density and compressive stress. Bombardment of the 50 eV film with 75 and 100 eV ions significantly reduced the stress in the film. Thus we are able to predict the characteristic dependence of compressive stress on ion energy seen in experiment.

If possible, a short video demonstrating the dynamics of film growth will be shown during the poster session.

References:

[1] D.R. McKenzie, D. Muller and B.A.Pailthorpe, Phys. Rev. Lett. **67**, 773 (1991).
[2] H.-P. Kaukonen and R.M. Nieminen, Phys. Rev. Lett. **68**, 620 (1992).

ACCUMULATED PHOTON ECHOES IN Nd^{3+}–DOPED CaF_2 AND DISORDERED CaF_2–YF_3 CRYSTALS

Roger J. Reeves‡, Keith W. Ver Steeg, Alexander Ya. Karasik†,
Richard C. Powell, and Tasoltan T. Basiev,
University Center for Laser Research,
Oklahoma State University, Stillwater, OK 74078, U.S.A.

The theory of homogeneous line broadening rare-earth ions is well developed for crystals but less so for disordered materials. For example, the temperature dependences of the homogeneous spectral width (Γ_h) corresponding to relaxation by direct-phonon absorption and two-phonon Raman scattering have been well documented for crystals while in glasses Γ_h exhibits a range in temperature dependence of the form $\Gamma_h \sim T^s$ where $1.7 < s < 2.2$. In order to better understand host–matrix influences on rare-earth ion transition broadening we have measured the inter–Stark relaxation of Nd^{3+} ions in disordered CaF_2–YF_3 crystals. Although differing structurally from glass, these highly disordered crystals possess inhomogeneous linewidths similar to those found in glasses. Accumulated photon echoes were used to measure the dephasing time (T_2) for the $^4I_{9/2} \rightarrow {}^4G_{5/2},{}^2G_{7/2}$ transition of Nd^{3+}. T_2 decreased from subnanosecond values for excitation of low lying Stark levels to subpicosecond values for excitation of high lying levels. The temperature dependence of Γ_h from 9 – 100 K was found to be well described by an exponential function corresponding to a resonant, single-phonon absorption process. In CaF_2:Nd^{3+} quantum beats in the echo decay signal infer a pair interaction between Nd^{3+} ions in a cluster.

‡New Address: Department of Physics and Astronomy, University of Canterbury, Christchurch, New Zealand.

†Permanent address of Profs. Karasik and Basiev is: General Physics Institute, 38 Vavilov St., 117333, Moscow, Russia.

ZEEMAN SHIFTS AND SPLITTINGS OF HYDRIDE VIBRATIONAL LINES IN RARE-EARTH DOPED CALCIUM FLUORIDE

G Jones and N Strickland
Department of Physics and Astronomy, University of Canterbury
PB 4800, Christchurch, 8020, New Zealand

Hydride ions can be introduced into rare-earth doped calcium fluoride crystals with the formation of tetragonal symmetry rare-earth centres charge compensated by hydride ions. The doubly degenerate, transverse (X,Y) hydride ion local mode vibrations of these centres are frequently found to be split into components (separated by up to 3 cm^{-1}) by the electron-local mode interaction. Through this, the resulting local mode vibronic states possess a magnetic moment from the admixture with the rare-earth electronic states. Thus these lines are observed to shift and split in applied magnetic fields. Infra-red spectra showing the varied Zeeman behaviour observed for several different rare-earth ions will be presented, together with their interpretation.

NEUTRON DIFFRACTION MEASUREMENTS OF TIME-DEPENDENT TRANSFORMATION OF PLASTICALLY DEFORMED Mg-PSZ

W.J. Batchelor and T.R. Finlayson

Department of Physics, Monash University, Clayton, 3168

Magnesia-Partially-Stabilized Zirconia (Mg-PSZ) is a ceramic with very good strength and toughness.[1] These properties arise from a metastable dispersion of tetragonal precipitates within a cubic matrix. Under stress, these precipitates can transform to monoclinic symmetry with the resultant volume expansion of ~4.5% producing compressive stresses around stress points. One of the consequences of this stress-induced transformation is that under stress, Mg-PSZ samples can undergo considerable plastic deformation, with permanent strains of up to 1.8% having been reported. It has further been noted in thermal expansion measurements[2] and in some limited neutron diffraction measurements[3] that samples which have been previously plastically deformed will undergo additional transformation, if they are left to sit for long enough periods. This process has been investigated by measuring the phase contents of two samples of Mg-PSZ, that had been previously plastically deformed, using Rietveld analysis of neutron diffraction data[4] at a number of different times throughout 1992/93. The results show that any additional transformation occurs at a much lower rate than would have been expected from the previous measurements.

References

[1] D.J. Green, R.H.J. Hannink, and M.V. Swain, Transformation Toughening of Ceramics, CRC Press, Boca Raton, Florida, 1989.

[2] W.J. Batchelor, T.R. Finlayson, and J.R. Griffiths, Thermal Expansion Measurements on Creep Tested Mg-PSZ, Thermochemica Acta **218**, 113–133 (1993).

[3] E.H. Kisi, 1991, Private communication.

[4] C.J. Howard, E.H. Kisi, R.B. Roberts, and R.J. Hill, Neutron Diffraction Studies of Phase Transformations between Tetragonal and Orthorhombic Zirconia in Magnesia-Partially-Stabilized Zirconia, J. Am. Ceram. Soc. **73**, 2823–2833 (1990).

Orientation and Polarization effects in the Raman spectroscopy of (100) diamond faces in CVD deposited diamond films.

Paul S. Weiser, Steven Prawer and Kerry W. Nugent.
School of Physics, University of Melbourne, Parkville, Victoria, 3052.

Raman spectroscopy is a widely used analysis technique for determining the quality of Chemical Vapour Deposited (CVD) diamond films. It is approximately fifty times more sensitive to sp^2 bonded carbon than sp^3 bonded carbon, and the different carbon allotropes have distinct peaks (diamond 1332 cm^{-1}, amorphous carbon ~1530 cm^{-1}, and graphitic carbon 1350 and 1580 cm^{-1}). The quality of the deposited diamond film is often determined by calculating the ratio of the intensity of the diamond peak to the intensity of the amorphous carbon background peak [1].

In the present experiment a diamond film was deposited on a (100) Si wafer which was seeded by abrading with 9μm diamond paste. The CVD diamond deposition system consists of a waveguide plasma applicator encasing a 1" quartz tube containing the reactant gases (CH_4/H_2), which are excited using a frequency of 2.45 GHz. The substrate was orientated so that the incoming gases were perpendicular to the abraded substrate surface and an optical pyrometer was employed to measure the sample temperature during the deposition. The CVD deposition parameters used were: pressure 20 Torr; total flow rate 100 sccm; CH_4:H_2 1:99; temperature 1050°C; and a deposition time of 4 hours.

Raman spectra were taken in a backscattering geometry from the (100) diamond faces within the film. When the analyser polarization is perpendicular to the incident laser polarization it was found that the diamond line intensity varies from a maximum to a minimum as the crystal is rotated through 45° about the (001) direction. The maximum occurs when the E vector of the incident laser light is parallel to the (100) direction in the (001) plane. However, the amorphous carbon background remains constant and is independent of the crystal rotation. Hence, the ratio of the intensity of the diamond to non-diamond line depends on the orientation of the crystal with respect to the E vector of the incident radiation.

The significance of this result lies principally with Raman spectroscopy when it is used for the analysis of large faceted, or single particle, CVD diamond. If a face of a particular particle is chosen, using micro-Raman mode, an assessment of the quality of the film (as judged by the $I_{diamond}/I_{non\text{-}diamond}$ ratio) can easily lead the investigator astray if the above polarization dependence of this ratio is not taken into account.

1. D.S. Knight and W.B. White, J. Mater. Res., 4(2), 1989, 385.

DIELECTRIC RELAXATIONS IN YTTRIA-STABILISED ZIRCONIA ALLOYS AT LOWER TEMPERATURES

Yu Chen Jeff R. Sellar
Department of Materials Engineering, Monash University
Willinton Road, Clayton, Victoria, Australia 3168

Fully stabilised zirconia alloys are well-known ionic conductors and commonly used as electrolytes in oxygen sensors, and in high-temperature solid state cells for energy conversion, storage and saving[1,2]. It is believed that oxygen vacancies formed to preserve local charge balance for the lower-valent dopant cations (e.g., Y^{3+}) are very mobile and responsible for the high ionic conductivity of these materials[1]. Many investigators have reported that at lower temperatures the oxygen vacancies are localised by association with the dopant cations due to Coulomb attractions or strain field interactions, and such associates or clusters will decompose as temperature rises so that the ionic conductivity increases rapidly with increase of temperature[3,4]. Such a model would lead to the conclusion that at lower temperatures, stabilised zirconia alloys should exhibit dipolar and conductivity relaxations due to the localisation of the oxygen vacancy and dopant cation clusters with dipole moments.

Dielectric properties of yttria-stabilised zirconias with yttria contents ranging from 9.5mol% to 18.0mol% alloys were measured over a temperature range from room temperature to 175°C and a frequency range from 15 to 10^5Hz. The dielectric properties of yttria-stabilised zirconia alloys were found to decrease with increase of yttria content within the cubic region. It is much like the ionic conduction trend with dopant content. A random potential energy model was used to interpret both a.c and d.c. phenomena. According to this model, an increase in dopant will give rise to an increase in activation energies for d.c. conduction and a decrease of dipole moments for dielectric properties so that both d.c.conduction and dielectric properties decrease with increase of dopant cations. By separating the contributions of dipolar and conduction relaxations to the dielectric properties, it was found that they occur concurrently in yttria-stabilised zirconia alloys with conduction relaxation as the dominant part at lower temperatures. Anisotropic dielectric properties of yttria-stabilised zirconia alloys were observed which are believed to be connected with dipole orientations.

REFERENCES

1. T. H. Etsell, and S. N. Flengas, *Chem. Rev.*, **70** (1970) 339-376
2. B. Riley, *J. Power Sources* , **29** (1990) 223-237
3. F. T. Ciacchi, and S. P. S.Badwal, *J. Euro. Ceram. Soc.*, **7** (1991) 197-206
4. J. A. Kilner, and R.J. Brook, *Solid State Ionics* , **6** (1982) 237-252

GLASSY THERMAL EXPANSION OF CUBIC STABILISED ZIRCONIA ALLOYS

Yu Chen J. R. Sellar
Department of Materials Engineering, Monash University
Willinton Road, Clayton, Victoria, Australia 3168

The thermal expansion behaviour of cubic yttria-stabilised zirconia single crystals with yttria contents ranging from 9.5mol% to 18.0mol% was measured over a temperature range from room temperature to 1200°C. The results showed that the expansion or contraction curves for the samples can be divided into three linear segments separated by two break-points. The lower break-point is at 400°C to 550°C and the upper break-point is at 850°C to 1000°C. With increase of the yttria content, the break-points shift to higher temperature. It was found that the heating expansion /cooling contraction cycle is not reversible. A small permanent expansion remains after a cycle of heating and cooling at fast heating and cooling rates, while a permanent contraction remains at slow heating and cooling rates.

The thermal expansion behaviour observed in our yttria-stabilised zirconia alloys illustrates two phenomena: The first is that the expansion coefficient of cubic yttria-stabilised zirconia changes rapidly at the break-points. The second is that there are structural relaxations within the cubic stabilised zirconia alloys which are dependent on the cooling rate.

We will present these and other results which demonstrate that bulk single crystals of yttria-stabilised cubic zirconia behave in a glassy manner during heating and cooling in the 400°C-1000°C range, which we label its "metastable" or "supercooling" range.

Formation of Iron Carbide-Nitrides by mechnochemical reaction between iron and organic H(CN)-ring compounds

I. Onyszkiewicz#, W. A. Kaczmarek*, A. Calka* and B.W. Ninham*

Institute of Physics, A. Mickiewicz University, 60-780 Poznan, Poland
* Research School of Physical Sciences and Engineering,
Australian National University, Canberra, A.C.T. 0200

Metal carbides are of interest because they exhibit technologically useful properties such as high degree of hardness, high melting point, and superconducting properties. Synthesis methods of many metal carbides are well known and the production of bulk materials is advanced. On the other hand metal nitrides technology is more complicated. Variety of different thermally activated chemical methods for producing thin surface nitride layers are in use [1]. However, nitrides are generally less stable than oxides. The highier stability of oxides relative to nitrides means not only that nitrides must be prpared at lower temperature, but also that oxygen and water must be completely excluded from the nitriding environment. Using traditional nitriding techniques it is not easy to achived this which leads to lack of activity in this field. Recently, the new method of nitrides synthesis by mechanical alloying process was reported [2-3]. This preparation procedure involves room temperature direct reaction of metals with N_2 or NH_3 atmosphere.

In this study dry milling was performed on pure iron powder (99.9 % at., average particle size 4 μm) and organic ring type compounds: piperazine $H_6(C_4N_2)$ and pyrazine $H_4(C_4N_2)$ powders respectively, to investigate the possibility of formation iron carbide-nitride composite material. The amount of piperazine or pyrazine compounds used in experiments were calculated for stoichiometric ratio (Fe/N) = 4:1.

X-ray diffraction and thermal analysis results obtained from 150 and 300 hours milled powders show nanostructural mixture of Fe-N phases (Fe_3N and Fe_2N) and traces of structurally transformed γ-Fe (α-Fe ⇒ γ-Fe). Additionally, we suspect that carbon containing phase exists in amorphous form. Analysis of lattice parameters in as milled and annealed samples, and thermal gravimetry results of thermal stability will be presented.

[1] L. E. Toth: *Transition metal carbides and nitrides*, Refractory Materials Series, vol. 7, Academic Press, New York-London 1972.

[2] A. Calka and J. S. Williams, *Synthesis of nitrides by mechanical alloying*, Mater. Sci. Forum 88-90 (1992) 787.

[3] T. Koyano, C. H. Lee, T. Fukunaga and U. Mizutani, *Formation of iron-nitrides by mechanical alloying in NH3 atmosphere*, Mater. Sci. Forum 88-90 (1992) 809.

CHARACTER OF ELECTROMECHANICAL COUPLING IN CERAMIC MATERIALS NEAR F-AF PHASE BOUNDARY

SUN Da-Zhi, DONG Xian-Ling, WANG Yong-Ling and LIN Sheng-Wei
Shanghai Institute of Ceramics, Chinese Academy of Sciences
Shanghai 200050, People's Republic of China

ABSTRACT $Pb(Hf_{1-y-x}Zr_yTi_x)O_3$ (PHZT) ceramic material near Ferroelectric (F) - Antiferroelectric (AF) phase boundary was prepared. The value of K_t and K_p in the system is 0.46 and 0.21, respectively. The character of electromechanical coupling is similar to that in $Pb(Zr_{1-x}Ti_x)O_3$ (PZT), $Pb(Sn_{1-y-x}Zr_yTi_x)O_3$ (PSZT) and $Pb_{1-y}La_y(Zr_{1-x}Ti_x)O_3$ (PLZT) systems[1,2] in which compositions are all near the F-AF phase boundary. The experimental results means that the F-AF phase boundary takes an important role in electromechanical coupling in piezoelectric ceramic materials. The influence of sintering time to the coupling factor in PLZT ceramics was investigated. The value of K_t is 0.52 in the sample that was sintered at 1320 °C for 3 hours when it is only 0.47 in the sample sintered at the same temperature for 1 hour. The size of grain in th ceramic material sintered for different time is different. It is important to control the process for preparing the ceramics with excellent electromechanical coupling character.

REFERENCES

1. Y. L. Wang, X. H. Dai and D. Z. Sun, Prpceedings of International Symposium on Applications of Ferroelectrics, (Urbana, USA) 22(1990)
2. D. Z. Sun, X. L. Dong and Y. L. Wang, Ferroelectrics, 127, 125(1992)

FIBRE OPTIC SENSORS FOR VIBRATION MONITORING OF CONCRETE BEAMS

Edward Tapanes*, Nick Pandelidis†, John Movrin†
Dr Jagoda Williams† and Professor Paul Rossiter*‡
Centre for Advanced Materials Technology*
Department of Civil Engineering†
Department of Materials Engineering*‡
Monash University
Clayton, Victoria 3168 Australia

A unique and practical multimode fibre optic interferometer is described for vibration monitoring of concrete structures. The fibre optic sensing technique takes advantage of the spatial coherence filtering properties of multimode optical fibres, thus yielding improved linearity in amplitude modulation, resulting in a significant reduction in signal fading and drifting. Jacketed and non-jacketed sensors were embedded in concrete beams (approximately 75 mm x 100 mm x 450 mm in dimension) and subjected to three-point dynamic loading on an MTS machine. The beams were cycled between 0 and 10 Hz at 0.5 Hz intervals. The resultant fibre optic interferometer output signals were monitored in real-time in comparison to the MTS load cell output. In field use, a Fast Fourier-Transform (FFT) analysis of the signals may be used to obtain information about modes as well as amplitudes of vibration frequency. For the beams studied, the fibre optic interferometer was found to provide very accurate modal analysis, even at loads as small as 20 kg.

FIBRE OPTIC CHEMICAL SENSORS

Edward Tapanes*, Jason Goode† and Professor Paul Rossiter *†
Centre for Advanced Materials Technology*
Department of Materials Engineering†
Monash University
Clayton, Victoria 3168 Australia

The development of an intrinsic fibre optic configuration based on evanescent wave absorption is reported. The technique is analogous to attenuated total reflectance (ATR) techniques utilised in bulk-optic spectroscopy. In the intrinsic configuration, the fibre buffer and cladding are removed from the desired sensing location(s) and the fibre is placed in the sensing medium. A chemical etching technique for removing the buffer and cladding have been utilised. The sensing medium surrounds the fibre and acts as the fibre cladding in the region(s) where the buffer and cladding have been removed. The evanescent wave of the fibre therefore propagates through the sensing medium as it passes through the sensing region. The sensing medium is absorptive at particular wavelengths corresponding to the chemical species present. These absorption peaks can be monitored in real-time using conventional spectroscopy techniques. Chemical sensors produced in this way have been tested in a range of solutions known to have absorption bands in the near infrared region. Fibre selection and the degree of cladding removal are important to the sensitivity of the technique and depend on the application. The information needed to make the appropriate selections will be discussed.

CURE MONITORING WITH FIBRE OPTIC SENSORS

Edward Tapanes*, Jason Goode†, Anita Hill† and
Professor Paul Rossiter*†
Centre for Advanced Materials Technology*
Department of Materials Engineering†
Monash University
Clayton, Victoria 3168 Australia

An intrinsic fibre optic configuration based on evanescent-wave absorption has been used to monitor the cure of epoxy resins by coupling to a Fourier Transform Infrared (FTIR) and Acousto-Optic Infrared (AOIR) spectrometer. To our knowledge, this is the first demonstration of this technique using standard silica fibre. In the intrinsic configuration, the fibre buffer and cladding are removed from the desired sensing location(s) and the fibre is embedded in the epoxy resin. The resin surrounds the fibre and acts as the fibre cladding in the region(s) where the buffer and cladding have been removed. The evanescent-wave of the fibre therefore propagates through the epoxy resin as it passes through the sensing region. The epoxy resin is absorptive at particular wavelengths corresponding to the chemical species present. These absorption peaks can be monitored in real-time during cure and their intensities can be related to the degree of cure. Fibre selection and the degree of cladding removal are important to the sensitivity of the technique and in some cases are resin dependent. The information needed to make the appropriate selections will be discussed.

MICRO-RAMAN STUDIES OF WEAR OF MG-PSZ

G.L. Kelly, W.J. Batchelor and T.R. Finlayson

Department of Physics, Monash University, Clayton, 3168

Mg-PSZ (magnesia partially stabilized zirconia) ceramics commonly contain a mixture of phases. Raman spectroscopy is one analytical technique which can be used to characterize the phase content of Mg-PSZ and study the stress-induced tetragonal to monoclinic and tetragonal to orthorhombic transformations. The sliding wear process has been found to induce both of these transformations. An ARC mechanism C grant has resulted in a micro-Raman facility with confocal scanning and a small sampling volume (typically 8 μm^3) being available for a study of the extent of these transformations as a function of depth into the sample.

The Raman spectrum of Mg-PSZ consists of distinct peaks, enabling easy recognition of the presence or absence of each phase. The advantages of micro-Raman spectroscopy include a small spot size which can be accurately placed at any point in the sample, short collection time and simplicity in obtaining spectra. It is also found however, that there are severe orientation effects associated with Mg-PSZ and spectra from different grains may vary dramatically. Micro-Raman spectroscopy has proved most effective when used to analyse trends occurring in phase content within one grain. Macro-Raman spectroscopy , with its larger spot size covering several grains, can be used to compare distant areas on a sample.

By comparing the sums of the integrated intensities of the peaks corresponding to each phase, the effect of the wear process on the phase content of the ceramic has been studied and depth profiles plotted. A decrease in the amounts of orthorhombic and monoclinic phases was found as the volume sampled was moved deeper into the sample.

Inelastic Neutron Scattering from Cubic Stabillsed Zirconia

D.N. Argyriou & M.M. Elcombe
Australian Nuclear Science and Technology Organisation. Private Mail Bag 1, Menai, N.S.W. 2234, Australia.

Phonon dispersion curves have been measured for three cubic stabilised zirconias (CSZ) with varying amounts of oxygen vacancies ($Zr(Y)O_{1.913}$, $Zr(Ca)O_{1.875}$, $Zr(Y)O_{1.805}$), using a triple axis spectrometer. We have been able to observe transverse (TA) and longitudinal acoustic (LA) branches for these crystals. However in agreement with previous work, and despite an exhastive search in (Q,ω) space, optic modes were not observed[1]. The behaviour of the LA and TA branches is atypical, in that phonons become increasingly broader, and weaker close to the Brillouin zone boundary. This is particularly the case for the $[\zeta\zeta 0]$ direction, where the TA_2 branch disapears beyond ζ=0.45. This atypical behaviour has been speculated to be caused by to the defect fluorite structure of CSZ.

Recently a reliable model of the static structure has been determined[2] and has been used here to explain the observed inelastic neutron scattering observations. To understand the effect of the defect structure of CSZ to the observed neutron mesurements, lattice dynamical calculations have been carried out on the basis of the static structure. These calculations show that the stability of CSZ is particular sensitive to the [100] interactions between oxygen atoms. They show that either relatively small variations in the force constants for this interaction, associated with variations of the O-O bondlengths in the defect structure, or the incorporation of vacancies into the structure can render the $[\zeta\zeta 0]$ TA_2 mode unstable. This is in agreement with the experimental results which shows that this mode disappears rapidly. These calculations also show a general broadening of all phonon branches. This makes the measurement of the optic phonon particularly difficult. It is found therefore that the static defect model of CSZ is consistent with the inelastic neutron scattering measurements.

1. D.W. Liu, C.H. Perry, A.A. Feinberg, R. Currat. *Phys Rev B* 35 (1987) 9212.
2. D.N. Argyriou, M.M. Elcombe, to be published.

Low Pressure Growth of Diamond Films.

L.Kostidis and S.Prawer,
Micro Analytical Research Centre,
School of Physics,
University of Melbourne,
Parkville, 3052.

ABSTRACT

In this work, we investigate the nucleation and growth of diamond on a silicon substrate by bias enhanced hot filament chemical vapour deposition. In addition, the effcts of growing diamond on thin silicon nitride tips and the consequences of biasing these tips was also investigated.

Transverse Microanalysis of 2.5 MeV H^+ Damage in Diamond.

Sean P. Dooley, David N. Jamieson, Kerry W. Nugent and Steven Prawer.

Micro Analytical Research Centre, School of Physics,
University of Melbourne, Parkville 3052, AUSTRALIA.

The damage produced at the end of range of an MeV light ion beam is too deep to be studied by conventional techniques such as visible micro-Raman spectroscopy and RBS channeling which cannot probe deeper than ~2 μm, meaning that numerical models such as TRIM-89 are relied upon in high energy ion implantation and analysis. Our alternative approach involves irradiating the edge of a crystal and performing the analysis with a focussed beam on the face of the crystal, perpendicular to the irradiation, to obtain a cross-sectional view of the damage.

A <100> type IIa diamond window with edges cut to the <010> and <001> axes was irradiated into the edge by a 2.5 MeV H^+ beam focussed to a 10 μm spot and scanned in an 80 x 120μm rectangle to beam doses of $2 \times 10^{17}/cm^2$. Both random and channeling alignments were used for the irradiations to study the effect of channeling on ion range and damage distribution. Diamond was chosen because it is clear but becomes dark where it has been irradiated, allowing easy analysis of the damage.

Optical microscope measurements showed that the deepest part of the damage was at 37.6 μm for random irradiation and 40.3 μm for channeled irradiation, the random figure comparing well with a Trim-89 calculation. Raman measurements showed little deviation in the diamond Raman peak except near the end of range region of the H^+ implants where it broadened and shifted to lower wavenumbers indicating severe damage. The end of range of the H^+ irradiation showed almost no diamond Raman peak in the random irradiated regions indicating possible amorphization (see figure). The channeled irradiation at the same dose showed less damage at the end of range due to the greater effective longitudinal straggling of channeled ions. Channelling Contrast Microscopy results were consistent with the Raman results.

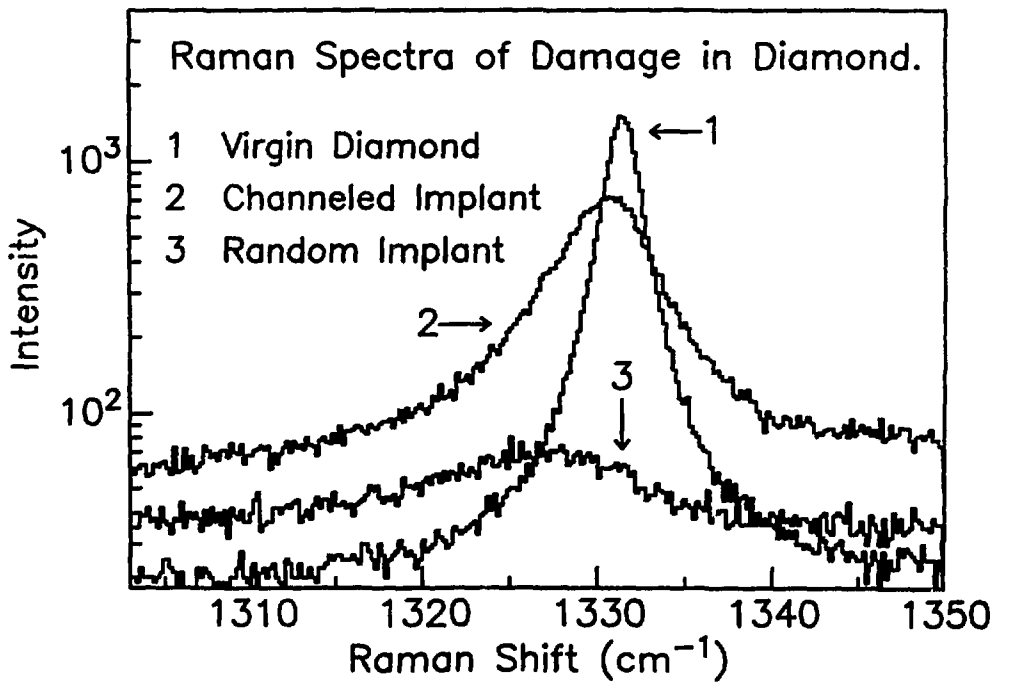

ZIRCONIUM X-RAY EMISSION SPECTRA BY AN ELECTRON PROBE MICROANALYSER

A. Duncan and T. Warmiński

Telecom Australia Research Laboratories, 770 Blackburn Road, Clayton, Victoria 3168.

Zirconium is considered to be a crucial element in a variety of modern ceramics, including the infrared transparent fluorozirconate glasses. Many of us researchers see these glasses as promising materials for optical amplifier components in the 2^{nd} generation optical fibre trunk systems, along with some esoteric applications that use the long wave length transmission window. Zirconium usually has a complex interaction with non-metals, such as Oxygen, Carbon, and Fluorine. This makes for an impossible task for the EDS detection unit operator to chemically identify a micron sized Zirconium based inclusion, but one which can be solved with the WDS unit that is part of the electron beam activated X-ray emission microprobe. The **L** and **M** core level to valence band transitions are the ones being analysed here. A few practical examples of unambiguous Zirconium compound identifications will be demonstrated. Also, we will show some details of our handling of the WDS data recording and spectra processing procedures that are suitable for work with insulating materials.

CELL PARAMETERS AND THE ORTHORHOMBIC TO CUBIC TRANSFORMATION IN STRONTIUM SUBSTITUTED PEROVSKITE ($CaTiO_3$)

C. J. Ball, B. D. Begg and E. R. Vance
Advanced Materials Program, Ansto, Menai, NSW 2234.

The departure of the orthorhombic unit cell of perovskite ($CaTiO_3$) from the cubic symmetry can be characterised by the angle of shear, ϕ, of the pseudo-cubic sub-cell. We have determined ϕ for a series of strontium-substituted perovskites, of general formula $Ca_{1-x}Sr_xTiO_3$, at room temperature. ϕ decreases linearly with increases in x and extrapolates to zero at $x \approx 0.4$, in fair agreement with previous work. For $x > 0.4$ the structure is cubic, contrary to previous reports.

The Micropore Structure of Concrete Determined by Small Angle Neutron Scattering

T.M. Sabine , W.K. Bertram, and L.P. Aldridge

Advanced Materials Program, ANSTO

Small angle neutron scattering (SANS) is a complementary technique to electron microscopy for the elucidation of the shape and size of inhomogenities in the nanometric size range. SANS has the advantage that a large volume (~ 0.5 cm^3) of the specimen is illuminated by the beam, and experiments can be carried out at atmospheric pressure on water saturated samples. It has the disadvantage that, except for very simple systems, interpretation of the experimental data is not unambiguous.

We have collected SANS data on a range of samples of concrete containing different water/cement ratios.

The data was collected on the LOQ instrument at the ISIS spallation neutron source. The range of q $\left(=\frac{4\pi \sin\theta}{\lambda}\right)$ was 0.005 - 0.2 A^{-1}.

We discuss interpretation of the data in terms of microscopic inhomogenities in the structure of concrete.

MODELLING THE MICROSTRUCTURE OF CEMENT

W.K. Bertram, T.M. Sabine , and L.P. Aldridge

Advanced Materials Program, ANSTO

To gain a better understanding of the factors that influence the strength and durability of concrete the microporosity of hydrated cement paste has been investigated by small-angle neutron scattering (SANS). The great advantage that SANS has over the more conventional methods of microporosity analysis such as mercury or gas intrusion , is that for SANS measurements it is not necessary to dehydrate the samples and the process is non-intrusive .

However the results from SANS are often open to several different interpretations and it is necessary to obtain additional information where possible .One method of obtaining such additional information is through computer modelling of the process of cement hydration.

In this poster we present the results of a 3- dimensional computer model that simulates the growth of a layer of calcium-silicate-hydrate (CSH) on a surface. The model used is similar to that for random aggregates (T.A Witten and L.M . Sanders, Phys. Rev. Lett. 19, 1400 (1981)). The model calculates the porosity and the pore size distributions, which can then be compared with those obtained from SANS measurements.

LONG-RANGE TWO-HOLE BOUND STATES IN THE t-J MODEL

M. Yu. Kuchiev* and O. P. Sushkov†

School of Physics, The University of New South Wales

P.O.Box 1, Kensington, NSW 2033, Australia and

**A.F.Ioffe Physical-Technical Institute, 194021 St. Petersburg, Russia*

†*Budker Institute of Nuclear Physics, 630090 Novosibirsk, Russia*

Several series of shallow large-size ($r \gg$ *lattice spacing*) two-hole bound states are found [1] in the two-dimensional t-J model which is closely related to high-T_c superconductivity. The ground state of the t-J model possesses the long-range Néel antiferromagnetic order. The one-particle excitations are holes and spin-waves on the Néel background.

Consider the two holes on the antifferomagnetic background with $\mathbf{P} = 0$ and $S_z = 0$. We show that the single-magnon exchange results in the long-range interaction between these holes described by the static potential $V(r) = \lambda/r^2$, where r is the separation between the holes and λ depends on the symmetry of the wave function of the two holes and the parameters of the $t - J$ model. We find several cases of symmetry when λ is negative. In each case there appears an infinite series of bound states with the energies

$$E_n \sim -\exp\left\{-2\pi(n+3/4)/\sqrt{|\lambda|}\right\}\ , \qquad n = 0, 1, \ldots$$

For physically reasonable parameters of the $t-J$ model the absolute value of λ is not large, $|\lambda| \leq 1$. Therefore the binding energies are shallow, the corresponding wave functions possess a large radius. There are the states with positive and negative parity which is related to the number of nodes $2l, l = 0, 1, \ldots$, of the angular wave function in the coordinate representation by the unusual relation: $\mathcal{P} = -(-1)^l$.

The energies E_n vary sharply with λ. This property makes the states found interesting for high-T_c superconductivity. In the ensemble of holes a stronger interaction between holes and a larger effective constant $|\lambda|$ can be expected. Therefore the found attractive potential λ/r^2 should result in the strong superconducting pairing.

[1] M.Yu.Kuchiev, O.P.Sushkov. Physica C **218**, 197-207 (1993)

Flux jumps in magnetization loops of melt-textured Y-Ba-Cu-O

K.-H. Müller and C. Andrikidis

CSIRO Division of Applied Physics, Sydney 2070, Australia.

As the applied field acting on a type II superconductor is increased beyond the instability field, it is possible for a disturbance cycle to become initiated that leads to a macroscopic ingress of flux usually referred to as flux jump. Flux jumps have been studied extensively in conventional type II superconductors, in particular in connection with wires and magnetic coils.

We have measured the magnetization of a melt-textured Y-Ba-Cu-O superconducting sample in magnetic fields up to 5.5 Tesla using a SQUID magnetometer[1]. Partial flux jumps were observed below the temperature of 7.6 K. With the applied field parallel to the sample's c-axis, the upper bound of the instability field was found to be the maximum applied field while with the applied field perpendicular to the c-axis, the sample's dimensions determined the upper bound. Magnetization loops with flux jumps were calculated employing a critical state model which incorporates the flux-jump instability criterion and considers the incompleteness of jumps. The different shapes of the magnetization loops are determined by four model parameters of which the instability field of the first virgin jump has the strongest effect on the loop shape. To predict the observed loop asymmetry and the appearance of solitary jumps, the simple Bean critical state model was found to be insufficient. Instead, a critical state model where the critical current density decreases as a function of the magnetic field is needed. It is shown that the use of a simple Kim-type critical current density is adequate to explain in detail all our experimental flux jump data.

Because of the large instability fields in melt-textured Ya-Ba-Cu-O the concept of producing superconducting permanent magnets seems to become applicable.

1) K.-H. Müller and C. Andrikidis, Phys. Rev. B 49 (January 1994)

STRAIN TOLERANT MULTIFILAMENTARY BiPb-2223 TAPES FOR POWER APPLICATIONS

John Yau, *S.X. Dou and Nick Savvides

CSIRO Division of Applied Physics, Lindfield, Australia 2070
*University of Wollongong, Wollongong, Australia 2522

Multifilamentary BiPb-(2223) silver-sheathed tapes are candidates for large scale applications in the electrical power industry, and in high field ($B \geq 20$ T) superconducting magnets operating at ≤ 20 K. The strain tolerance of the superconducting tapes, namely their ability to withstand considerable mechanical stress/strain during handling and fabrication into cables or winding into coils without any detereoration of the critical current density, is important. For the most demanding magnet applications the conductor must have a minimum strain tolerance or ϵ_{irr} of about 0.4%.

We report measurements of the critical current density, J_c, at 77 K as a function of bending radius (∞–10 mm) and bend strain (0–2.5%) for BiPb-2223 silver-sheathed tapes. The powder-in-tube method was used to prepare monofilament tapes and multifilament tapes (up to 49 filaments), 0.3–0.5 mm overall thickness, with 5–20 vol% superconductor. The irreversible strain limit, ϵ_{irr}, for the onset of bend strain damage is found to increase from 0.1–0.3% for monofilament tapes to 0.8–1.5% for 49-filament tapes. The 49-filament tapes are exceptionally strain tolerant and retain 85–90% of the initial critical current at 2.5% strain.

Hall Effect in Zn-doped Y-124

Anne Mawdsley

New Zealand Institute for Industrial Research

P.O.Box 31310, Lower Hutt, New Zealand

We have measured the Hall effect in ceramic samples of $YBa_2Cu_{4-x}Zn_xO_8$. As the concentration of Zn is increased T_c is suppressed and the magnitude of the resistivity increases. The magnitude of the Hall coefficient varies only slightly with Zn concentration. The Hall angle is linear in T^2 with a constant slope and a temperature-independent term that increases with Zn concentration. The implication of these results, according to the Anderson charge-separation picture (1,2), is that the Zn suppresses T_c by substituting for the copper on the planes and acting as an in-plane scatterer, rather than changing the hole concentration as would be expected if it substituted on the chain copper site.

1. P.W.Anderson, Phys.Rev.Lett. 67, 2092 (1991).
2. T.R.Chien, Z.Z.Wang and N.P.Ong, Phys.Rev.Lett. 67 (15), 2088 (1991).

A Study of Transition Metal Implanted Single Crystal $YBa_2Cu_3O_{7-\delta}$

J. W. Martin [1], G. J. Russell [1], D. D. Cohen [2], P. J. Evans[2] and A. Hartmann[1]

1. School of Physics, University of N.S.W.

2. Australian Nuclear Science and Technology Organisation.

Abstract ;

The modification of materials by ion-implantation is a method by which the structure and properties of a material can be altered in a controlled fashion and the study of these modified structures can lead to a better understanding of the parent material. The application to the field of high temperature superconductors has been present ever since the discovery of the new oxides. In this study, high quality single crystal $YBa_2Cu_3O_{7-\delta}$ was implanted separately with several different transition metal ions. The implantation was carried out using a metal vacuum vapour arc (MEVVA) ion source operated at 30kV with an approximate dose of $1x10^{17}$ ions/cm^2 being applied. The resulting crystals were subsequently annealed in two separate anneal cycles in an oxygen atmosphere at 550°C for a total of 108 hours.

The sample analysis techniques involved the use of rutherford backscattering spectroscopy (RBS), at both 2 and 3.07MeV, a.c. susceptibility measurements, X-ray diffraction (XRD) and X-ray photoelectron spectroscopy (XPS) for compositional, superconductivity, crystal structure and bonding analysis respectively.

This paper will report on the results of this study which have shown that the implantation of nickel increased the rate of oxygenation in the near surface region, obtaining a transition temperature of 92°K after only 108 hours anneal time, whereas the implantation of iron was deleterious with a transition temperature of only 78°K reached after the same anneal cycles.

This worked has been kindly supported by AINSE.

AN ELASTIC RECOIL TIME OF FLIGHT SPECTROMETER FOR MATERIALS ANALYSIS

J. W. Martin [1], D. D. Cohen [2], N. Dytlewski [2], G. J. Russell [1] and D. B. Garton[2].

1. School of Physics, University of N.S.W.

2. Australian Nuclear Science and Technology Organisation.

Abstract ;

A heavy ion elastic recoil time of flight (ERTOF) spectrometer has been built on the ion beam analysis (IBA) beam line of the 8 MV tandem particle accelerator at the Australian Nuclear Science and Technology Organisation (ANSTO). The spectrometer consists of two electrostatic mirror time detectors, as described in the literature by Whitlow et. al.[1] and Busch et. al.[2], at the forward scattering angle of 45°, and an ion-implanted surface barrier energy detector. The flight length of 750mm gives a typical timing resolution of a few hundred pico-seconds.

The use of high energy heavy ions in recoil spectrometry is ideally suited to the analysis of light ions in heavy matrices, though the analysis of recoil spectra presents some ambiguity due to the overlap of individual depth profiles. An ERTOF spectrometer, with incident 77MeV $^{127}I^{10+}$ as designed here, allows individual depth profiling of most elements contained within the matrix, even those in close proximity in the periodic table, therefore providing an unambiguous profile and greater certainty in sample analysis.

This paper will outline the design and principles of the ERTOF spectrometer built on the IBA beam line at ANSTO. The application of this technique to materials analysis and such examples as YBCO superconductors and AlGaAs semiconductors systems will also be presented.

[1] H. Whitlow, B. Jakobsson, and L. Westerberg, Nucl. Instr. and Meth. A310 (1991) 636.

[2] F. Busch, W. Pfeffer, B. Kohlmeyer, D. Schull and F. Puhlhoffer, Nucl. Instr. and Meth. 171 (1980) 71.

This worked has been kindly supported by AINSE.

THEORY OF FREEZING OF A FLUX LATTICE IN HIGH T_c SUPERCONDUCTORS

D. J. C. Jackson & M. P. Das
Department of Theoretical Physics
Research School of Physical Sciences and Engineering
The Australian National University, Canberra, ACT 2601
Australia

In the mixed state of conventional type II superconductors magnetic field penetrates in quantized flux lines by maintaining the material superconducting except in the cores of the vortices. The vortices are pinned by the defects and form a regular lattice known as the Abrikosov vortex lattice.

In high T_c oxide superconductors the resistivity in magnetic fields remains nonzero well below the onset transtion temperature. This happens due to the motion of the vortices, which experience little pinning force. This phase is analogous to that of a classical liquid. When the temperature is reduced in presence of the magnetic field, the vortices form a solid superconducting structure with zero resistance. The temperature at which the vortex liquid forms a vortex solid is the freezing temperature.

In this paper we describe the phase transition of vortex matter by using the density functional theory. For a given magnetic field we know the density of the vortices. The change in the free energy near the freezing transition is obtained (to second order) in terms of the solid density and the correlation function of the liquid phase. The solid liquid phase boundary in the (H-T) plane is obtained where the free energy difference is zero. Implication of these results in the context of high T_c oxides are discussed.

Current-carrying length scale in silver sheathed Bi-Pb-Sr-Ca-Cu-O tapes

K.-H. Müller, C. Andrikidis, H.K. Liu* and S.X. Dou*

CSIRO Division of Applied Physics, Sydney 2070, Australia.

* School of Materials Science and Engineering,
UNSW, Sydney 2033, Australia

We have measured the magnetization of silver sheathed Bi-Pb-Sr-Ca-Cu-O tapes at different temperatures and fields up to 5.5 Tesla using a SQUID magnetometer. The current-carrying length scale has been determined using formulas for the magnetization of a disc-shaped type II superconductor in perpendicular field. We found that the induced current (even in strong magnetic fields), unlike in polycrystalline samples, flows over the whole tape indicating a relatively strong intergranular current and weak intragranular pinning.

Exposing a tape to different bending strains, we found that the current-carrying length scale started to decrease at a relative bending strain of 1 % and that at 10 % the length scale had decreased by a factor of two.

In order to gain better insight into the interplay between intergranular and intragranular currents we have measured the magnetization of single grains of typically 100 x 100 x 30 μm^3, taken from inside the tape material and compared it with the magnetization of the whole tape.

Magnetization Studies of Superconducting V_3Si

D.B.Lowe and T.R.Finlayson

Department of Physics, Monash University, Clayton, Victoria, 3168.

The magnetic phase diagram of high temperature superconductors (HTS) has been under close examination since their discovery. Of particular interest is the observed boundary between reversible and irreversible regions in the H-T plane and much debate has centred upon the correct description for this behaviour : flux lattice depinning or flux lattice/glass melting. This has led to a re-investigation of the same phenomena in conventional superconductors.

We have conducted magnetization measurements on V_3Si in both a Quantum Design SQUID magnetometer and an "in-house" built vibrating sample magnetometer (VSM). We have observed a reversible region in both instruments but the measurements do not coincide. This has been attributed to the sample undergoing minor magnetic hysteresis loops when traversing the detector coils in the SQUID magnetometer during a measurement. Zero-field-cooled (ZFC) and field-cooled (FC) measurements and magnetic relaxation measurements are used to distinguish between different flux pinning models.

QUENCH RECOVERY PROCESSES ASSOCIATED WITH DEFECT BEHAVIOUR IN YBCO NEAR THE CRITICAL TEMPERATURE

Sujito, A.R. Anderson, G.Godamanne, G.J. Russell
School of Physics
University of NSW
PO Box 1 Kensington 2033

Utrasonic measurements at 85 kHz were made on YBCO polycrystalline samples following quenching from room temperature to just above the critical temperature. Quenching experiments provide a means of studying activation energies and processes associated with active species in HTSCs.

Internal friction measurements indicated that there are defect recovery processes occurring after the samples have reached a constant temperature following quenching. Modulus measurements have indicated that the overall YBCO structure stabilises quickly, while the defect recovery processes are occurring. Results show that there are at least two proceses involved. These can be indentified by the different time constants involved. A short term process significantly decreases the overall damping while a second longer term process marginally increases the final value of the damping.

It is thought that these two processes are related to the internal friction relaxation peaks in the 120 K region [1].

References

1. Effects of Grain Size and Silver Doping on Ultrasonic Propagation in YBCO Ceramics, A.Anderson, G.J. Russell, K.N.R. Taylor, D.N. Matthews and J.I. Dunlop, Physica C, 185, 1389,1991.

THERMOELECTRIC POWER OF YBCO: Ag COMPOSITE SUPERCONDUCTORS

Sujito, A.R. Anderson, G.J. Russell and G. Godammane

Advanced Electronic Materials Group
School of Physics, The University of New South Wales
P.O. Box 1, Kensington NSW 2033

ABSTRACT

The temperature (77-300K) and magnetic field (0-5000 Oe) of the thermoelectric power for bulk $YBa_2Cu_3O_{7-\delta}$ and $YBa_2Cu_3O_{7-\delta}$ with 10%, 20% wt of silver have been studied. The Seebeck Coefficient (S) was found to have a zero value for the superconducting state, rising to a positive value for the normal state, with S decreasing with increasing Ag content.

These results are compared with those from resistivity, ac susceptibility and XRD measurements. It is apparent that the silver does not enter the grains, but remains between for these composite materials.

ACTIVATION ENERGY OF OXYGEN DEFICIENT YBCO

H.B. Sun and G.J. Russell

Advanced Electronic Materials Group, School of Physics, The University of New South Wales,
P.O. Box 1, Kensington NSW 2033

ABSTRACT

The activation energy of oxygen deficient YBCO has been studied by the methods of (i) a.c. susceptibility with a superimposed d.c. field, (ii) magnetic relaxation, (iii) electric resistivity and (iv) thermoelectric power. The values of the activation energy obtained from these different methods are consistent and similar to the results reported by other workers. The dependence of the activation energy on applied d.c. field and temperature for samples with various oxygen content has also been investigated. The results show that the activation energy decreases as the applied field and temperature increase and as the oxygen deficiency increases. The field dependence of the activation energy decreases as the oxygen concentration in the samples is reduced. All these variations are compared with other reported data and discussed in terms of pinning force.

ELECTROMAGNETIC RESPONSE OF HIGH-T_c THICK FILMS

J.W. Cochrane and G.J. Russell

School of Physics, University of New South Wales

PO Box 1, Kensington NSW 2033 Australia

ABSTRACT

High quality microstrip resonators have been fabricated from thick films of YBCO and YBCO/metal composites on yttria stablised zirconia substrates. A network analyser was used to determine the Q of these resonators as a function of temperature for the frequency range 300 kHz to 3.6 GHz. Surface resistance, penetration depth and attenuation coefficient for the different thick films have been derived from the measurements and the results are compared with known thin film data.

ANOMALOUS TIME-DECAY IN NEUTRON DEPOLARISATION BY HIGH-T_c SUPERCONDUCTORS

Miles P.A.[**],Kennedy S.J., Taylor K.N.R.[*], Russell G.J.[**] & Wang J.[**],
Gu G.D.[**], Takamura K.[***] & Koshizuka N.[***]
ANSTO, Neutron Scattering Group
P.M.B. 1, Menai NSW 2234
** Advanced Electronic Materials, Physics,
University of N.S.W. P.O. Box 1, Kensington, N.S.W. 2033
* University of Tasmania, Physics Dept, Hobart, Tas
*** ISTEC, 10-13 Shinonome I-chome, Koto-ku, Tokyo 135, Japan

In studies of the field and time dependence of the polarisation state of a polarised neutron beam transmitted through single crystals of $YBa_2Cu_3O_{7-\delta}$ (YBCO) and $Bi_2Sr_2CaCu_2O_{8+\delta}$ (BSCCO), we have observed some unusual behaviour for temperatures > 60°K for YBCO and 30>T>40°K.

The observed results suggest that at these temperatures, after removing an external magnetic field, the trapped flux density seen by the neutrons is essentially zero for all time less than ≈ 200msecs. With increasing time, the sampled flux density increases in magnitude, reaching the values observed in long time (20secs) measurements only after a delay of several seconds. At this time, the trapped flux density reaches a maximum and subsequently decays logarithmically at a rate determined by the effective pinning energy U(H,T). Possible mechanisms responsible for the inverse flux decay are considered.

Large anisotropy in this behaviour is observed with the effect not being observed at all with H∥ab for BSCCO and no marked temperature onset with YBCO with H∥ab. For both YBCO and BSCCO the H∥c observed flux decay show this behaviour.

We conclude that the observed results follow, not from a change in the magnitude of the trapped flux, but rather from a change in the flux distribution within the sample. We interpret this in terms of a domain structure in the flux lattice system which is associated with the fringing closure flux which remains once the external applied field is removed.

VARIABLE RANGE HOPPING CONDUCTIVITY IN Y_{123}:Y_{211} COMPOSITES CLOSE TO THE PERCOLATION LIMIT

H.S. Gamchi, K.N.R. Taylor and G.J. Russell

AEM, School of Physics, The University of New South Wales
P.O. Box 1, Kensington, NSW 2033, Australia

ABSTRACT

The normal state resistivity of the Y_{123} - Y_{211} percolation is best represented by a variable range hopping (VRH) model in which the electronic states of the system are localized. The characteristic temperature T_o, in the VRH representation $\rho = \rho_o(T_o/T)^{1/4}$ has been used to deduce the hopping length (α^{-1}), and we find that as the percolation limit is approached α^{-1} decreases.

Superconductivity of Fe-substituted $Bi_2Sr_2Ca_1Cu_2O_x$ Single Crystals

J.W. Cochrane
G. D. Gu, Y. Zhao*, ~~J. Cochrane~~, A. R. Anderson and G. Russell

AEM, School of Physics, Univeristy of New South Wales, PO Box 1, Kensington, NSW, 2033, Australia

*School of Materials Science and Engineering, University of New South Wales, PO Box 1, Kensington, NSW, 2033, Australia

K. Takamuku and N. Koshizuka

Superconductivity Research Laboratory, ISTEC, 10-13, Shinonome 1-chome, Koto-ku, Tokyo 135, Japan

Fe-substituted Bi-2212 single crystals of composition $Bi_{2.1}Sr_{1.9}Ca_1(Cu_{1-y}Fe_y)_2O_x$ with y<=0.03 have been successfully grown by floating zone method(FZM). Fe substitution in the feed rods depresses the crystal growth stability of the Bi-2212 phase and results in a planar S/L interface to break down into a cellular growth front. The size of the as-grown single crystals decreases with increase of y. The maximum thickness along the *c*-axis is over 2 mm for y=0, and is only 0.4 mm for y=0.03. There are no sizable and visible Bi-2212 crystals in the as-grown rod with y=0.06. The maximum solubility limit of the as-grown crystals in the rods of $Bi_{2.1}Sr_{1.9}Ca_1(Cu_{1-y}Fe_y)_2O_x$ is only 0.025 at.%. AC susceptibility measurements show that Fe substitution in single crystals significantly depresses not only the superconducting transition temperature, but also the superconducting homogeneity of the crystals. The rate of *Tc* decrease with actual Fe content is 16.7 K/(Fe/(Cu+Fe)) at.% for the as-grown crystals with y<=0.01, and 7.3 K/(Fe/(Cu+Fe)) at.% for the as-grown crystals with y in the range 0.01--0.03 and annealed crystals which have y<=0.03, respectively.

THE RELATION BETWEEN THE ULTRASONIC PROPERTIES AND THE CRITICAL TEMPERATURE IN FE DOPED BSCCO

G.Godamanne, A.R. Anderson, Gu Genda, G.J. Russell
N. Koshizuka * and S. Tanaka*
School of Physics, University of NSW, PO Box 1 Kensington 2033
* ISTEC 10-13 Shinonome 1 chrome koto-ku, Tokyo, Japan

Measurements of the ultrasonic properties of pure and Fe doped BSCCO single crystals at 85 kHz indicate that the changes in the critical temperature in the doped samples are reflected in the ultrasonic damping properties of the materials.

Previous ultrasonic work [1,2] has strongly supported the possibility of a phase change at approximately 165 K as samples are cooled from room temperature. This conclusion is based on characteristic changes in both internal friction and velocity measurements. When pure BSCCO samples are cooled below 165 K the internal friction decreases rapidly as the critical temperature is approached.

The addition of small amounts of impurity to BSCCO samples enable some of the mechanisms associated with superconductivity to be studied. In the present work measurements were conducted on BSCCO single crystals containing 6% Fe. The addition of iron significantly depresses the critical temperature. Measurements on the doped sample still provide support for the phase change at 165 K, however the rapid decrease in internal friction which is evident in the pure sample does not occur until lower temperatures. The depression of the critical temperature in the doped sample is comparable with the temperature depression of the internal friction curve.

References.

1. Evidence for Low Temperature Phase Changes in Single Crystal Bi(2212) A.R.Anderson, Gu Genda, G. Farrow, M.I.Darby, G.J. Russell and K.N.R. Taylor, Proc. Beijing International Conference on High Tc Superconductivity, Beijing (1992).
2. Oxygen-Deficiency Based Anomalies in the Ultrasonic Properties of Bi (2212) Crystals, A.R. Anderson, Gu Genda, K.N.R. Taylor and G.J.Russell, Supercond. Science and Technology , 5,258,(1992).

OXYGEN STOICHIOMETRY MEASUREMENTS IN POLYCRYSTALLINE $YBa_2Cu_3O_{7-x}$ BY MICRO-RAMAN SPECTROSCOPY

J.M. Long,* T.R. Finlayson,* C.S. Lim,*† and T.P. Mernagh**

*Department of Physics, Monash University, Clayton, VIC 3168
**Australian Geological Survey Organisation, GPO Box 378, Canberra, ACT 2601

Micro-Raman spectroscopy is a useful probe for identifying phases present, measuring oxygen stoichiometry, and determining the orientation of single grains in $YBa_2Cu_3O_{7-x}$ (YBCO) and similar superconducting materials.[1-3] Of particular interest is the oxygen stoichiometry, $7-x$, on which the superconducting transition temperature depends.

The frequency of the Raman A_g spectral peak for YBCO near 500 cm^{-1} has been found to depend on $7-x$.[4,5] Many groups use the position of this peak to provide a measurement of $7-x$. Normally, this peak is detected only when components of the polarisations of incident and scattered laser beams are parallel to the long axis (c) of the YBCO unit cell. Another A_g peak occurs near 335 cm^{-1}, and is detected when components of the polarisations of incident and scattered laser beams are perpendicular to the c axis. Little change is observed in the position of this second peak as $7-x$ changes. However, this peak is asymmetric for orthorhombic YBCO, and symmetric for tetragonal YBCO. We have observed a variation in the asymmetry of this second peak in spectra obtained from single grains of YBCO with various values of $7-x$ as determined by Raman spectroscopy.

We propose the use of the asymmetry of the peak near 335 cm^{-1} as a means to determine quantitatively the oxygen stoichiometry of YBCO. Such a method would by useful when the peak near 500 cm^{-1} is not detected in a Raman spectrum. Raman spectra obtained from a number of single grains in a polycrystalline YBCO sample will be presented. The grains have mixed orientations such that both Raman peaks near 335 and 500 cm^{-1} were detected in each spectrum. The grains also have various values of $7-x$, allowing the investigation of the asymmetry of one peak as a function of the position of the other. This study thus yields a quantitative measure of the variation of the asymmetry of the peak near 335 cm^{-1} with oxygen stoichiometry.

[1] J.M. Long, T.R. Finlayson, C.S. Lim, and T.P. Mernagh, Fifteenth Annual A.I.P. Condensed Matter Physics Meeting (Wagga Wagga, N.S.W.), 6–8 February 1991.

[2] C.S. Lim, J.M. Long, T.R. Finlayson, and T.P. Mernagh, *Bull. Am. Phys. Soc.* **36**, p. 365 (1991).

[3] J.M. Long, C.S. Lim, T.R. Finlayson, and T.P. Mernagh, Australian Institute of Physics Tenth National Congress (Melbourne), 10–14 February 1992.

[4] R. Feile, *Physica C* **159**, p. 1 (1989).

[5] C. Thomsen and M. Cardona, in *Physical Processes in High Temperature Superconductors I*, edited by D.M. Ginsberg (World Scientific, Singapore, 1989), pp. 409–507.

†Current address: CSIRO Division of Mineral and Process Engineering, Pvt. Mail Bag 5, Menai, NSW 2234.

Spectral Cathodoluminescence Studies in $YBa_2Cu_3O_{7-x}$ and its related components.

G. Stockton, M.R. Phillips and L.Kirkup
Department of Applied Physics
University of Technology, Sydney
P.O Box 123 Broadway
N.S.W. 2007

ABSTRACT

The identification of the impurity phases present on the surface of bulk superconductors is important in the preparation of low resistance contacts in these materials. These impurity phases can be identified using the technique of cathodoluminescence.

Non spectral Cathothodoluminescence (CL) measurements have shown that the superconducting $YBa_2Cu_3O_{7-x}$ phase is less luminescent than related impurity phases[1]. This enables the high T_c phase to be distinguished from its impurity phases.

Spectral CL measurements have the advantage over nondispersive measurements, in that it is possible to identify various phases at a high spatial resolution[2]. This is especially useful in a multiphase region.

In this work spectral CL measurements were made on a bulk sample of YBCO before and after exposure to atmospheres of varying humidity. Characteristic spectra of the starting materials (Y_2O_3, $BaCO_3$, CuO) were also obtained and used to assist in the identification of new luminescent impurities formed on the surface of the bulk sample as a result of its reaction with water.

(1) J. H. Miller, J. D. Hunn, S. L. Holder, A. N. DiBianca, and C.R. Bagnell, Appl. Phys. Lett. **56**, 89 (1990).

(2) Z. Barkay, G. Deutscher, E. Grunbaum, and B. Dwir, Appl. Phys. Lett. **61**, 25 (1992).

MICROSTRUCTURE DEVELOPMENT AND PHASE TRANSFORMATION OF Ag-SHEATHED BI-2223 TAPES

H.K. Liu, S.X. Dou, E.W. Collings* and M.D. Sumption*

Centre for Superconducting and Electronic Materials
University of Wollongong, Northfields Av.,
Wollongong, NSW 2522, Australia

* Metals and Ceramics Department, Battelle Memorial Institute, Columbus Division, 505 King Ave. Columbus, Ohio 43201-2693, USA

Abstract

Two sets of Ag-clad Bi-based superconducting tapes fabricated using the powder-in-tube process have been treated at different temperatures and investigated with J_c measurements, XRD, SEM and EDS. The first batch of the tapes which was annealed at lower temperatures (828°C), consisted of high fraction 2223 phase and lower fraction of impurity and low T_c phases, but the grain size is small, and grain alignment is poor, and hence the J_c is low. For second batch, annealing at higher temperatures(832 - 838°C), results in a desirable microstructure in which grain alignment and grain connectivity are improved and grain size is large and hence the J_c is higher than first batch even though the tapes contain a higher fraction of impurity phases. The critical current density of Bi-based superconducting tape was very sensitive to the powder quality and heat-treating procedures. The J_c showed a rapid increase during the period of grain growth. The tapes selected from several batches show that the highest value of J_c always occurs at the ratio of 2212/2212+2223 around 4 - 10 %.

OXYGEN ANNEALING OF $Bi_2Sr_2Ca_1Cu_2O_{8+x}$ SINGLE CRYSTALS

H.M.Ionescu[a], S.X.Dou[a], R.Ramer[b]

[a] Centre For Superconducting And Electronic Materials, University of Wollongong, Northfields Av., NSW 2522.
[b] University of NSW, School of Electrical Engineering, PO Box 1, Kensington, NSW 2033.

The oxygen content and the homogeneity of its distribution in the Bi-based superconductors are important parameters for the transport properties of this material since a p-type carrier concentration per CuO_2 plane is believed to have a strong influence on the superconducting transition temperature T_c.

$Bi_2Sr_2Ca_1Cu_2O_{8+x}$ crystals grown by slow cooling in a large temperature gradient were used to study the kinetics of oxygen diffusion in and out of the crystals in a series of annealing experiments , between 400°C and 800°C.

The variation of the *c* parameter of the unit cell with the annealing temperature was investigated and a nonliniar correlation was found.

Also, the width of the superconducting transition temperature ΔT_c measured by a.c. susceptibility was found to be strongly influenced by the level of oxygen content.

MICROSTRUCTURAL AND SUPERCONDUCTING PROPERTIES OF Bi(2223)/Ag TAPES DURING HEAT TREATMENT PROCESS

Y.C. Guo, H.K. Liu and S.X. Dou

Centre for Superconducting and Electronic Materials, University of Wollongong, Northfields Avenue, Wollongong, NSW 2522, Australia

The variation of phase constitution, microstructure and superconducting properties (critical temperature, T_c, and critical current density, J_c) in silver-clad $(Bi,Pb)_2Sr_2Ca_2Cu_3O_{10}$ composite tapes during the heat treatment process was investigated using X-ray diffraction (XRD), scanning electron microscopy (SEM) and electrical measurements. The high-T_c phase formation kinetics was analysed by using the Avrami equation, and the results showed that the conversion process of low-T_c (2212) to high-T_c (2223) phase was a diffusion-controlled, two-dimensional reaction. Microstructural observations revealed that grain alignment, grain growth and intergrain connectivity improved during the entire heat treatment process, with a large grain growth during 100-160 h (834°C) sintering period and significant grain alignment during 160-240 h. Resistivity measurements indicated that zero resistivity at above 77 K was not obtained immediately after the high-T_c (2223) phase appeared (sintering at 834°C for 50 h) but after continuous high-T_c phase paths formed (sintering at 834°C for 100 h); in particular, a sharp, one-step transition with T_c(zero resistivity) = 107 K was observed after sintering at 834°C for 240 h. The correlation between the high-T_c phase fraction, microstructure and superconducting properties at different sintering stages was also studied.

ELECTRON PARAMAGNETIC RESONANCE, MAGNETIC SUSCEPTIBILITY AND RESISTANCE MEASUREMENTS ON Mn DOPED 1:2:3 HIGH TEMPERATURE SUPERCONDUCTORS

Bowden G J, La Robina M, and Ploenjes E C

School of Physics
University of New South Wales
PO Box 1 Kensington
NSW 2033
Australia

Abstract

EPR measurements at 9.2GHZ on Mn doped(0-6%) and Gd doped (5%) 1:2:3 high temperature superconductors, in the temperature range 77K - 300K, are reported. The results are also correlated with both AC and resistivity measurements. It is shown that the addition of small amounts of Mn into the superconducting CuO_2 planes leads to a rapid decrease in the amount of superconducting phase at 92 K, while at the same time giving rise to an increase in the resistivity in the normal regime. It is argued that this is the classic response of a superconductor to the presence of localized magnetic moments in the superconducting lattice. It is also shown that the Mn EPR signal in the 2 and 4% Mn doped samples disappears below T_c, presumably due due to rf-shielding by the superconducting Cooper pairs. However, by way of contrast the Gd EPR signal does not vanish below T_c, but appears t be enhanced. It is argued that both these apparently unreconcilable results can be explained in terms of the non-anisotropic nature of the superconductivity in the 1:2:3 structure.

THE DEFECTS OF HIGH J_c MELT TEXTURED $YBa_2Cu_3O_{7-x}$ SUPERCONDUCTORS+

J.A. Xia, P.R. Munroe, Y.Zhao, H.K. Liu*, S.X.Dou*,

School of Materials Science and Engineering, University of N.S.W., P.O.Box1, Kensington, N.S.W. 2033, Australia.

**Centre for Superconducting and Electronic Materials, University of Wollongong, Northfields Avenue, Wollongong, N.S.W. 2522, Australia*

Abstract

The microstructures of melt textured $YBa_2Cu_3O_{7-x}$ superconductors with high J_c were investigated by means of X-ray diffraction, optical polarised microscopy, scanning electron microscopy (SEM) and transmission electron microscopy (TEM). The structures of the samples were highly dense and aligned. The microcompositions were also determined by energy dispersion spectrometry (EDS). The distributions of the Y_2BaCuO_5 (211) phase in the 123 matrix were examined. Defects including the 211 phase, twins, dislocations, grain boundaries and other defects were examined. The relationship between microstructure and superconducting properties has been examined which indicates that dislocations and 211 phases, which may act as flux pinning centres, play a significant role on improvement of critical current density.

+ This work was supported by the Metal Manufactures Ltd., the Commonwealth Department of Industry, Technology and Commerce, and the Australian Research Council.

Vortex-Glass Superconductivity in Low Magnetic Field In $YBa_2Cu_3O_{7-y}/V_2O_5$ Composite

Y.Zhao

School of Materials Science and Engineering, University of New South Wales, P.O. Box 1, Kensington, NSW 2033, Australia

Y.Y. He

Cryogenic Laboratory, Chinese Academy of Sciences, Beijing, P.R. China

Vortex glass superconductivity is studied in an extreme weak-link system of $YBa_2Cu_3O_{7-y}/V_2O_5$ composite by measuring the resistive transition as well as the I-V curve in low magnetic fields. The feature of the vortex glass transition, i.e. the changes of the curvature of the I-V curves from the positive to negative are observed and the equilibrium phase boundary line between the normal and superconducting phases in H-T plane is obtained. The equilibrium phase boundary line H-T determined from the resistivity measurement is well consistent with that determined by the I-V characteristic measurement, thus it provides us with a simple and reliable method to distinguish the vortex-glass state from vortex-liquid state. In addition, it is found that as the magnetic field is lower than 132 Oe, the system shows a magnetic-field-independent scaling behaviour; but a magnetic-field-dependent scaling behaviour is observed in higher fields. A relatively low value of the dynamic exponent z, suggests that the dynamics of vortex glass in the weak-link network system is different from that in the superconducting single crystal system.

References:

1. M.P.A. Fisher, **Phys. Rev. Lett.**,62, 1415 (1989); D.S. Fisher, M.P.A. Fisher, and D.A. Huse, **Phys. Rev.B**, 43, 130 (1991).
2. R.H. Koch, V. Foglietti, W.J. Gallagher, G. Koren, A. Gupta, and M.P.A. Fisher, **Phys. Rev. Lett.**, 63, 1512 (1989).
3. P.L. Gammel, L.F. Schneemeyer, and D.J. Bishop, **Phys. Rev. Lett.**, 66, 953 (1991).
4. T.K. Worthington, E. Olsson, C.S. Nichols, T.M. Shaw, and D.R. Clarke, **Phys. Rev. B**, 43, 10538 (1991).
5 Y. Zhao, X.B. Zuge, J.M. Xu, and L.Cao, **Phys. Rev. B** (in press).

Structure and Superconductivity in $YBaSrCu_{3-x}Sn_xO_y$ Compound

Y. Zhao[1], G.D. Gu[2]. J.A. Xia[1], and G.J. Russell[2]

[1]School of Materials Science and Engineering, University of New South Wales P.O. Box 1, Kensington, NSW Australia

[2]School of Physics, University of New South Wales P.O. Box 1, Kensington, NSW Australia

The compound $YBaSrCu_{3-x}Sn_xO_y$ with x = 0 to 0.3 has been synthesised. The structure and superconductivity of the sintered and annealed samples under different conditions have been investigated. A non-monotonic variation of the superconducting transition temperature as well as the structural parameters with the Sn content has been observed. This is in contrast to those previously reported, and suggests the existence of two types of occupation states for Sn atoms in the structure. The relationship between the T_c and Sn content can be interpreted with the charge-transfer model which shows that the mobile hole concentration in the CuO_2 planes is influenced by the electronic state of the CuO chains. Our results further reveal that the mobile hole concentration is predominant mechanism associated with the superconducting transition temperature of the cuprates.

References:

1. B.W. Veal, et al., **Appl. Phys. Lett.** 51, (1987).
2. Y. Zhao, et al, **Physica C**, 152 513 (1988).
3. Y. Zhao, et at., **Physica C**, 212, 451 (1993).
4. H. Zhang, et al., **Phys. Rev.**, B 42, 2253 (1990).
5. Y. Zhao, **Physica C**, 179, 207 (1991); **J.Phys:** Conden. Matter 4, 2263 (1992)
6. Y. Zhao, et al., **Supercond. Sci. & Technol.** 5, 295 (1992).

SPIN GAP BEHAVIOUR OF $YBa_2(Cu_{(1-x)}Zn_x)_4O_8$.

G V. M. Williams, J. L. Tallon and R. Meinhold,
New Zealand Institute for Industrial Research and Development,
P.O. Box 31310, Lower Hutt, New Zeaiand.

The electron spin dynamics in underdoped Zn substituted $YBa_2Cu_4O_8$ high temperature superconductors (T_c=82K, x=0) have been probed by Nuclear Magnetic Resonance (NMR), Susceptibility, Thermopower and Resistivity measurements. Previous Neutron scattering studies, for x=0, indicated a gap in the spin fluctuations ($\chi''(\omega)$) which begins to form at temperatures greater than the superconducting transition temperature[1]. A recent Nuclear Quadrupole Resonance (NQR) study has shown that Zn substitution for copper on the copper oxide planes reduces T_c and the antiferromagnetic part of $\chi''(\omega)$ near $q=(\pi,\pi)$[2]. Using NMR we have been able to study the real part of the spin susceptibility, $\chi'(\omega)$, about $q=(0,0)$ and the resultant spin gap as Zn is progressively substituted onto the plane copper site. We observe both the spin gap energy and T_c to be depressed with Zn substitution emphasising the close relationship between superconductivity and the spin spectrum.

[1]K.Kakurai, S. Shamoto, T.Kiyokura, M. Sato, J.M.Tranquada and G. Shirane, Phys. Rev. B **48**, 3485 (1993).

[2]Guo-qing Zheng, Takahiro Odaguchi, Takeshi Mito, Yoshio Kitaoka, Kunisuke Asayama and Yasuharu, J. Physical Soc. Japan **62**, 2591 (1993).

A SHOCK-HUGONIOT FOR $YBa_2Cu_3O_7$ POWDER.

J.R.Fitzsimmons*, P.D. Killen*, and N.W. Page$.

*Queensland University of Technology, Brisbane, Australia.

$The University of Queensland, St. Lucia, Australia.

The successful fabrication of bulk, polycrystalline, high temperature $YBa_2Cu_3O_7$ ceramic superconductor has proven to be extremely difficult. This is partly because of the poor physical properties of the material (it has low strength and ductility) and also because it is difficult to achieve good superconducting links between the powder particles. In order to determine the optimum shock conditions for densification, a series of experiments was undertaken to enable the calculation of the shock Hugoniot. The Hugoniot model used in this work is a further refinement by Page of the Petrie-Page shock Hugoniot model for powders[1] and is based on the model of Zeldovich and Raizer[2]. The refinements include the effects of the Hugoniot elastic limit and a procedure to calculate the continuum shock temperature. This Hugoniot model was validated by comparison of predicted and measured shock states. Measurements of the shocked state in the superconductor were determined by consolidating powdered $YBa_2Cu_3O_7$ in a die using shock waves generated by the impact of high speed, 6061T6 aluminium projectiles. The shock strength was determined using the impedance mis-matching technique described by Al-Tshuler[3] which requires knowledge of the shock Hugoniot for the projectile, the projectile velocity and the shock speed. Shock speeds were measured using strain gauges attached circumferentially to the die and longitudinally to a bar gauge which supported the powder from below. Transit times in the die and bar gauge were corrected for by ultrasound measurements of elastic longitudinal wave velocities.

REFERENCES

1. M.W.Petrie and N.W.Page, "An Equation of State for Shock Loaded Powders." *J.Appl. Phys.*, **69**, pp3517-3524, 1991

2. Y.B. Zel'dovich and Y.P. Raizer, Physics of Shock Waves and High-Temperature Hydrodynamic Phenomena Vol II Academic Press, New York, 1967, p.697

3. L.V.Al-Tshuler,K.K.Krupnikov,B.N.Ledenev,V.I.Zhuchiknin and M.I.Brazhnik,*Soviet Physics.* JETP **34**, 606 (1958)

ELECTRONIC STRUCTURAL CHANGES IN $Y_{1-x}Pr_xBa_2Cu_3O_{7-\delta}$ SINGLE CRYSTALS DUE TO Pr4f STATES

A. Hartmann[1], G.J. Russell[1], W. Frentrup[2] and K.N.R. Taylor[1]

[1]School of Physics, The University of New South Wales, P.O. Box 1, Kensington NSW 2033, Australia
[2]Humboldt-Universität zu Berlin, Invalidenstr. 110, D-1040 Berlin, Germany

ABSTRACT

Electronic structural changes in both tetragonal and orthorhombic $Y_{1-x}Pr_xBa_2Cu_3O_{7-\delta}$ (x = 0, 0.5, 1) single crystals due to Pr4f states have been studied using the techniques of EELS and NEXAFS. The EELS data from cleaved surfaces for the energy range 4-37 eV show no extra peaks due to Pr4f states, while the positions of the Y4d and Pr5d bands above E_F appear to be identical indicating a very similar DOS structure above E_F. The O1s-NEXAFS data shows empty p-states above E_F arising from unfilled Pr4f states hybridized with O2p states. The large relative intensity of the O2p-Pr4f hybrid-state peaks at ~3 eV, 5.5-6.0 eV for the tetragonal crystals and at ~4 eV, 6.3 eV for the orthorhombic crystals indicates very strong hybridization as the relative density of the empty Pr4f states is small. Intensity changes associated with a peak at 1.3 eV above E_F found for the tetragonal crystals, could indicate changes in $O2p-Cu3d_{(x^2-y^2),(3z^2-r^2)}$ hybridization with different Pr content.

^{197}Au MÖSSBAUER ANALYSIS OF GOLD-DOPED YBCO

D. Jinks, G. Ganakas, J.D. Cashion, G. Jakovidis and M.J. Morgan
Physics Department, Monash University, Clayton, Vic. 3168, Australia

It has been shown that the addition of gold to YBCO raises the critical temperature slightly, in contrast with other dopants. In two recent Mössbauer effect studies [1,2] with up to 10mol% Au, the samples have contained between 30 and 84% of the gold as Au(0), believed to be in the grain boundaries, with the dominant substitutional arrangement being Au(III) in the Cu(1) sites. This site has a square planar coordination to oxygen ions and hence is compatible with the d^2sp configuration of Au(III). As the oxygen concentration is reduced, an increasing proportion of the gold is converted [2] to Au(I), with the preferred linear coordination (sp) being achieved by the elimination of two of the neighbouring oxygens.

Our samples contained 4, 6 and 8 mol% of gold and were made by solid state reaction with successive crushing, reheating and extended oxygen annealling to produce stoichiometric material ($\delta \approx 0$). The dominant site in all samples was the substitutional Au(III) with concentrations of 93%, 85% and 73% respectively and only 4%, 8% and 14% of Au(0). The parameters of IS = 3.2 mm/s, QS = 3.5 mm/s agree well with refs. 1 and 2. However, an additional Au(III) site with IS = 5.1 mm/s, QS = 6.8 mm/s was also seen, with an intensity equal to that of Au(0) and the absence of Au(1) agrees with ref 2 for $\delta = 0$. There is little relevant data available on appropriate IS-QS combinations to help in interpreting this second site, because there is no other material in which gold is known to be coordinated to oxygens, and all conductors (metals) are cubic (except $AuTe_2$). The first site has parameters which are close to those for sulphur coordination, with an increased QS probably due to distortion of the site from square planar. However, the second site is in a region characterised by softer ligands such as CN and its interpretation is not yet clear.

1. A.T. Mailybaev et al., Bull. Acad. Sci. USSR, Phys. Ser. 54 89-94 (1990).
2. M. Eibshutz et al., Appl. Phys. Lett., 62 1827-9 (1993).

THE BEHAVIOUR OF OXYGEN REALATED DEFECTS IN BSCCO NEAR THE CRITICAL TEMPERATURE

A.R. Anderson, G.Godamanne, Gu Genda, G.J. Russell,
N. Koshizuka * and S. Tanaka*
School of Physics, University of NSW, PO Box 1 Kensington 2033
* ISTEC 10-13 Shinonome 1 chrome koto-ku, Tokyo, Japan

Ultrasonic measurements at 85 kHz have enabled the behaviour of oxygen related defects to be studied in single crystals of BSCCO near the critical temperature (77 K - 140 K) as the main part of the acoustic damping is due to these defects. A relaxation model has been developed which explains the changes in internal friction as a function of temperature in terms of a single relaxation process, where because of the low activation energy (24 meV), the defect concentration varies significantly over the temperature range involved. This modifies the traditional Debye relaxation curve. The model explains the results of slow thermal cycling below room temperature to 77 K and rapid quenching experiments from room temperature.

When BSCCO samples are cooled slowly from room temperaure there is strong ultrasonic evidence from both the changes in velocity and and internal friction that a phase change occurs at approximately 165 K [1]. Below this temperature the internal friction decreases substantially as the critical temperature is approached. The modified relaxation model can quantitatively explain the results obtained.

In the quenching experiments samples were cooled, over a period of 10 minutes, from room temperature to temperatures between 77 K and 140 K. While velocity measurements indicate that the overall BSCCO structure quickly stabilises, there are further changes in the internal friction which can be explained in terms of the change in the concentration of defects as thermal equilibrium is achieved.

Preliminary analysis also indicates that the model can also be used to explain the internal friction results in YBCO between 77 K and room temperature.

Reference.

1. Oxygen-Deficiency Based Anomalies in the Ultrasonic Properties of Bi (2212) Crystals, A.R. Anderson, Gu Genda, K.N.R. Taylor and G.J.Russell.Supercond. Science and Technology , 5,258,(1992).

THE EFFECT OF SILVER ON THE I-V CHARACTERISTICS OF BSCCO SILVER-SHEATHED TAPES.

D.N. Matthews[+], K.-H. Muller[+], C. Andrikidis[+], H.K. Liu[++] and S.X. Dou[++] .
[+] CSIRO Division of Applied Physics, Sydney, Australia.
[++] School of Materials Science and Engineering, University of New South Wales, Sydney, Australia.

ABSTRACT.

Measurements of the I-V characteristics at various fields and temperatures give insight into the pinning mechanisms of a type II superconductor. For BSCCO silver-sheathed tapes a complication arises from the effect of the silver on the current distribution. Several groups have reported on the I-V characteristics of such tapes (e.g. see refs. [1-3]) but the majority tend to ignore the effect of the silver when analysing the results. In this paper we report on a method by which the measured data can be corrected and we make a comparison between the raw and processed data at 4.2 and 77 K in various magnetic fields (0 - 1.7 T). It will be shown that a drastic effect is observed at 4.2 K and even at 77 K the effect of the silver is significant. It will also be shown that the downward curvature often observed in the log(I)-log(V) plots, which is sometimes interpreted in terms of the collective creep model, is entirely due to the silver and not a charactisitic of the BSCCO superconductor.

In addition we will discuss the influence of the silver on the value of the critical current density using different E-field criteria at 4.2 and 77 K.

REFERENCES.

[1] J.E. Tkaczyk, R.H. Arendt, M.F. Garbauskas, H.R. Hart, K.W. Lay and F.E. Luborsky. Phys. Rev. B. 45, 12506 (1992).

[2] L.N. Bulaevskii, L.L. Daemen, M.P. Maley and J.Y. Coulter. Phys. Rev. B. 48, 13798 (1993).

[3] A. Gurevich, A.E. Pashitski, H.S. Edelman and D.C. Larbalestier. Appl. Phys. Lett. 62, (14), 1688, (1993).

NOISE IN HIGH-T_c R.F. SQUIDS

G.J.Sloggett, D.L.Dart†, C.P.Foley, R.A.Binks, N.Savvides and A.Katsaros

CSIRO Division of Applied Physics, P.O. Box 218, Lindfield 2070, N.S.W., Australia.
†BHP Research, Newcastle Laboratories, P.O. Box 188, Wallsend 2287, N.S.W., Australia.

The noise of a number of thin-film $YBa_2Cu_3O_7$ r.f. SQUIDs fabricated on MgO substrates with single step-edge Josephson junctions has been measured. A substantial range of noise levels has been observed for devices having similar electrical parameters (inductance, critical current, r.f. frequency). When operated at a frequency of 170-200 MHz and a temperature of 77 K, the best devices have white noise levels below $10^{-4}\ \phi_0 Hz^{-1/2}$, where $\phi_0 = 2.07 \times 10^{-15}$ Wb is the magnetic flux quantum, and have 1/f noise corners of a few Hertz. Measurements of the V_{rf} vs I_{rf} characteristics of one SQUID indicate that intrinsic device noise dominates the measured total noise of these devices. The white noise of all devices excedes the predictions of the theory of Kurkijarvi *et al.* [1-3] by a large factor, apparently because of non-ideal behaviour of step-edge Josephson junctions.

1. J.Kurkijarvi and W.W.Webb, Proc.Applied Superconductivity Conf., 1972, 581.
2. J.Kurkijarvi, J. Appl. Phys. **44**, 3729 (1973).
3. L.D. Jackel and R.A.Buhrman, J. Low Temp. Phys. **19**, 201 (1975).

JOSEPHSON BEHAVIOUR AND FLUX TRAPPING EFFECTS IN YBCO STEP EDGE JUNCTIONS.

C.P. Foley, G.J. Sloggett, D.N. Matthews, K.-H. Muller, S. Lam, N. Savvides and A. Katsaros.

CSIRO Division of Applied Physics, Sydney 2070, Australia.

ABSTRACT

YBCO Josephson junctions prepared over step edges in (100) MgO substrates show the presence of two dominant junctions in series with different critical currents, I_c. These junctions exhibit resistively-shunted-junction (RSJ) behaviour and in one junction the lower I_c has a close to ideal magnetic response, sin(x)/x, in a perpendicular magnetic field. When the magnetic field is increased to a particular level, flux trapping occurs resulting in a hysteretic behaviour in the I_c versus H response. We have investigated the effect of this flux trapping on the two critical currents and have found that it occurs as a continuous process rather than as discrete quantised steps. We show that the onset of trapping occurs at approximately the same field for both junctions and at surprisingly large values of H. This suggests that flux is trapped in the main body of the film once the applied field has exceeded the lower critical field H_{c1}, and not in the junctions themselves.

This paper will also explore the effect of the step edge profile, junction dimensions [1] and flux focusing from nearby superconducting material on the magnetic characteristics of the Josephson step edge junctions.

REFERENCES

[1] P.A Rosenthal, M.R. Beasley, K. Char, M.S. Colclough and G. Zaharchuk. Appl. Phys. Lett. **59**, 26 (1991).

YBCO Thin Film Deposition by Cathodic Arc and Laser Ablation

B. Jenkins, D.R. McKenzie
School of Physics, University of Sydney
NSW, 2006, Australia

and

C.P. Foley, G.J. Sloggett
CSIRO Dision of Applied Physics,
P.O. Box 218, Lindfield
NSW, 2070, Australia

High-T_C YBCO films of thickness 100-200nm have been deposited by pulsed cathodic arc ablation and pulsed Nd:YAG laser ablation.

Plasma filtering by a curved magnetic duct produces arc-deposited films free of large particulates. This deposition technique maintains the stoichiometry required for films to exhibit high-T_C superconductivity with zero resistance at 85K.

The pulsed laser ablation technique was used to prepare highly c-axis oriented films with zero resistance at 88K and critical current of $7x10^5 A/cm^2$. Josephson juctions have been fabricated by deposition onto a step edge substrate. At 77K, the Josephson critical current is of order 20uA.

Anomalous Flux Pinning by Twin Boundaries in Single-Crystalline $YBa_2Cu_3O_7$

J.N. Li, A.A. Menovsky and J.J.M. Franse

Van der Waals-Zeeman Laboratorium, University of Amsterdam
Valckenierstraat 65, 1018 XE Amsterdam, The Netherlands

Abstract:

Pinning by twin boundaries in single-crystalline $YBa_2Cu_3O_7$ has been investigated by measuring the field-induced resistivity for flux lines moving within twin boundaries, crossing twin boundaries perpendicular and crossing twin boundaries with an angle of about 45°. It is found that the strong pinning effect of the twin boundaries depresses the flux movement in the flux-creep regime for fields aligned along the twin boundary for all directions of the flux-line movement. For this field orientation the flux-creep regime persists to higher temperatures. In the flux-flow regime, the effect of the twin boundaries is not significant for flux lines crossing the twin boundaries, while for flux lines moving within the twin boundaries, the twin boundary seems to act as a "flux-flow channel" enhancing the flux movement.

EFFECT OF COLUMNAR DEFECTS ON THE CRITICAL CURRENT ANISOTROPY OF EPITAXIAL $YBa_2Cu_3O_{7-\delta}$ THIN FILMS AND $YBa_2Cu_3O_{7-\delta}/PrBa_2Cu_3O_{7-\delta}$ MULTILAYERS

B Holzapfel*, L Schultz* and G Saemann-Ischenko†

* Institute of Metallic Materials, IFW Dresden, PO Box 01171 Dresden, Germany

† Physikalisches Institut, Universität Erlangen, Erwin-Rommel-Str.1, D-91058 Erlangen, Germany

Expitaxial $YBa_2Cu_3O_{7-\delta}$ (YBCO) thin films, which were prepared by a new laser deposition technique (the so-called off-axis laser deposition), and $YBa_2Cu_3O_{7-\delta}/PrBa_2Cu_3O_{7-\delta}$ (Y/Pr) multilayers were irradiated with high energy heavy ions (770 MeV ^{208}Pb and 340 MeV ^{129}Xe) under various directions ϕ relative to the c-axis. The irradiation resulted in columnar defects tilted by ϕ from the c-axis. The angular dependence of their pinning activity was studied by measuring the anisotropy of the critical current density. The $J_c(B,T,\vartheta)$ behaviour of the irradiated YBCO thin films showed an additional peak, which exceeds the intrinsic pinning peak, exactly at the irradiation direction. The Y/Pr multilayers, however, showed an isotropic J_c-enhancement by a factor of 5, without any additional structure in the $J_c(B,T,\vartheta)$-curve.

PRODUCTION OF SUPERCONDUCTING THICK FILMS THROUGH CATION CHELATED ORGANIC PRECURSORS

M.YAVUZ AND S.X.DOU

The Centre of Superconducting and Electronic Materials- Northfields Ave. NSW 2522

The process involves dissolution of cations from oxides and carbonates in polyhydroxyl alcohol, and ethylene glycol based solutions, which is able to produce high-T_c superconducting Y-Ba-Cu-O thick films of desired thickness.

The process has the advantages of homogeneity (prevention of formation of undesirable phases such as green phase Y-Ba-Cu-O_4, abnormal grain growth), reproducibility, precise control of cation stoichiometry, and enhanced physical and mechanical properties.

CHARGE COMPENSATION MECHANISMS FOR ALIOVALENT IMPURITIES IN PEROVSKITE AND ZIRCONOLITE

E. R. VANCE, R. A. DAY, B. D. BEGG and M. G. BLACKFORD,
Advanced Materials Program, Ansto, Menai, NSW 2234.

As part of the chemical design of Synroc-type ceramics for the immobilisation of different high-level radioactive wastes from nuclear fuel reprocessing, it is necessary to understand the various possible charge compensation mechanisms which occur when up to tens of atomic percent of rare earths and actinides are incorporated in solid solution in perovskite ($CaTiO_3$) and zirconolite ($CaZrTi_2O_7$). In particular the solid solution of Gd in the Ca site of perovskite and the incorporation of Nd, Ce, U, Np and Pu in the Ca and Zr sites of zirconolite have been studied by XRD, SEM, TEM, and XANES. The essential conclusions are that in formulations where charge compensating ions are made available, then this is the preferred mechanism for incorporation of these cations in Ca and Zr sites. However in formulations where such compensators are not made available, it is possible for charge compensation to take place via significant abundances of cation vacancies, or by the appearance of unexpected valence states stabilised by crystal-chemical forces. An example of the latter is the probable stabilisation of Ti^{3+} in Ti sites, and of trivalent Ce and actinides in Ca and Zr sites, even under quite oxidising conditions.

A complication in these studies is the effect of prevailing or inherited redox conditions. Redox conditions influence phase abundances and compositions as they control the valencies of cations capable of more than one oxidation state. There is also an indication that reducing conditions can promote oxygen site deficiencies in some formulations. Other complicating factors relate to sample fabrication, arising from the need to make extremely chemically uniform phases having the desired composition. This requires prolonged heating at high temperatures to achieve complete solid-state reaction that may result in selective losses due to volatilisation. Incipient melting due to localised eutectic formation and the apparently straightforward task of efficient stoichiometric mixing on a 1 to 10 μm scale are other problems which have had to be overcome in sample fabrication.

NAME	INITIALS	INSTITUTION	PAPERS/POSTERS
Anderson	**Dr A R**	University of NSW St. George Campus	TP44, TP45, TP50, TP51,TP65
Andrikidis	**Mr C**	CSIRO Division of Applied Physics	TM06, TP36, TP42, TP66
Argyriou	**Mr D N**	ANSTO Neutron Scattering	TP28
Baker	**Mr R J**	University of Wollongong Department of Physics	WP65
Bakshi	**Dr E**	Swinburne Uni. of Tech. Department of Physics	WP63
Barczynska	**Ms J**	UTS Dept of Applied Physics	TP10
Bartel	**Mr A G**	Swinburne Uni. of Tech. Department of Physics	WP63
Bartels	**Dr D**	University of NSW	WE04
Begg	**Mr B D**	ANSTO Advanced Materials	TP32, TP73
Bell	**A/P J M**	UTS Dept of Applied Physics	WP67, TP09, TP10
Bertram	**Dr W K**	ANSTO Advanced Materials	TP33, TP34
Bhasale	**Mr R D**	University of Wollongong Centre for SC & Elec. Mat.	TM06
Blach	**Mr T**	Griffith University Science and Technology	WP19
Bourgeois	**Ms L N**	University of Melbourne School of Physics	
Bowden	**A/P G J**	University of NSW School of Physics	WP14, WP15, WP40, TP57
Bubb	**A/P I**	RMIT	WP72, WP73
Burke	**Mr M D**	UTS Dept of Applied Physics	WP43
Bursill	**Dr L A**	University of Melbourne School of Physics	WP42, FM05
Butcher	**Mr K S A**	Macquarie University Physics Department	WP48
Cashion	**A/P J D**	Monash University Department of Physics	WP20, WP21, WP22, TP64
Chaplin	**A/P D H**	University College, ADFA Department of Physics	WP17
Chen	**Mr Y**	Monash University Materials Engineering	TP20, TP21
Clark	**Prof R G**	University of NSW School of Physics	WE03

NAME	INITIALS	INSTITUTION	PAPERS/POSTERS
Cochrane	**Mr J W**	University of NSW School of Physics	TP47, TP50
Collings	**Dr E W**	Batelle Engineering Mechanics	TA01, TP54
Collins	**Dr J G**	CSIRO Division of Applied Physics	
Collocott	**Dr S J**	CSIRO Division of Applied Physics	
Con Foo	**Ms J**	LaTrobe University Department of Physics	WP32
Crew	**Mr D C**	University of W A Mechanical Engineering	
Crisp	**A/P R S**	University of W A Department of Physics	WP52
Das	**Dr M P**	A N U, Theoretical Physics R S of Physical Sciences	WP47, TM04, TP41
Davis	**Dr R L**	ANSTO Neutron Scattering	WP63, FM04
den Hartog	**Mr B C**	Monash University Department of Physics	
Di	**Dr L**	ANU EME	
Dobbie	**Mr E**	Javac Pty. Ltd.	
Dooley	**Mr S P**	University of Melbourne School of Physics	TP30
Dou	**Prof S X**	University of Wollongong Centre for SC & Elec. Mat.	WP08, WP09, WP14, TM06, TP37, TP42, TP54, TP55, TP56, TP58, TP66, TP72
Duncan	**Mr A M**	Telecom Research Labs	TP31
Dunlop	**Dr J B**	CSIRO Division of Applied Physics	
Dyson	**Mr A J**	University of Newcastle Department of Physics	WP54
Edge	**Dr A V J**	University College, ADFA Department of Physics	
Ediriweera	**Dr R N**	Uni of Technology, Sydney Centre for Materials Tech.	TP06, TP07
Edwards	**Dr C**	University of W A Department of Physics	
Ersez	**Mr T**	Monash University Department of Physics	WP06
Eska	**Prof G**	University of Bayreuth Physical Institute	TM01

NAME	INITIALS	INSTITUTION	PAPERS/POSTERS
Etheridge	**Mr G T**	Monash University Department of Physics	WP30
Fell	**Mr C J**	University of Newcastle Department of Physics	WP68
Finlayson	**A/P T R**	Monash University Department of Physics	WP01, WP04, TP18, TP27, TP43, TP52
Finnemore	**Prof D K**	Iowa State University Department of Physics	FM01
Fisher	**Prof P**	University of Wollongong Department of Physics	WP65, FM06
Fisher	**D**	University of Wollongong Department of Physics	WP61
Fitzsimmons	**J R**	QUT School of Physics	TP62
Folks	**L**	University of WA Department of Physics	
Forsyth	**Mr A J**	Monash University Department of Physics	WP60
Geoghegan	**Mr D S**	University of WA Department of Physics	WM05
Gerstner	**Mr E G**	University of Sydney Dept. of Applied Physics	TP14
Godamanne	**Dr G**	University of NSW School of Physics	TP44, TP45, TP51, TP65
Gu	**Dr G**	University of NSW School of Physics	TA03, TP48, TP50, TP51, TP60, TP65
Guan	**Mr P**	University of Sydney Dept. of Applied Physics	WP31
Guo	**Mr Y C**	University of Wollongong Centre for SC & Elec. Mat.	TP56
Gwan	**Mr P B**	CSIRO Division of Applied Physics	
Hall	**Mr L E**	University of Sydney Dept. of Applied Physics	FM04
Harker	**Mr S J**	University College, ADFA Department of Physics	WP23
Harris	**Mr R**	Oxford Scientific Pty. Ltd.	
Hicks	**Dr T J**	Monash University Department of Physics	WP02, WP06, WP30
Hutchison	**Dr W D**	University College, ADFA Department of Physics	WP17
Ionescu	**Mr H M**	University of Wollongong Centre for SC & Elec. Mat.	WP13, TM06, TP55

NAME	INITIALS	INSTITUTION	PAPERS/POSTERS
Jackson	**Mr D**	A N U, Theoretical Physics R S of Physical Sciences	TP41
Jacyna-Onyskiewicz	**Dr J H**	Australian National University Applied Maths	WP11, TP22
Jafar	**Mr M**	University of NSW School of Physics	WP56
Jamieson	**Dr D N**	University of Melbourne School of Physics	WA03, WP66, TP30
Jenkins	**Mr B**	University of Sydney Dept. of Applied Physics	TP69
Jiang	**Z T**	La Trobe University Department of Physics	TP01
Johnston	**Dr P**	RMIT	WP72, WP73
Jones	**Dr G**	University of Canterbury Physics and Astronomy	TP17
Jurczyk	**Dr M**	CSIRO Division of Applied Physics	
Kaczmarek	**Dr W A**	Australian National University Applied Maths	WP05, WP10, WP11, WP27, WP28, TP22
Katsaros	**Mr A**	CSIRO Division of Applied Physics	TA02, TP67, TP68
Kelly	**Miss G L**	Monash University Department of Physics	TP27
Kennedy	**Dr S J**	ANSTO Neutron Scattering	WP02, WP06, WP30, WP75, TP48
Kenny	**Dr M J**	CSIRO Division of Applied Physics	WP74, TP03
Kent	**Dr A J**	University of Nottingham Department of Physics	TM02
Ketabi	**Mr G H**	University of NSW School of Physics	
Khachan	**Dr J**	University of Sydney Plasma Physics	WP03
Kijek	**Dr M**	RMIT	WP71
Killen	**Dr P D**	QUT School of Physics	WP18, TP62
Kinnear	**Dr R W N**	University College, ADFA Department of Physics	
Kisi	**Dr E H**	University of Newcastle Mechanical Engineering	WP07, WP75
Koshizuka	**Dr N**	SRL -ISTEC	TA03, TP48, TP50, TP51, TP65, FM02

NAME	INITIALS	INSTITUTION	PAPERS/POSTERS
Kostidis	**Mr I L**	University of Melbourne School of Physics	TP29
Kucheiv	**Dr M Yu**	University of N.S.W. School of Physics	TM05, TP35
Kumar	**Dr S**	Macquarie University Physics Department	TP04
Laird	**Mr J S**	University of Melbourne School of Physics	WP64
Leckey	**Prof R**	LaTrobe University Department of Physics	WP32, WP46, WP58
Lee	**Ms G**	RMIT	WP71
Lerch	**Mr M L F**	University of Wollongong Department of Physics	WP44
Lewis	**Dr R A**	University of Wollongong Department of Physics	FM06
Li	**Dr J N**		TP70
Li	**Dr H S**	University of N.S.W. School of Physics	WP08, WP09, WP12, WP14, WP15, WP23
Li	**Dr D**	University of NSW School of Physics	WP50
Liesegang	**A/P J**	La Trobe University Department of Physics	WM03, TP01
Lim	**Mr S S**	Monash University Materials Engineering	WP41
Liu	**A/P H K**	University of Wollongong Centre for SC & Elec. Mat.	WP08, WP09, WP14, TM06, TP42, TP54, TP56, TP58, TP66
Liu	**Dr M**	Monash University Department of Physics	WP01
Lowe	**Mr D B**	Monash University Department of Physics	TP43
Lower	**Dr J C A**	A N U R S of Physical Sciences	
Lumley	**Mr G**	Coltronics Systems	
Luo	**Mr H**	Monash University Materials Engineering	TP12
Maddison	**Dr D S**	DSTO Materials Research Labs	TP02
Manson	**Dr N B**	ANU Laser Physics Centre	
Margarian	**Mr A**	CSIRO Division of Applied Physics	

NAME	INITIALS	INSTITUTION	PAPERS/POSTERS
Marks	**Mr N A**	University of Sydney Dept. of Applied Physics	WP31, TP15
Marshal	**Mr C J**	Balzers Australia Pty. Ltd.	
Martin	**Mr J W**	University of N.S.W. Advanced Electronic Materials	WP72, TP39, TP40
Maslen	**Dr V W**	CSIRO Division of Materials Science and Technology	
Matthews	**Dr D N**	CSIRO Division of Applied Physics	TP66, TP68
Mawdsley	**Dr A**	New Zealand Institute for Industrial Research	TP38
McCubbery	**Mr M D**	La Trobe University Chemistry Department	WP45
McKean	**Mr N S**	Swinburne Uni. of Tech. Department of Physics	WP63
McKinnon	**Ms B A**	Monash University Department of Physics	TP05
Michalewicz	**Dr M T**	CSIRO Supercomputing	WP35
Miles	**Mr P A**	University of NSW School of Physics	TP48
Miller	**A/P D J**	University of NSW School of Physics	WP16, WP51, WP59
Müller	**Dr K-H**	CSIRO Division of Applied Physics	TM06, TP36, TP42, TP66, TP68
Murray	**Mr K**	Oxford Instruments Pty Ltd	
Norman	**Dr P D**	Monash University Department of Physics	WP33
Oitmaa	**Prof J**	University of NSW School of Physics	WP24
Oliver	**Mr D R**	Monash University Department of Physics	WP04
Orloh	**Mr D**	Monash University Department of Physics	WP22
Orlov	**Mr A V**	University of Melbourne School of Physics	TP08
Osotchan	**Mr T**	Macquarie University Physics Department	WP49
Paley	**Mrs A V**	UTS Dept of Applied Physics	WP39
Peng	**J L**	University of Melbourne School of Physics	WP42, TP08, FM05
Petravic	**Mrs J**	University College, ADFA Department of Physics	WP34

NAME	INITIALS	INSTITUTION	PAPERS/POSTERS
Pillai	**Dr S M**	UTS Dept. of Materials Science	TP11
Prawer	**Dr S**	University of Melbourne School of Physics	TP08, TP19, TP29, TP30, FM05
Puclin	**Mr T**	Australian National University Applied Maths	WP10
Qian	**Mr H**	University of Melbourne School of Physics	WP42
Radny	**Dr M W**	University of Newcastle Department of Physics	WP55
Ramer	**Dr R P R**	University of NSW Electrical Engineering	WP13, TP55
Reeves	**Dr R J**	University of Canterbury Physics and Astronomy	TP16
Reza	**Dr K A**	University of NSW School of Physics	WP12
Ricketts	**Dr B W**	CSIRO Division of Applied Physics	WP70
Riegel	**Prof D**	Hahn Meitner Institute Berlin	WM01
Rossiter	**Prof P L**	Monash University Materials Engineering	WP41, TP12, TP24, TP25, TP26
Russell	**A/P G J**	University of NSW School of Physics	TA03, TP39, TP40, TP44, TP45, TP46, TP47, TP48, TP49, TP50, TP51, TP60, TP63, TP65
Ryan	**Mr D S**	University of Wollongong Department of Physics	WP65
Sabet Dariani	**Mr R**	University of NSW School of Physics	WP52, WP57
Sabine	**Prof T M**	ANSTO Advanced Materials	WP43, TP33, TP34
Sarwar	**Mr M**	CSIRO Division of Applied Physics	
Savvides	**Dr N**	CSIRO Division of Applied Physics	TA02, TM06, TP37, TP67, TP68
Schultz	**Prof L**	IFW, Dresden	WM04, WP25, TP71
Scott	**Mr M D**	CSIRO Division of Applied Physics	TP03
Sedghi-Gamchi	**Mr H**	University of NSW School of Physics	TP49
Sellar	**Dr J R**	Monash University Materials Engineering	TP20, TP21
Shakhmuratova	**Prof L**	Kazan State Pedagogical Institute	WA01

NAME	INITIALS	INSTITUTION	PAPERS/POSTERS
Sheils	**Mr W**	La Trobe University Department of Physics	WP58
Sholl	**A/P C A**	University of New England Department of Physics	WM06, WP38
Skryabin	**Dr I**	UTS Dept of Applied Physics	WP67, TP09
Sloggett	**Dr G J**	CSIRO Division of Applied Physics	TP67, TP68, TP69
Smith	**Prof T F**	La Trobe University	WP01
Smith	**A/P P V**	University of Newcastle Department of Physics	WP54, WP55
Smith	**Prof G B**	UTS Dept of Applied Physics	WP37, WP39, TP09
Stephenson	**Mr P C L**	University of New England Department of Physics	WP38
Stewart	**Dr G A**	University College, ADFA Department of Physics	
Stewart	**Dr A M**	Australian National University Applied Maths	WP36
Stockton	**Mr G**	UTS Dept of Applied Physics	TP53
Storer	**Dr P J**	Flinders University Electronic Materials Centre	WA02, TP13
Street	**Prof R**	University of W A Department of Physics	WM02, WM05, WP26
Studd	**Mr W**	RMIT	WP72, WP73
Suharyana	**Mr H**	University of NSW School of Physics	WP14, WP15
Sujito	**Mr S**	University of NSW AEM - Physics	TP44, TP45
Sun	**S D Z**	Shanghai Inst. of Ceramics	TP23
Sun	**Mrs H B**	University of NSW School of Physics	TP46
Swierkowski	**Dr L**	University of NSW School of Physics	FM03
Szymanski	**Dr J**	Telecom Research Labs	FM03
Thakur	**Dr J S**	University of NSW School of Physics	TM03
Thompson	**P J**	University of WA Department of Physics	WP26
Troup	**Dr G J**	Monash University Department of Physics	WE01
Unsworth	**Prof. J**	Uni of Technology, Sydney Centre for Materials Tech.	TP06, TP07, TP11

NAME	INITIALS	INSTITUTION	PAPERS/POSTERS
Usher	**Dr B F**	Telecom Research Labs Photonics Section	WP53
Vagov	**Mr A V**	A N U, Theoretical Physics R S of Physical Sciences	WP37, WP39
Vance	**Dr E R**	ANSTO Advanced Materials	TP32, TP73
Vos	**Dr M**	Flinders University Department of Physics	WA02, TP13
Walker	**Mr S**	RMIT	WP72, WP73
Wang	**MR G**	University College, ADFA Department of Physics	WP11
Warminski	**Dr T**	Telecom Research Labs	TP31
Weiser	**Mr P S**	University of Melbourne School of Physics	TP19
White	**Dr G K**	CSIRO Division of Applied Physics	
Wielunski	**Dr L S**	CSIRO Division of Applied Physics	WP74, TP03
Wildes	**Mr A R**	Monash University Department of Physics	WP02
Wilkins	**Dr S W**	CSIRO, Division of Materials Science and Technology	WE02
Williams	**Dr G V M**	New Zealand Institute for Industrial Research	TP61
Witham	**Mr L G**	University of Melbourne School of Physics	WP66
Wu	**Mr S**	University of NSW School of Physics	WP62
Xia	**J A**	University of NSW Materials Science and Eng.	TP58, TP60
Xiong	**Mr Z**	University of NSW School of Physics	WP51, WP59
Xu	**Dr W**	A N U, Theoretical Physics R S of Physical Sciences	WP47
Yau	**Mr J K F**	CSIRO Division of Applied Physics	TM06, TP37
Yavuz	**Mr M**	University of NSW Materials Science and Eng.	TP72
Yazidjoglou	**Dr N**	University College, ADFA Department of Physics	WP17
Yin	**Dr Y**	University of Sydney Dept of Applied Physics	FM07

NAME	INITIALS	INSTITUTION	PAPERS/POSTERS
Zhang	**Mr F**	University of Newcastle Department of Physics	WP69
Zhao	**Dr Y**	University of NSW Materials Science and Eng.	TA03, TP50, TP58, TP59, TP60
Zhao	**Mr X**	University College, ADFA Department of Physics	WP29

Printed by University College, UNSW Canberra